ORINCON CORPORATION

OCR 98-4320-U-0295

AUTONOMOUS UNDERGROUND MICROBORER FOR CHARACTERIZATION OF DEEPLY BURIED UNDERGROUND FACILITIES

Final Report

16 July 1998

Sponsored by Defense Advanced Research Projects Agency STO
ARPA Order No. D611, Amdt. 27

Issued by U.S. Army Missile Command Under Contract No. DAAH01-98-C-R026
CDRL No. A002/0001AB

Principal Investigator: Dr. S. Lawrence Marple, Jr.
ORINCON Corporation
9363 Towne Centre Drive
San Diego, CA 92121
(619) 455-5530, ext. 460

Submitted to:
Commander, U.S. Army Aviation and Missile Command
Redstone Arsenal, AL 35898-5248

Contract Effective Date: 17 November 1997
Contract Expiration Date: 16 July 1998

ORINCON CORPORATION

3 August 1998

Project Ref: 4320

Commander
U.S. Army Aviation and Missile Command
Attn: AMSMI-RD-WS-DP-SB (Mr. Charles R. Piner, Technical Monitor)
Bldg. 7804, Room 222
Redstone Arsenal, AL 35898-5248

Subject: Contract No. DAAH01-98-C-R026
Delivery of Final Technical Report

Dear Mr. Piner:

Enclosed is the *Autonomous Underground Microborer for Characterization of Deeply Buried Underground Facilities* Final Technical Report, CDRL No. A002/0001AB, submitted under the subject contract. With this delivery, all work under this contract is considered complete.

A DD Form 250 is attached for this deliverable. Since payment is dependent upon your acceptance, please execute as soon as possible and forward the original DD250 to the agency in Block 12 for payment, along with a copy to the undersigned at the address in Block 9 for ORINCON's records. Your expeditious handling is appreciated and will avoid unnecessary financial burden to ORINCON.

Should you have any questions concerning this report, please contact Dr. S. Lawrence Marple at (619) 455-5530, extension 460.

Sincerely,

Alan Ledbetter
Contract Administrator

Distribution:

AMSMI-RD-WS-DP-SB	2/0
AMSMI-RD-CS-R	1/0
AMSMI-RD-WS	1/0
DARPA/STO	1/0
DARPA OASB/ARPA Library	1/0
DARPA OASB/SBIR	1/0
DTIC	2/0

9363 Towne Centre Drive, San Diego, CA 92121 Phone: (619) 455-5530 FAX #: (619) 453-9274

REPORT DOCUMENTATION PAGE

Form Approved
OMB No. 0704-0188

1. AGENCY USE ONLY (Leave blank)	2. REPORT DATE	3. REPORT TYPE AND DATES COVERED
	3 August 1998	Final Report 11/17/97-7/16/98

4. TITLE AND SUBTITLE

Autonomous Underground Microborer for Characterization of Deeply Buried Underground Facilities

5. FUNDING NUMBERS

C
DAAH01-98-C-R026

6. AUTHOR(S)

Dr. S. Lawrence Marple, Jr.

7. PERFORMING ORGANIZATION NAME(S) AND ADDRESS(ES)

ORINCON Corporation
9363 Towne Centre Drive
San Diego, CA 92121

8. PERFORMING ORGANIZATION REPORT NUMBER

98-4320-U-0295

9. SPONSORING/MONITORING AGENCY NAME(S) AND ADDRESS(ES)

Commander, U.S. Army Aviation and Missile Command
Attn: AMSMI-RD-WS-DP-SB (Mr. Charles R. Piner, Tech Monitor)
Bldg. 7804, Room 222
Redstone Arsenal, AL 35898-5248

10. SPONSORING/MONITOR AGENCY REPORT NUMBER

11. SUPPLEMENTARY NOTES

12a. DISTRIBUTION/AVAILABILITY STATEMENT 16 Jul 98

Distribution limited to U.S. Government agencies only; Test and Evaluation; ~~(3 August 1998)~~. Other requests for this document must be referred to Director, Advanced Research Projects Agency, Attn: Tech Information/Ms. Amick, 3701 North Fairfax Drive, Arlington, VA 22203-1714.

12b. DISTRIBUTION CODE

13. ABSTRACT (Maximum 200 Words) Although construction and entrances of deeply buried underground facilities (UGFs) may be detected by remote surveillance assets available to U.S. forces, detailed internal characterization and 24-hour monitoring of denied access facilities cannot be accomplished by current remote sensors and have therefore depended heavily on human intelligence (humint) resources, which are often not available or may be unreliable. An innovative underground intelligence (UGINT) system concept and its technical feasibility is presented in which a stealthy autonomous underground microborer (AUM) is used to deliver sensors to designated positions exterior to or interior within a UGF by microboring through the ground with a rock-melting penetrator. For a UGF entrance monitoring mission, the AUM would carry low-light-level electro-optic/infrared (EO/IR) imaging and/or acoustic sensors periscoped to ground level near an entrance. For a UGF mapping mission, the AUM would carry a ground-penetrating radar transmitter working in conjunction with stealthily placed unattended ground sensors (UGS) or an ELF antenna working in conjunction with the HAARP system in Alaska to perform bistatic tomographic imaging of the UGF. For an internal penetration access mission, the AUM would carry EO/IR, audio, and/or radiological/chemical sniffers to be placed in or through walls of a UGF chamber. The monitoring mission is proposed as a near-term technology development capability, and the internal access mission is proposed as a far-term technology capability.

14. SUBJECT TERMS	15. NUMBER OF PAGES
Underground facilities, Microboring, Rock melt, Ground-penetrating radar, Unattended ground sensors, Autonomous air vehicle	77
	16. PRICE CODE

17. SECURITY CLASSIFICATION OF REPORT	18. SECURITY CLASSIFICATION OF THIS PAGE	19. SECURITY CLASSIFICATION OF ABSTRACT	20. LIMITATION OF ABSTRACT
Unclassified	Unclassified	Unclassified	SAR

TABLE OF CONTENTS

LIST OF FIGURES

LIST OF TABLES

LIST OF SYMBOLS, ABBREVIATIONS, AND ACRONYMS

ASIC	Application-Specific Integrated Circuit
AUM	Autonomous Underground Microborer
DSWA	Defense Special Weapons Agency
ELF	Extremely Low Frequency
EM	Electromagnetic
EO/IR	Electro-Optical/Infrared
GPR	Ground-Penetrating Radar
HAARP	High-Frequency Active Auroral Research Program
HAE	High Altitude Endurance
HF	High Frequency
HVAC	Heat, Ventilation, Air Conditioning
IUGS	Integrated Unattended Ground Sensors
JPL	Jet Propulsion Laboratory
LASL	Los Alamos Scientific Laboratory (Former Name)
LANL	Los Alamos National Laboratory
LLNL	Lawrence Livermore National Laboratory
LOC	Line Of Communications
LPI	Low Probability Of Interception
MAE	Medium Altitude Endurance
MIR	Micropower Impulse Radar
NTS	Nevada Test Site
PCB	Printed Circuit Board
PRF	Pulse Repetition Interval
SATCOM	Communications Satellite
UAV	Unmanned Air Vehicle
UGF	Underground Facility
UGINT	Underground Intelligence
USP	Unmanned Space Plane
UWB	Ultrawideband
VLF	Very Low Frequency
WMD	Weapons Of Mass Destruction

1.0 SUMMARY

In order to maintain vigilance to military threats, to support military operations, to enable treaty verification, and to document UN sanction violations, the United States depends on the world's most sophisticated surveillance and remote sensor technology. These sensors have been placed in space (e.g., the reconnaissance spacecraft of the NRO or the future DARPA Discoverer II space-borne radar), in air (e.g., the U2 or the DARPA UAV programs), in oceans underwater (e.g., the SOSUS arrays), and on the earth's surface (e.g., the DSWA Tactical Unattended Ground Sensors (TUGS) program or the DARPA Internetted Unattended Ground Sensors (IUGS) program). The one domain where the United States has no sensor emplacement capability, or the technology development program to lead to such a capability, is deep underground. The case for urgently developing such deep underground sensor emplacement technology and associated sensor capabilities for continuous monitoring is compelling. The construction of underground facilities (UGFs) has been accelerating as many countries, particularly those that are targets of US surveillance, have been moving their weapons of mass destruction (WMD) development, manufacturing, and stockpiling to such facilities. Deep underground command and control facilities that are impervious to knockout by non-nuclear weapons are also now common. To illustrate the inadequacies of existing above-ground sensors, one need only look to the recent nuclear tests in India and Pakistan, which hid their tests from US space-borne sensors primarily by use of UGFs, and the extensive use of UGFs by Iraq (including Sadam's many "palaces") to continue hiding its nuclear and biological agent weapon programs before and after the Gulf War. If there were a technology developed that could permit stealthy placement of underground sensors near, or inside of, UGFs suspected of having WMD associations, then the surveillance gap where the US is now blind could be filled.

DARPA has been the DOD's research leader in the development of novel, high-risk technology and is, therefore, the natural choice to be the technology visionary that takes the initiative to develop such technology for underground sensors and the unmanned autonomous emplacement of such sensors. This Phase I SBIR report provides one possible technology roadmap and a feasibility evaluation to provide such a critical through-ground technology in a system concept called the *autonomous underground microborer* (AUM). This name is intended to invoke the long DARPA legacy in autonomous technology system development. In *air*, it has been the unmanned air vehicle (UAV) through programs like Global Hawk and DarkStar. In *water*, it has been the autonomous underwater vehicle (AUV). On *land*, it has been the autonomous land vehicle (ALV). The AUM is envisioned as perhaps the most stealthy and unexpected approach to placing sensor assets in close access to, or inside of, UGFs in denied areas of interest to the United States. The AUM technology would also have commercial potential as a means for search

and rescue units to emplace sensors into inaccessible voids from mine accidents or collapsed structures due to earthquakes in order to monitor for entombed survivors.

The primary task for the Phase I project was to develop a feasible concept of operations together with the technology roadmap to accomplish the concept of operations (conops) and an estimate of the program cost if the roadmap were implemented. Four subsidiary tasks were also identified in the Phase I proposal to focus attention on the four most critical technologies of the roadmap. Specifically, these tasks were to (1) investigate a rock melt penetrator and determine its feasibility relative to other microboring approaches, (2) investigate underground navigation technologies that permit the boring system to determine its underground position and the target location, (3) provide a bistatic UGF imaging feasibility assessment, and (4) investigate data exfiltration techniques to transmit the sensor data that are extremely covert.

The original conops as presented in the Phase I proposal, captured by Figures 6, 9, 11, 12, 13 of Section 3, envisioned three mission variations: long-term external monitoring of UGF adits (entrances at ground level), volumetric imaging/mapping of the UGF layout by bistatic means, and long-term internal monitoring by penetrating UGF concrete chamber walls to emplace sensors. These missions are listed in order of increasing complexity, and we will conclude this summary by proposing a multiphase, multiyear program to stage the technology development and spread the risk to accomplish all three proposed missions.

In the original conops, the AUM would be precision (GPS accuracy) soft-landed for emplacement by a parasailing mini-UAV (unmanned aerial vehicle) deployed from a larger recoverable UAV such as Predator or Global Hawk (near term), or a mini USP (unmanned mini spaceplane) after re-entry from orbit or a suborbital trajectory (far term). The AUM was originally envisioned to be a self-contained, finite-length modular assemblage of diesel fuel and electronics (navigation and sensors) cylinders, tipped by the rock-melting penetrator head with propelling cleats, with a total length of a linear feet, that could microbore and navigate to a designated sensor emplacement location with no surface-based supporting equipment. A rock-melting approach was selected because it is the quietest method for boring to avoid detection and it is able to penetrate concrete and rebar as well as soil, soft rock, and hard rock. A 50-mm (roughly 2-inch) diameter for the AUM was needed to get sufficient fuel into the borehole and to contain the entire AUM below ground within two hours. Based on the estimated payload capability of the mini-UAV, the AUM would have sufficient fuel to penetrate approximately 100 meters. Because of the fairly short distance, the mini-UAV must accomplish its mission quickly and quietly under the cover of night — thus, the two-hour deployment assumption to minimize discovery. After deployment of the AUM to a point where the entire assemblage is in

the glass borehole created by the rock-melting action, the one-time-use mini-UAV would depart and self-destruct several kilometers away by navigating to isolated terrain or bodies of water that could hide the evidence of its presence. As the deployment site for the AUM under some scenarios might be hundreds of miles inside denied territories, it was desirable to develop a conops that allocated the maximum weight for the AUM and its penetration distance rather than fuel to recover the mini-UAV. To deploy the sensor(s), it was envisioned to have an offset drill in the cylinder behind the penetrator head penetrate the last few inches of ground or concrete. The sensor would be coaxially located within the drill body and would be pushed out of the drill tip to allow the sensor to look, listen, or sniff as required. In order to communicate the sensor data, the original conops envisioned a thin jacketed fiberoptics cable deployed as the penetrator bored, terminating at a camouflaged surface-based antenna configured to look like an indigenous cultural feature (e.g., a rock or a plant). The deployment sequence from the mini-UAV would position the camouflaged antenna to cover the borehole entrance to conceal it and would exfiltrate the navigational data as the AUM bored in order to monitor its progress, and then switch to sensor data after the target location was reached.

Due to the technology discoveries made during the Phase I study and some realities of physics and fuels, the conops was modified and improved. Of the many technologies considered in this study, there were three critical ones: (1) alternative rock-melting penetrator designs as a result of technical discussions with Los Alamos National Laboratory (LANL), (2) a sub-inch-size radar called the micropower impulse radar (MIR) pioneered by Lawrence Livermore National Laboratory (LLNL), and (3) integrated active antenna structures of Professor Tatsuo Itoh of the microwave engineering group at UCLA that are key to developing a stealthy exfiltration comm system. The conops modifications also made it possible to create a receiving extremely low frequency (ELF) antenna hundreds of meters in length behind the penetrating tip, making it possible to work with the High-frequency Active Auroral Research Program (HAARP) as a source of ELF waves to bistatically image the UGF, which was not feasible with the original technical concept for the AUM.

It seems technically feasible, after a series of technical dialogues with LANL, to construct a steerable rock-melt penetrating AUM with only a 10- to 12-mm diameter (less than 1/2 inch). As the energy for thermal microboring is essentially proportional to the square of the borer diameter, the 5X reduction in borer diameter from the original concept means a 25X greater tactical standoff range for deployment from the target point for the same weight in fuel. This makes it possible to have a 1-km or greater range for the mini-UAV method of soft-landed deployment, and possibly 2- to 3-km range if a 3- or 4-man special operations team does the deployment manually. Such large standoff ranges make it possible to use compact surface-based deployment

means operating in conjunction with a reduced complexity AUM (from the original concept) in the borehole because the deploying mini-UAV or SpecOps team is better able to conceal its activities for longer periods of time as it is no longer in the near vicinity of the targeted UGF. This will simplify the downhole component of the AUM design. The mini-UAV, which will have the surface-based deployment component of the AUM integrated into its structure, will stay until the penetrator has reached its target point, and then will depart the surface at completion of microboring, leaving nothing on the surface except the camouflaged data exfiltration antenna as described in the original conops scenario.

Figures 10, 14 and 15 in Section 3 depict the modifications to the AUM design and conops from the original design and conops in the Phase I proposal. The basic conops, which involved using a larger UAV like Predator or Global Hawk to launch a mini-UAV close to a targeted UGF and having that mini-UAV precision soft-land, deploy a AUM, and then take off for a destruction location, is identical to that originally proposed, except for the duration of time that the mini-UAV stays on the surface operating with the AUM. The AUM design changes from that of a set of linked cylinders to simply a unitary structure with a rock-melt penetrator component, a heat exchange component, and an electronics component with ground-penetrating radar as a navigating sensor, all connected to the surface via a coiled-tubing stem deployed with a reeled tubing injector unit on the surface (within the mini-UAV) to develop thrust for pushing the penetrator through the borehole. The tubing will carry pressurized fuel, possibly Navy torpedo fuel or one of the high-energy-density rocket propellant fuels being developed by NASA rather than the diesel originally envisioned, to the heater feeding energy through a heat pipe to the penetrator. The tubing will then carry residual exhaust gases out. Local means of propulsion close to the penetrator may prove useful, especially for purposes of steering, although differential heating rates in the tip are expected to be adequate for steering the penetrator. The final placement of the sensors is accomplished by first letting the penetrator head cool and then drilling directly through the penetrator tip, perhaps up to 10 cm, to the desired final location. In contrast to the offset drilling proposed originally, this scheme is more efficient and easier to design and fabricate. A shaped charge to blow the sensor stem through may also be possible.

The final technological conclusions for underground navigational aids are to use both micro-sized ground-penetrating radar (GPR) and micro-sized inclinometers. The change in conops to use a compact coiled-tubing approach, which (1) provides a propulsion force downhole to the penetrator as it melts, (2) delivers surface-ambient cool fuel under pressure to the combustion chamber behind the penetrator head from a surface tank or bladder, and (3) provides comm and power links between the downhole penetrator assembly and the surface equipment and

exfiltration antenna via electrical cabling internal to the tubing, also provides a method to determine depth of penetration simply by sensing periodic insertion length markings on the side of the tubing as it is inserted into the microborehole. Three-axis micro-inclinometers, a by-product of the video gaming industry, carried along with the penetrator assembly would be sampled periodically in coordination with the tubing insertion length readings to determine the downhole penetrator's 3-D orientation. By a simple integration process using both insertion length and orientation measurements, it is possible to determine the exact 3-D underground location of the penetrator relative to the borehole surface geoposition.

The GPR would be used as a look-ahead sensor (1) to determine the presence of significant obstacles or voids to be avoided, (2) to determine the nearness to the ground surface if the AUM is being used to deliver sensors for a monitoring mission external to the targeted UGF in order to terminate the penetration and initiate final emplacement of the sensor (exterior monitoring mission), or (3) to determine the position and thickness of UGF chamber walls or air vents being approached to terminate the penetration and initiate final sensor emplacement (interior penetration mission). We propose that the application specific integrated circuit (ASIC) chip version of the LLNL micropower impulse radar (MIR) be used, as the chip size and 1.5-linear-inch dipole antenna would be consistent with the proposed 10-mm diameter AUM assembly. Five of these chips would be used to form an array of five dipole antennae equi-spaced around the circumference of a section of the AUM assembly away from the hot penetrator tip, slightly tilted to transmit energy not only to the sides of the AUM but also toward the penetrating direction. Such an array configuration would yield a 360-degree view around the AUM in azimuthal resolution increments of 72 degrees. Due to the forward motion of the penetrator, a synthetic aperture processing approach makes it possible to achieve high-resolution along-axis imaging. If the section of the AUM containing the MIR array can be made to slowly rotate as the AUM penetrates, then azimuthal synthetic aperture processing can provide high angular resolution imaging around the AUM as well. The MIR array is anticipated to provide approximately a 1-meter look-ahead (beyond the penetrator tip) capability, depending on how much multipulse integration is performed and the conductivity condition (primarily determined by moisture content) of the material being penetrated. Due to the positioning of the dipole antennae, it will not be possible to radar image directly in front of the penetrator tip, but only in the areas from about 10 degrees and beyond from the AUM centerline. Because ground surfaces and walls cover a wide area, this blind spot directly in front will not be a problem as the ground/air or wall/air boundary will be apparent in the look-ahead imaging available to either side of the AUM centerline.

Although the NRO and CIA were contacted regarding available highly classified wireless data exfiltration comm schemes and devices, none were found to be entirely appropriate for this application. A highly innovative new approach was invented for the data exfiltration component of the AUM based on the use of a retrodirective array implemented as an active integrated antenna. Such antennae combine the antenna patch elements and the active electronics into a single substrate, typically on thin microstrip material. This makes it possible to form thin conformal antenna structures, such as a rock shape, that may be required to camouflage the antenna on the surface. The design of active integrated antenna arrays has been pioneered by Dr. Itoh at UCLA. Data exfiltration is activated only upon receipt of pulses from a friendly radar system, such as that from a JSTARS surveillance radar plane, the future DARPA Discoverer II space-based radar, or other classified national assets that will not be discussed here in order to maintain this report at an unclassified level. Any radar pulse received by the retrodirective antenna array causes a simultaneously transmitted pulse of the same form to be transmitted back only in the direction of the received pulse. A spread-spectrum modulation on top of the return pulse contains the data to be exfiltrated. This exfiltration scheme essentially hides the data in the return radar echoes. It is inherently low probability of intercept (LPI) due to (1) the array directivity in which the strongest return signal energy is only in the direction of the interrogating radar and (2) the use of spread-spectrum modulation that places the data intelligence perhaps 80 dB below the radar pulse signal level. The AUM will exfiltrate both compressed imagery from the GPR and other navigational data regarding the boring progress, and then shift to exfiltrating compressed data from its sensors once they are in position near or inside the UGF.

As a result of the refined concept of operations and technologies identified in this report to create a feasible AUM, we are proposing a $23.5M 6-year new program start for DARPA to fully develop the technology concepts for delivery of a new capability for US armed forces and intelligence agencies for close access characterization of underground facilities. Figure 1 summarizes the six proposed phases of the project, which include a sequence of three specific missions of increasing complexity and approximate costs associated with each phase. This cost does not include the costs for development of specialized sensors that would be carried and emplaced by the AUM. As there are numerous sensor possibilities (image—e.g., low-light-level EO and IR, acoustic—e.g., microphones, thermal, seismic, chemical sniffers, biological agent detectors, nuclear detectors), the sensor or sensors for each of the three missions will need to be determined as part of the requirements planning and the cost of sensor development added to the costs for the AUM development shown in Figure 1. The costs and schedule are first-order estimates, based on preliminary discussions with the sources of the various technologies described in this report, and they will need to be revised and solidified during Phase 0 as a detailed set of program requirements are established.

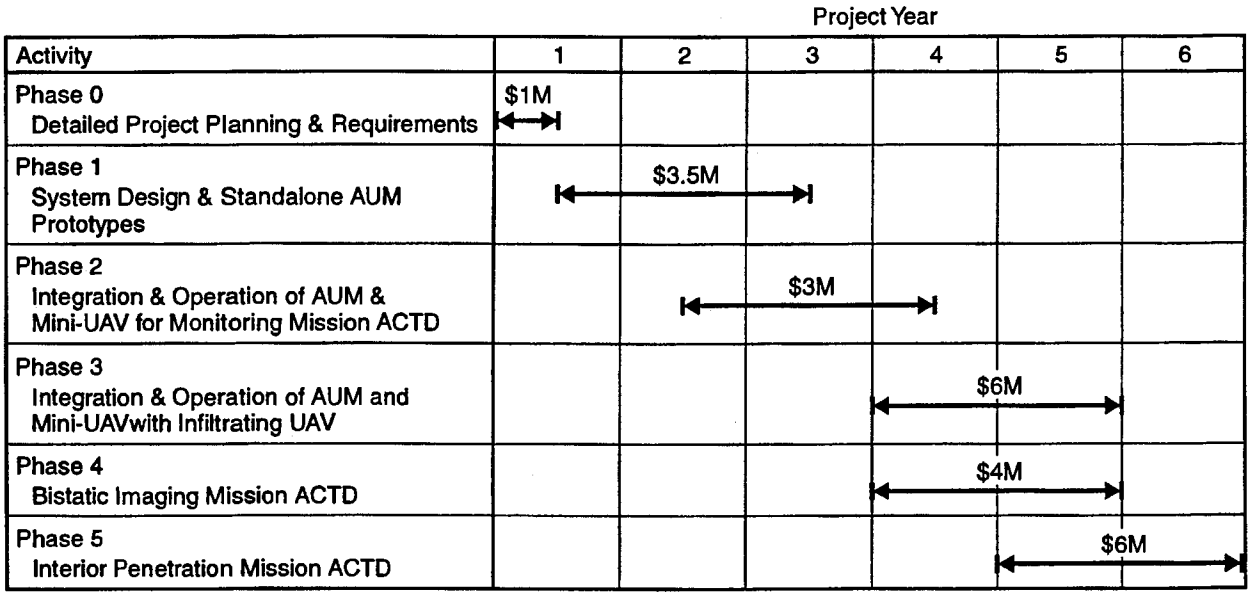

Figure 1. Proposed Program Plan, Schedule, and Projected Costs

Phase 0 will define the entire program plan for the AUM, including test sites and specific sensors to be deployed in addition to the usual program requirements. Preliminary contracts to LANL, LLNL, and UCLA to study critical issues with the rock-melt penetrator technology, the ground-penetration radar technology, and the data exfiltration technology to perform studies or initial experiments are likely needed in order to quantify some requirements for the program. A system engineering contractor will be needed to prepare the program specs and requirements documents. A Phase II SBIR effort with ORINCON could potentially provide about half the estimated costs of the Phase 0 effort. The Phase 0 would conclude with a Broad Area Announcement (BAA) initiating the program and soliciting alternative or supporting technologies to achieve a demonstrable AUM capability. Starting with Phase 1 and beyond, a system integrator would be added to the picture. Phase I would develop the critical nonflight portions of the AUM and more detailed system design, concentrating on the key penetrator technology and its navigation. The objective of Phase 1 would be the accurate penetration of a few hundred meters from a static insertion point to validate the rock-melting approach and the ability to accurately reach a target location. Phase 2 would be the first phase in which a specific mission capability would be demonstrated, namely the external monitoring mission. The objective of this phase is the integration of the AUM assembly with the mini-UAV and short flights to the surface followed by autonomous penetration to positions near adits of UGFs at the test site.

Beginning with Phase 3, the mini-UAV would be integrated with either a Predator or Global Hawk to perform a full mission as envisioned by the concept of operations cited in this report. The Predator or Global Hawk would carry the mini-UAV under its wings and would have as its objective the demonstration of these larger UAVs to infiltrate a denied area (the test range). Radar and other observables measured during the test will help determine how stealthy the

placement of an AUM can be made. Phase 4 would add further mission capabilities to the overall system, specifically a bistatic imaging demonstration with either the GPR on the AUM working in conjunction with surface-based UGS or ELF waves generated by the HAARP array in Alaska and intercepted by the ELF antenna along the AUM coiled tubing stem, or perhaps both techniques. Finally, Phase 5 would have as its objective the demonstration of the most complex mission envisioned: actual penetration of the interior walls of an underground sensor. This will require refinements/improvements in the navigational sensors and the positioning accuracy of the AUM. This last demonstration would also entail the longest microboring distance: over 1 km!

2.0 THE UNDERGROUND FACILITY ACCESS PROBLEM

There is increasing evidence from aircraft and satellite imagery of denied geographical areas that significant activities related to weapons of mass destruction (WMD) (specifically nuclear, biological, and chemical weapons) and command, control, and communications (C^3) are being placed into deeply buried and hardened underground facilities (UGF) accessible only by tunnel. Figure 2 is an artist's rendering of overhead imagery of one such facility near Tarhunah, Libya, suspected to be an underground chemical plant. The increasing use of such facilities stems apparently from lessons learned by nations observing the success of US intelligence assets and precision munitions during the Persian Gulf War when facilities are at or close to the surface. As the recent nuclear tests in India and Pakistan illustrate, underground facilities also deny surveillance by current remote sensors. It is conjectured, based on the number of known UGFs, that there are likely 500 or more suspected UGF sites, many yet undiscovered. While tipoff due to construction or visible tunnel entrances may help detect the existence of an underground facility, underground facilities such as that shown in Figure 2 are probably immune from characterization by existing remote surveillance systems that cannot penetrate the deep ground cover that can be hundreds of feet deep. UGFs are also probably survivable from use of precision munitions as employed in the Gulf War due also to the deep ground cover and the use of multiple blast doors at the tunnel entrances. Figure 3 depicts a prototypical underground facility and the difficulties to gain entry or to place weapons for destruction. Some nations have underground facilities in urban areas, such as that depicted in Figure 4, which are entered via normal building entrances or through public facilities such as subways. It appears that the only way to get close access function characterization and physical characterization of deep UGFs is to place, by stealthy means, sensors close to or inside the facility. This requires a fundamentally new approach to the UGF characterization and surveillance problem.

There are six operational steps in dealing with the underground facilities problem: (1) tip-off, (2) detection, (3) characterization remotely, (4) characterization by close access (interior or within the perimeter), (5) defeat/neutralization, and (6) post-defeat/neutralization assessment. The first four are part of the normal intelligence collection efforts against UGFS, whereas the last two are performed only in the event of hostilities. Tip-off is the analysis of correlative activity that would suggest the possibility of an underground facility, such as excavation tunnels or observed traffic of empty trucks coming from a site where there is no apparent stockpiling of material. Detection is the determination that a facility actually exists at a specific location, such as tunnel entrances observed in aerial imagery. Remote characterization is the determination of the purpose of the

Figure 2. Artist Rendering from Actual Aerial Imagery of Suspected Underground Chemical Plant Near Tarhunah, Libya. Note the three tunnel entrances that are sufficiently large for trucks to enter.

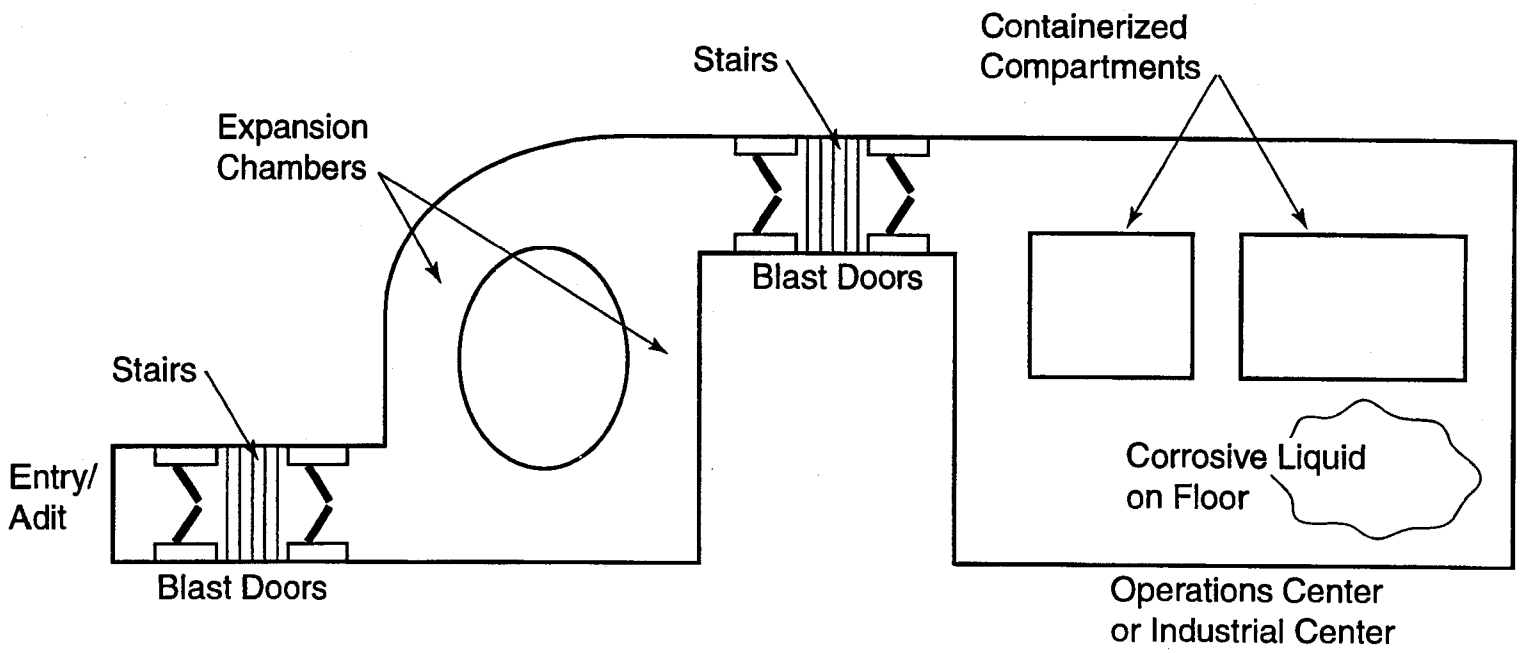

Figure 3. Prototypical Underground Facility System Layout, Overhead View

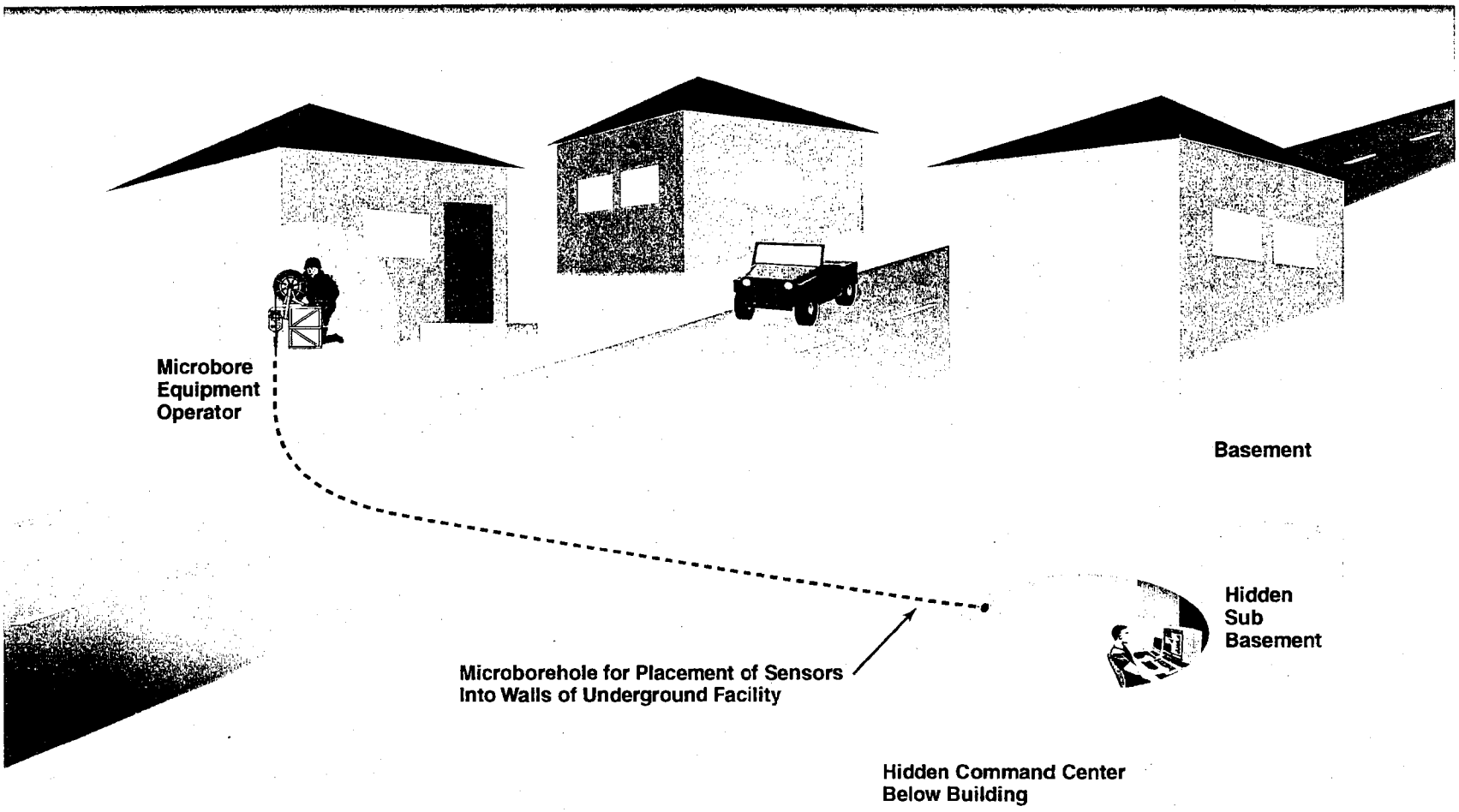

Figure 4. Depiction of Surveillance Situation for Subterranean Facility in Urban Setting

UGF by fusing remote ground, air, and space sensor data of external observables. This could be electro-optical imagery, infrared imagery, radar imagery, and acoustic array data. Typically, remote characterization is inadequate, especially if observables denial is practiced by the state operating the facility. This was the case in the recent Indian and Pakistani nuclear tests. Close access characterization, the focus of this report, provides access technology to place sensors close to or into the UGF to make a firm characterization. The defeat/neutralization (D/N) operation is a covert special operations or overt military action (e.g., airstrike) to deny the functional use of the facility. Having close access sensors near or into the UGF after a D/N operation is needed to validate the destruction or nonoperational status of an attacked UGF.

The types of surveillance requirements, or underground intelligence (UGINT), for the characterization of UGFs include: (1) construction practices, (2) mission of the UGF (manufacturing nuclear weapons?, storing chemical munitions?, etc.), (3) functional operations (how is the facility used?, is it a command center?, etc.), (4) infrastructure, meaning the layout, operations, power source(s), fuel source(s), cooling, ventilation, and communications nodes, (5) failure point locations (i.e., UGF vulnerabilities), (6) means of functional defeat without destruction (cut the power line by special operations?, blow out a door?, drop a guided munition down an air shaft?, etc.), and (6) post-strike damage assessment if destructive force is used. All of these requirements can be satisfied by the AUM device proposed in this report for delivery of sensors that can address all the characterization issues with long-term monitoring. DSWA has been funding the DOE national labs to develop air-dropped sensors shaped like stakes that use the kinetic energy of the free fall to implant themselves into the ground, typically in advance of an airstrike operation. These sensors are short-lived, are not stealthily or precision emplaced, and are not able to penetrate deeply, in contrast to the autonomous microborer approach, which is long-lived, stealthy, precision emplaced, and able to go deep.

3.0 CONCEPTS OF OPERATION

The autonomous underground microborer (AUM) collection system is envisioned as perhaps the most stealthy and unexpected approach to placing sensor assets for close access to or within denied UGFs. The AUM is a more realistic and feasible approach to accessing UGFs than alternative proposals to DARPA TTO to utilize very small robots that can hitch-hike on vehicles of opportunity traveling to or through a UGF adit, or that can navigate internal to conduits or air intake/exhaust vents accessible at ground level, in order to deliver sensor assets very close to or inside hard targets. However, in order to remain stealthy, the robots will likely have to be of insect size and scale, which limits the amount of power for mobility and sensor data acquisition, limits the operational lifetime, and makes it more difficult to overcome large physical obstacles in the path. As shown in Figure 3, steps, doors, and corrosive liquids on the floor are but some of the many obstacles that a robotic device would have to overcome. Furthermore, robots able to get inside a UGF will need some method to exfiltrate the surveilled data out from the UGF. Communication antennae and electronics with sufficient gain to transmit to satellite or loitering aircraft will be too large and power consuming to fit on an ultraminiature robot. In contrast, the autonomous underground microborer can make its own path to any targeted point for sensing and will have larger power and volume capability for carrying surveillance and data exfiltration comm electronics.

To get the AUM or microrobots close to a denied area UGF, it is proposed to use a combination of an available unmanned air vehicle (UAV) with a launchable para-wing mini-UAV that contains the AUM or robot payload. The large UAV would penetrate the denied territory and launch the mini-UAV with sensor payload at a target standoff where it is not likely to be detected, perhaps several miles from the sensor placement point. The mini-UAV, which is much quieter (using an electrically powered prop), would precision land, under GPS control, the sensor payload at an even closer location to the target UGF, perhaps 1 km from a UGF entry or vent. The infiltrating, payload-carrying UAVs currently in the inventory are the General Atomics Predator, the Teledyne-Ryan Global Hawk, and the Lockheed-Martin DarkStar. The Predator already has wing points for mounting wing-carried payload. The Global Hawk wings have the capability to carry payload, but wing mounts are not on the first or second factory units. DarkStar is designed to be a stealth UAV, so will not have wing mounts, and is also unlikely to be able to open the payload doors in flight to launch a secondary mini-UAV. Table 1 provides some of the key characteristics of the three UAVs. Of particular interest are: Predator medium altitude endurance (MAE) UAV has an operating altitude of 15,000 ft and range of 500 nm and payload capacity of 450 pounds with communication links of LOC (20 MHz), MILSATCOM (4.8 kbps), and SATCOM (1.544 Mbps); Global Hawk high-altitude endurance (HAE) UAV has an

Table 1. Key Attributes of Three UAVs as Possible Delivery Vehicles for the Autonomous Microborer



	Characteristics		Tier II MAE UAV Predator		Tier II+, CONV, HAE UAV Global Hawk		Tier III-, LO HAE UAV Darkstar	
Operational	Altitude:	Maximum (km, ft)	7.6 km	25,000 ft	19.8 km	65,00 ft	>13.7 km	>45,000 ft
		Operating (km, ft)	4.6 km	15,000 ft	15.2-19.8 km	50,000-65,000 ft	>13.7 km	>45,000 ft
	Endurance (Max):	(hrs)	>20 hours		>40 hrs (24 hrs at 5,556 km/3,000 nm)		>8 hours (at 926 km/500 nm)	
	Radius of Action:	(km, nm)	926 km	500 nm	5,556 km	3,000 nm	>926 km	>500 nm
	Speed:	Maximum (km/hr, kts)	204-215 km/hr	110-115 kts	>639 km/hr	>345 kts	>463 km/hr	>250 kts
		Cruise (km/hr, kts)	120-130 km/hr	65-70 kts	639 km/hr	345 kts	>463 km/hr	>250 kts
		Loiter (km/hr, kts)	111-120 km/hr	60-65 kts	630 km/hr	340 kts	>463 km/hr	>250 kts
	Climb Rate (Max):	(m/min, fpm)	168 m/min	550 fpm	1,036 m/min	3,400 fpm	610 m/min	2,000 fpm
	Deployment Needs:* *Depends on equipment & duration		Multiple* C-130 sorties		AV: Self-Deployable GS: Multiple* C-141, C-17, or C-5 sorties		Multiple* C-141, C-17, or C-5 sorties	
Air Vehicle	Propulsion:	Engine(s)	One Fuel-Injected Recip; 4-stroke		One Turbofan		One Turbofan	
		– Maker	– Rotax 912/Rotax 914		– Allison AE3007H		– Williams FJ44-1A	
		– Rating	63.4/75.8 kw	85/105 hp	32 kN	7,050 lb static thrust	8.45 kN	1,900 lb static thrust
		– Fuel	AVGAS (100 Octane)		Heavy Fuel (JP-8)		Heavy Fuel (JP-8)	
		– Capacity (L, gal)	409 L	108 gal	8,176 L	2,160 gal	1,575 L	416 gal
	Weight:	Empty (kg, lb)	544 kg	1,200 lb	4,055 kg	8,940 lb	1,978 kg	4,360 lb
		Fuel Weight (kg, lb)	295 kg	650 lb	6,668 kg	14,700 lb	1,470 kg	3,240 lb
		Payload (kg, lb)	204 kg	450 lb	889 kg	1,960 lb	454 kg	1,000 lb
		Max Takeoff (kg, lb)	1,043 kg	2,300 lb	11,612 kg	25,600 lb	3,901 kg	8,600 lb
	Dimensions:	Wingspan (m, ft)	14.8 m	48.7 ft	35.4 m	116.2 ft	21.0 m	69 ft
		Length (m, ft)	8.1 m	26.7 ft	13.5 m	44.4 ft	4.6 m	15 ft
		Height (m, ft)	2.2 m	7.3 ft	4.6 m	15.2 ft	1.5 m	5 ft
	Avionics:	Transponder	Mode IIIC IFF		Mode I/II/IIIC/IV IFF		Mode IIIC IFF	
		Navigation	GPS and INS		GPS and INS		GPS and INS	
	Launch & Recovery:		Runway (760 m/2,500 ft)		Runway (1,524 m/5,000 ft)		Runway (<1,219 m/<4,000 ft)	
	Guidance & Control:		Prepgmd/Remote Control/Autonomous		Preprogrammed/Autonomous		Preprogrammed/Autonomous	
Payload and Links	Sensor(s):		EO,IR, and SAR		EO, IR, and SAR		EO or SAR	
	Data Link(s): Type		C-band/LOS; UHF/MILSATCOM; Ku-band/SATCOM		Ku-band/SATCOM; X-Band CDL/LOS		Ku-band/SATCOM; X-Band CDL/LOS	
	Bandwidth:	(Hz)	C-band/LOS: 20 MHz UHF/MILSATCOM: 25 kHz Ku-band/SATCOM: 5 MHz		UHF/MILSATCOM: 25 kHz Ku-band/SATCOM: 2.2-72 MHz X-band CDL/LOS: 10-120 MHz		UHF/SATCOM: 25 kHz Ku-band/SATCOM: 2.2 MHz X-band CDL/LOS: 10-60 MHz	
	Data Rate:	(bps)	C-band/LOS: 20 MHz Analog UHF/MILSATCOM: 4.8 kbps Ku-band/SATCOM: 1.544 Mbps		UHF/MILSATCOM: 19.2 kbps Ku-band/SATCOM: 1.5-50 Mbps X-band CDL/LOS: 274 Mbps		UHF/SATCOM: 19.2 kbps Ku-band/SATCOM: 1.5 Mbps X-band CDL/LOS: 137 Mbps	
	C2 Link(s):		UHF/MILSATCOM		UHF/MILSATCOM; Ku-band/SATCOM; UHF/LOS; X-band CDL/LOS		UHF/MILSATCOM; Ku-band/SATCOM; UHF/LOS; X-band CDL/LOS	
System and Support	System Composition:		4 AVs, 1 GCS, 1 Trojan Spirit II Dissemination System, GSE		AVs (TBD); HAE CGS		AVs (TBD); HAE CGS	
	Prime/Key Contractor(s):		General Atomics-Aeronautical Systems		Teledyne Ryan Aeronautical		Lockheed Martin Skunk Works/ Boeing Military Aircraft Division	
	Major Subcontractors: –Air Vehicle, Propulsion, Avionics, Payloads, Information Processing, Communications, Ground and Support Systems		Boeing Defense & Space; Litton; LMTCS (Ku-band SATCOM); Magnavox/Carlyle Gp; Northrop Grumman (SAR); Rotax Cp; Versatron Cp		Allison Engine/Rolls Royce; Raytheon E-Systems; GDE Systems/Tracor; Héroux; Hughes Aircraft; Lockheed Martin Wideband Systems; Rockwell International; Aurora Flight Sciences		ABS Cp; Adv. Composites; Aydin Vector; CI Fiberite; Hexcel; Honeywell Avionics; Litton G&C; Lockheed Martin Wideband Sys; Recon/Optical; Rockwell Collins; Rosemount Aerospace; Northrop Grumman; Williams Int'l	

Legend:

ADR: Air Data Relay
A-Gear: Arresting Gear
AV: Air Vehicle
AVGAS: Aviation Gasoline
CDL: Common Data Link
CGS: Common Ground Segment
EO: Electro-Optical
FLIR: Forward-Looking Infrared
GCS: Ground Control Station
GPS: Global Positioning System
GSE: Ground Support Equipment
HAE: High Altitude Endurance
IFF: Identification Friend or Foe
INS: Inertial Navigation System
IR: Infrared
JP: Jet Petroleum
KHz: Kilohertz
LHA: Landing Helicopter Amphibious
LHD: Landing Helicopter Dock
LOS: Line of Sight
LPD: Landing Platform Dock
LRE: Launch & Recovery System
MAE: Medium Altitude Endurance
MHz: Megahertz
MMF: Mobile Maintenance Facility
MMP: Modular Mission Payloa
MOGAS: Mobility Gasoline
MOSP: Multi-mission Optronic Stabilized Payload
MPS: Mission Planning Station
PCS: Portable Control Station
RATO: Rocket-Assisted Takeo
RRS: Remote Receiving Statio
RVT: Remote Video Terminal
SATCOM: Satellite Communications (Military)
TML: Truck-Mounted Launcher
UHF: Ultra High Frequency

operating altitude of 65000 ft and range of 3000 nm and payload capacity of 1960 pounds with LOC (274 Mbps) and two SATCOM (19.2 kbps and 1.5-50 Mbps) comm links; DarkStar low observable (LO) HAE UAV has an operating altitude of >45000 ft, a range >500 nm, a payload capacity of 1000 pounds, and LOS (37 Mbps), and several SATCOM (19.2 kbps and 1.5 Mbps) comm links. Because the Predator has the smallest payload capability and would likely be the UAV most available for testing the concept of operations to be described, the 450- pound payload capability becomes a driving design factor in the operational concept. Assuming approximately 250 pounds for the mini-UAV, this leaves approximately 200 pounds for the AUM or robots.

A longer term possibility for delivery of the AUM into denied areas is the Boeing-North American unmanned space vehicle (USV) (a small reusable mini-spaceplane) that becomes the reusable upper stage of a launch system that is carried to hypersonic speeds by a larger aircraft or is ground launched. The payload capability will be in the 1200- to 2000-pound range in a bay 4 ft in diameter by 7 ft long. Figure 5 is a Boeing-North American-produced viewgraph showing another type of payload being considered for the USV as a suborbital delivery of munitions for a precision strike. A scaled version was rolled out in November 1997 for a test program that will run seven years.

Figure 6 illustrates the deployment steps expected of the mini-UAV, which should have a low radar cross-section and low acoustic levels. One company, Omega Aerospace of Everett, Washington, has a paragliding UAV called the Tactical Unmanned Surveillance Aircraft (TUSA) vehicle that could potentially satisfy the mini-UAV requirements. Such a mini-UAV would be dropped from the larger delivering UAV (Predator or Global Hawk) toward the target UGF area at an appropriate standoff distance and altitude to prevent detection. A likely scenario is a drop at an altitude of 1000 feet with a standoff of 10 to 20 miles from the target for final delivery of the penetrator and exfiltration antenna under precision GPS or terrain mapping correlation to a preplanned penetration site that is within one km or two from the desired sensor location, as depicted in Figure 6. The penetration site is selected to be a ravine, forested area, or other terrain feature that will serve to hide its presence, yet be as close as possible to the final sensor placement location consistent with not being detected. Delivery will likely occur at night to minimize visibility. The paragliding TUSA is not only very quiet, but also takes only a very short distance of a few feet to land and take off (minimizing the terrain impact due to its presence), and its parasail deflates on landing to minimize its visible cross-section.

In order to remain covert, the AUM upon deployment from the mini-UAV should keep its deployment time to a minimum while entering the ground, should not generate visible, seismic,

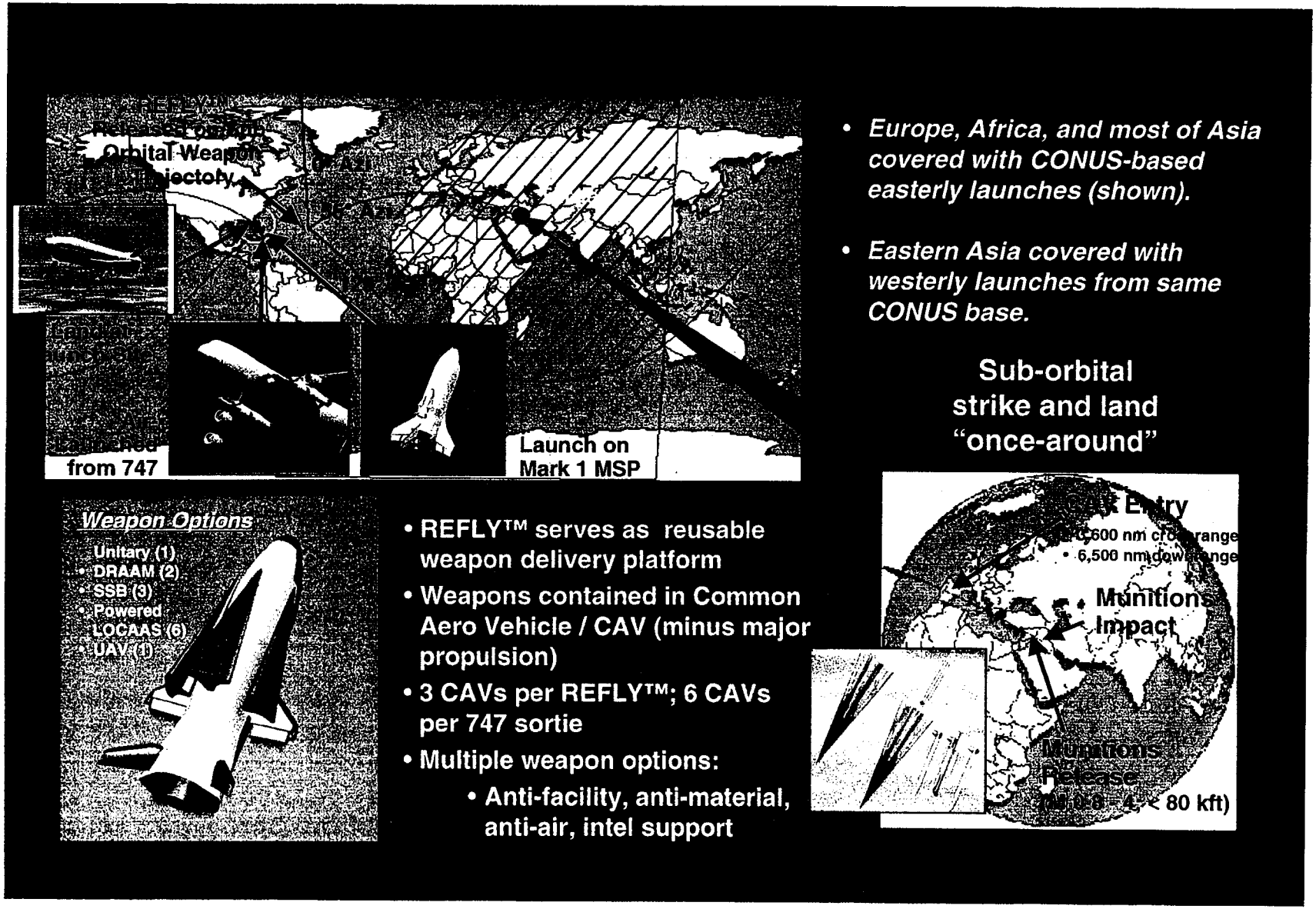

Figure 5. Illustration of Boeing North American Mini Space UAV for Delivery of Fast Reaction Precision Strike. Same capability could be used to deliver an AUM to a designated site from space (figure courtesy of Boeing North American).

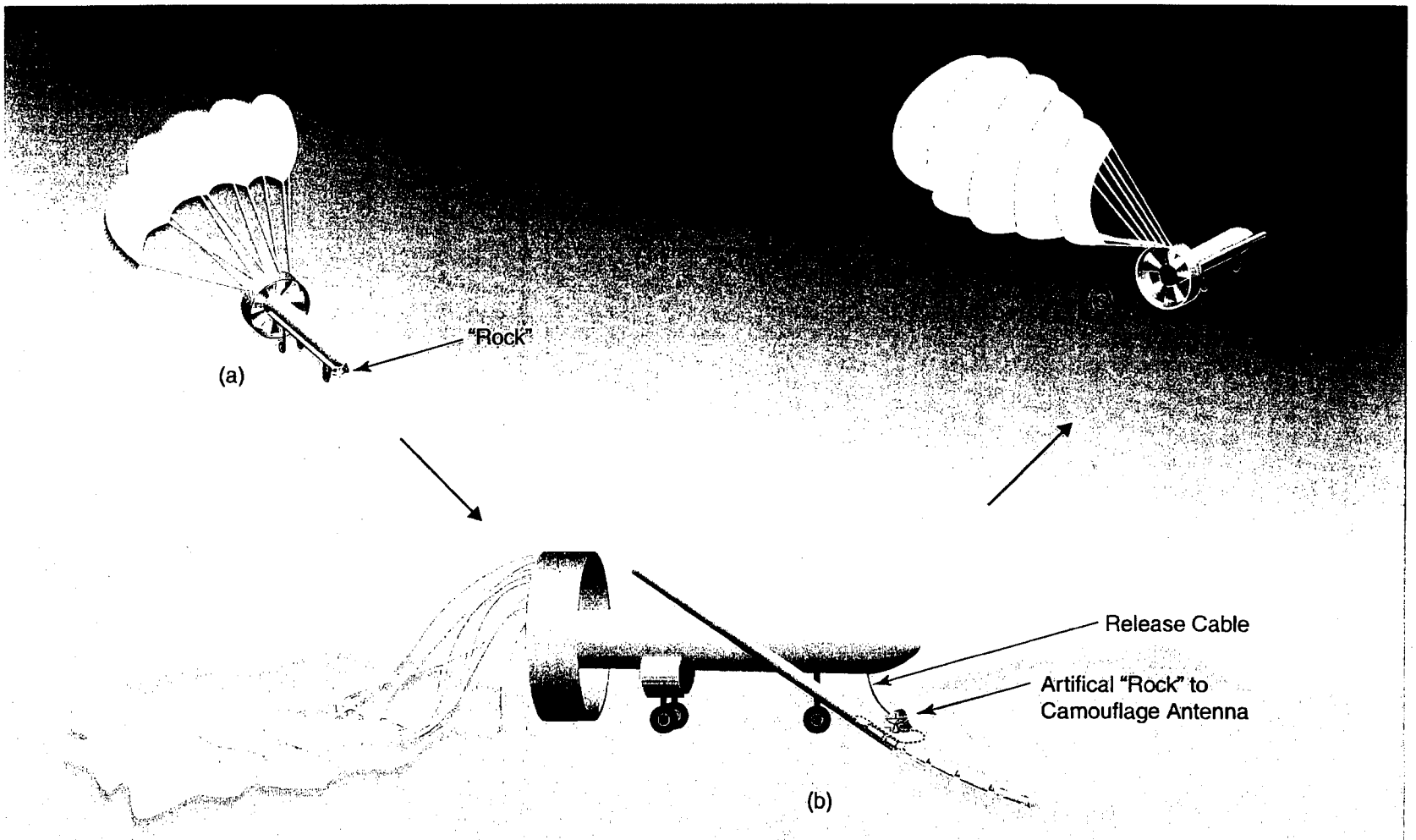

Figure 6. Deployment of Penetrator and Camouflaged Exfiltrating Antenna to Insertion Target Point. (a) Para-wing daughter UAV brings penetrator and antenna quietly to the surface. (b) The insertion tube tilts and penetration begins; antenna is deployed adjacent to insertion hole. (c) After deployment, daughter UAV quietly leaves ground, leaving only the concealed antenna on the surface.

or acoustic signatures that can be detected while penetrating, and should deploy microsensors to minimize their visual detectability, once positioned by the AUM at the final sensor location. Covert low probability of intercept (LPI) communication schemes should also be used to minimize the detectability of exfiltrated surveillance data. The AUM should be able to deploy voice-activated acoustic sensors, radiation sensors, chemical and biological sniffers, low-light-level EO and IR imaging sensors, and sensors that can detect items that have been covertly tagged (for example, a magnetic stripe on a crate that indicates a piece of equipment built in Germany is being delivered to a UGF in Libya).

Figures 7, 8, and 9 illustrate three concepts of operations with microrobots that utilize the dual large/mini UAV delivery scheme to stealthily place the energy-limited microrobots within a short distance of an underground facility. In Figure 7, the large UAV (Predator shown) drops the mini-UAV carrying the microrobots at a standoff range from the UGF. The mini-UAV flies quietly closer to the UGF and lands in a covered position 1 km or less from the targeted sensor placement points. The microrobots are deployed from the mini-UAV, and attempt entry through air-intake or exhaust vents associated with the UGF or, if under construction, might even attempt entry through the tunnels to assess the internal structure by imagery collection. The microrobots then make their way back to the mini-UAV, where the collected data is transferred to the UAV comm equipment, where it is then exfiltrated out by communication with a passing SATCOM or loitering UAV (perhaps the one that dropped the mini-UAV in the first place). Once the robots are recovered, the mini-UAV takes off and self-destructs a few kilometers away in a forested or body-of-water terrain area to leave no trace of the activity except the possibility of a few feet of tire tracks on the surface at the mini-UAV landing site. Having the one-time-use mini-UAV self-destruct simplifies the UAV design because it reduces its size and complexity by not having to structure a design with long flight distance in order to recover it.

Figure 8 presents an alternative robots-delivered-by-UAV concept of operations. This scenario can use the technology developed under a separate DARPA 1997 SBIR topic for a robotic hitch-hiker. Here the idea is for the microrobot, which might look like road kill, to place itself after deployment from the mini-UAV, in the middle of a road that leads to the UGF. The robot would attach itself to a passing vehicle like a truck, unattach at the site, take sensor data, reattach to the vehicle, ride the vehicle out of the UGF area, detach itself at the right place for ambling back to the mini-UAV, pass the data it collected to the mini-UAV comm equipment that would exfiltrate the data out of the area as previously described.

Figure 9 presents yet another robot-delivered-by-UAV concept of operations. In this scenario, a long-term monitoring mission is envisioned in which a larger robot capable of burrowing its

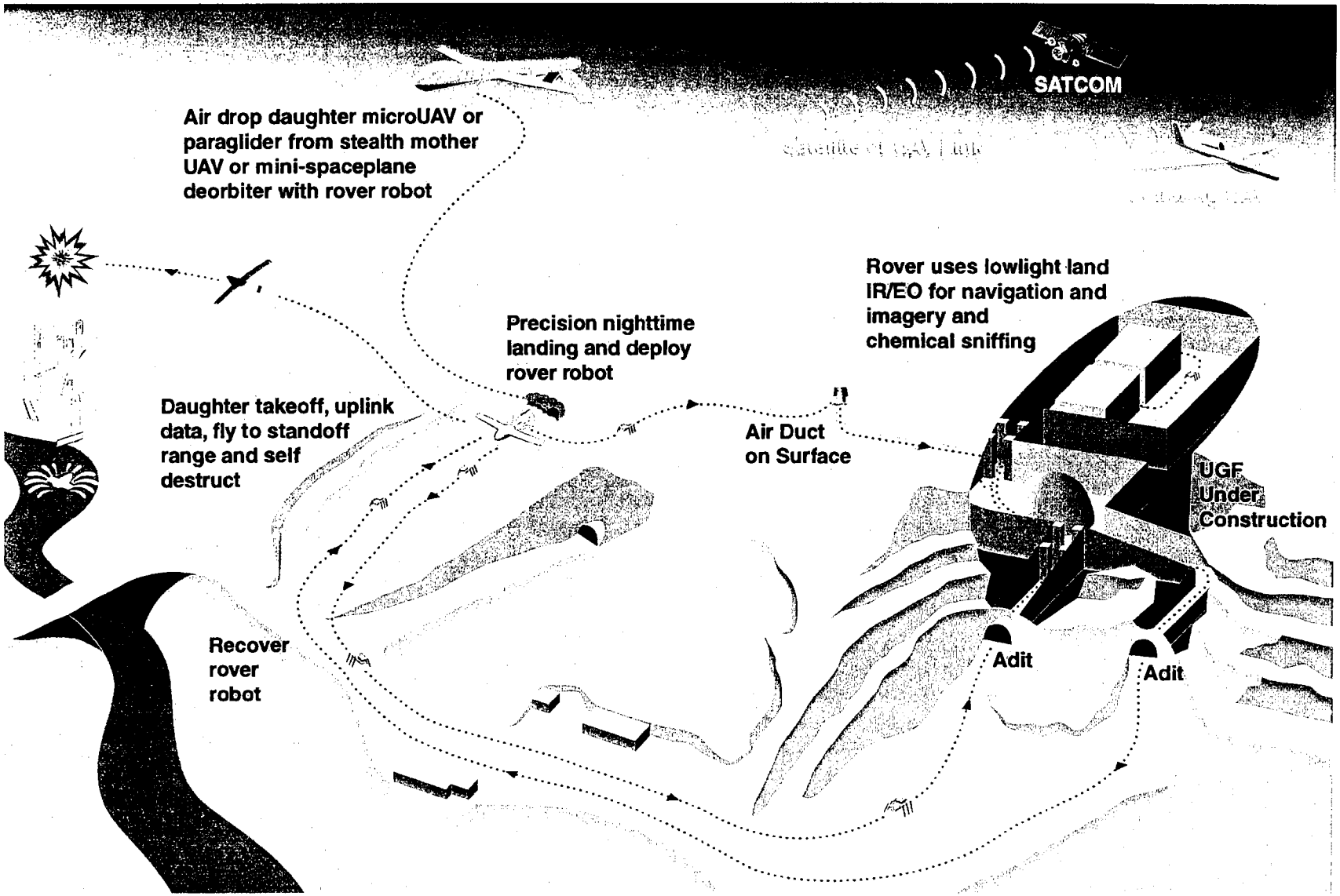

Figure 7. Underground Facility Close Access Characterization Concept Of Operation: Roving Robot Infiltration

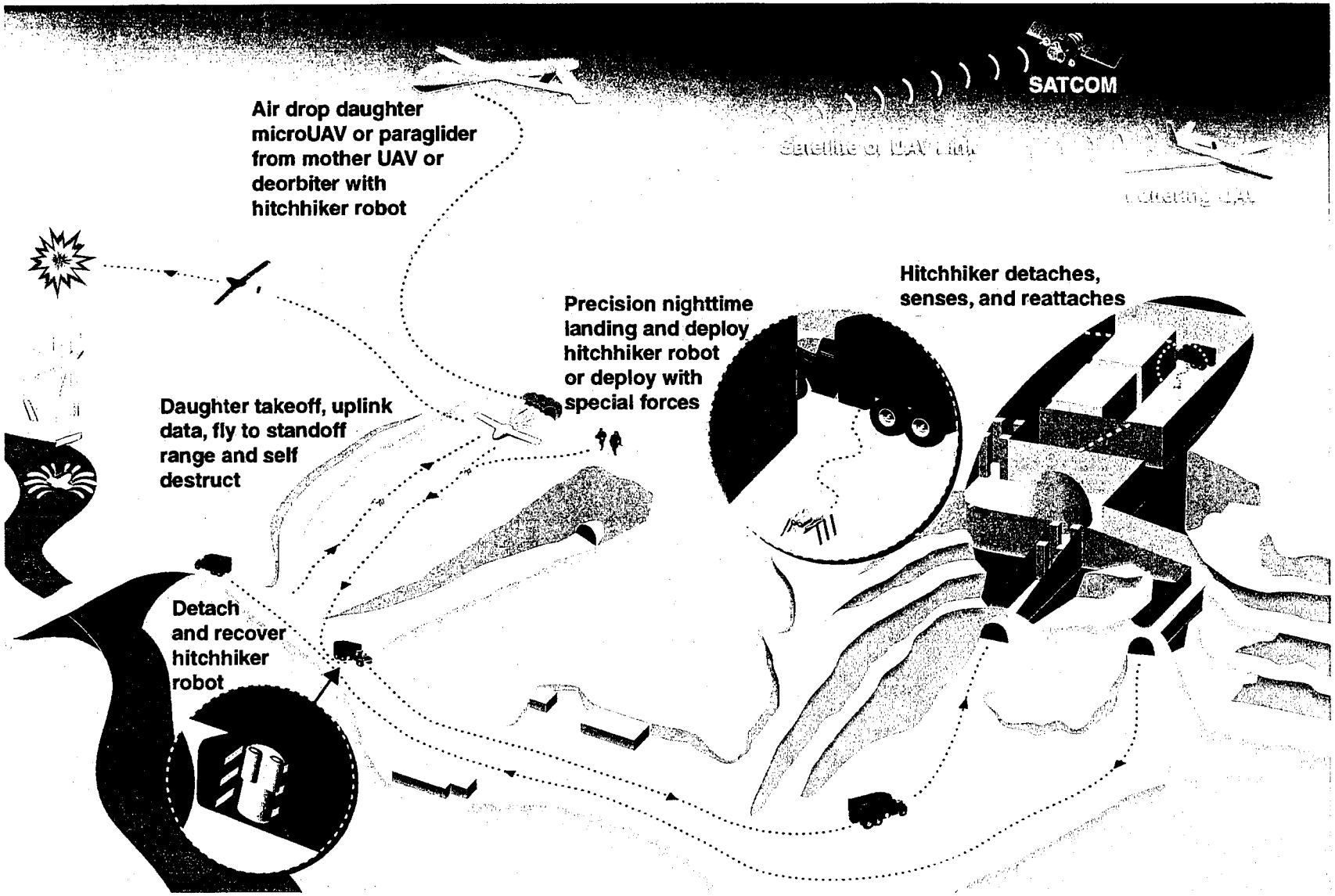

Figure 8. Underground Facility Close Access Characterization Concept Of Operation: Hitch-Hiking Robot Infiltration

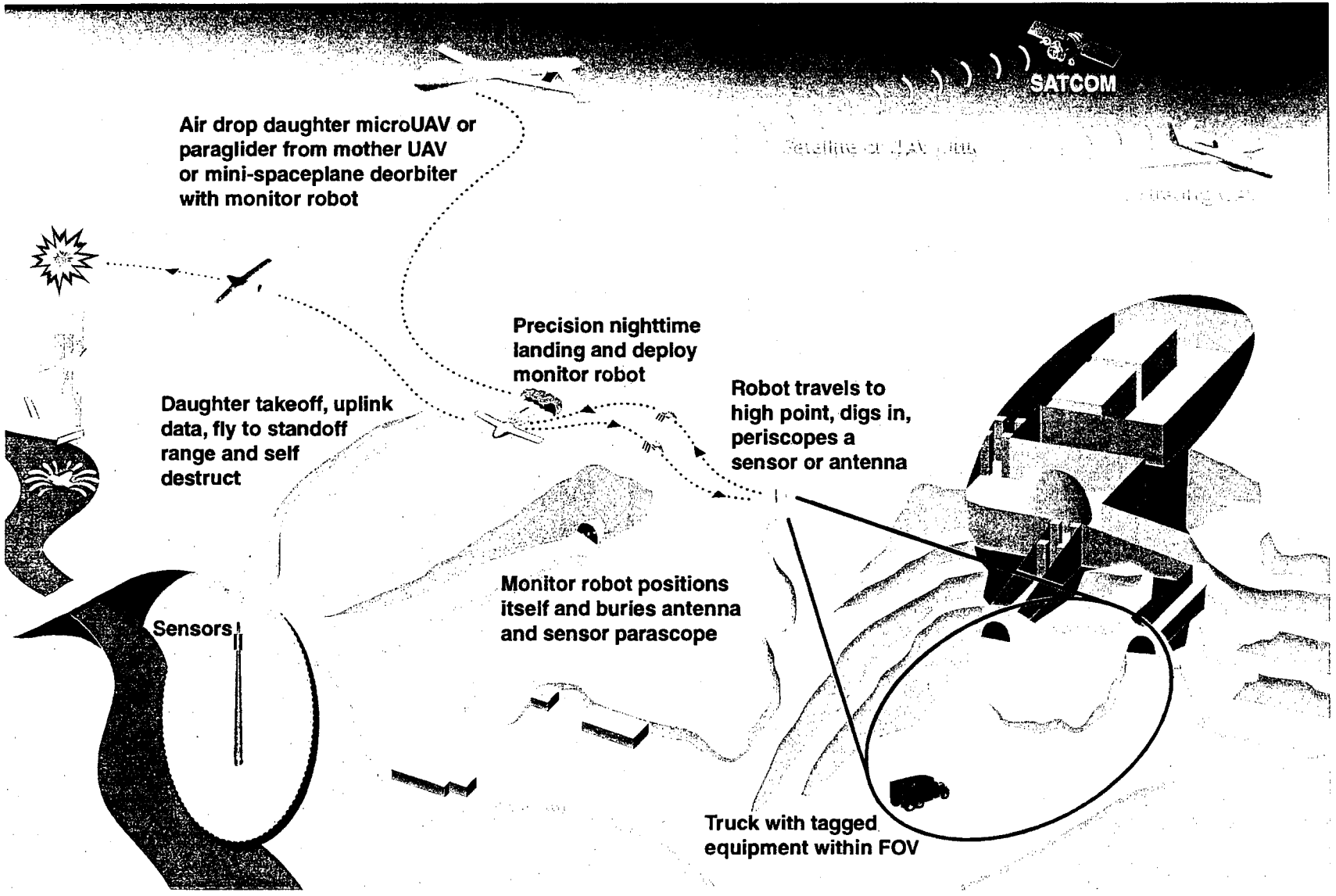

Figure 9. Underground Facility Close Access Characterization Concept of Operation: Continuous Entry Monitoring

entire mass just below ground is deployed from the mini-UAV. The mini-UAV would immediately depart after deployment and would fly away to self-destruct. The burrowing robot would place itself in a position to place sensor up through the ground on a slim periscoping stem to minimize detection (perhaps only periscoping up at night). The stem also serves as an antenna for more conventional spread-spectrum LPI comm link to exfiltrate the sensor data out from the site. The robot must carry sufficient battery power to run the sensors and comm link for long-term monitoring (typically several weeks or months).

3.1 Close Access Long-Duration Perimeter Monitoring

In most stealthy insertions of a sensor package to an operational UGF, it will not be possible to use surface-based robots that can be seen, nor will it likely be possible to land the mini-UAV in such close proximity to the UGF. A standoff landing of 0.5 to 2 km will probably be required in most conops in order to remain undetected. This means that the sensors will need to be moved underground a distance of 0.5 to 2 km in order to position them close to the entrances of a UGF for long-term monitoring about the UGF entrance perimeter. The autonomous underground microborer (AUM) is the proposed device to accomplish this.

Deployment. After landing the AUM to the surface via the large/mini-UAV conops, the original Phase I SBIR proposal had attached a tube containing the penetrator assembly to the mini-UAV, as indicated in Figure 6 (b). On the other side is a communication antenna concealed in a culturally blending form, such as a rock shape with color indigenous to the target area or a plant indigenous to the area. If there is sufficient payload capability, a second AUM could be carried by the mini-UAV so that two penetrations could be attempted with one landing of the mini-UAV. This would provide higher assurance of intelligence collection from the UGF site. In the updated scenario, the mini-UAV would not have straight launching tubes, but would use a coil-tube drill stem approach to inserting the AUM into the ground.

Emplacement. Once on the surface, the original Phase I SBIR proposal had the mini-UAV stay only long enough for the penetrator to fully enter the ground and the camouflaged antenna to move over the borehole (a few hours). After deployment of the penetrator, the UAV would take off and self-destruct over terrain that can hide its presence, such as a lake, river, deep forest, or difficult-to-access terrain. The penetrator would then advance another km or so to the target point. Alternatively, if the mini-UAV landing spot is close enough to be the observation point for the monitoring, then a simple one-step shallow microboring followed by sensor insertion could be performed while the mini-UAV stays on the ground, as illustrated in Figure 10. When the UAV departed the scene, it would then be able to take the penetrator assembly along with it for self-destruction. If the landing site is well concealed and 1 or 2 km from the targeted sensor

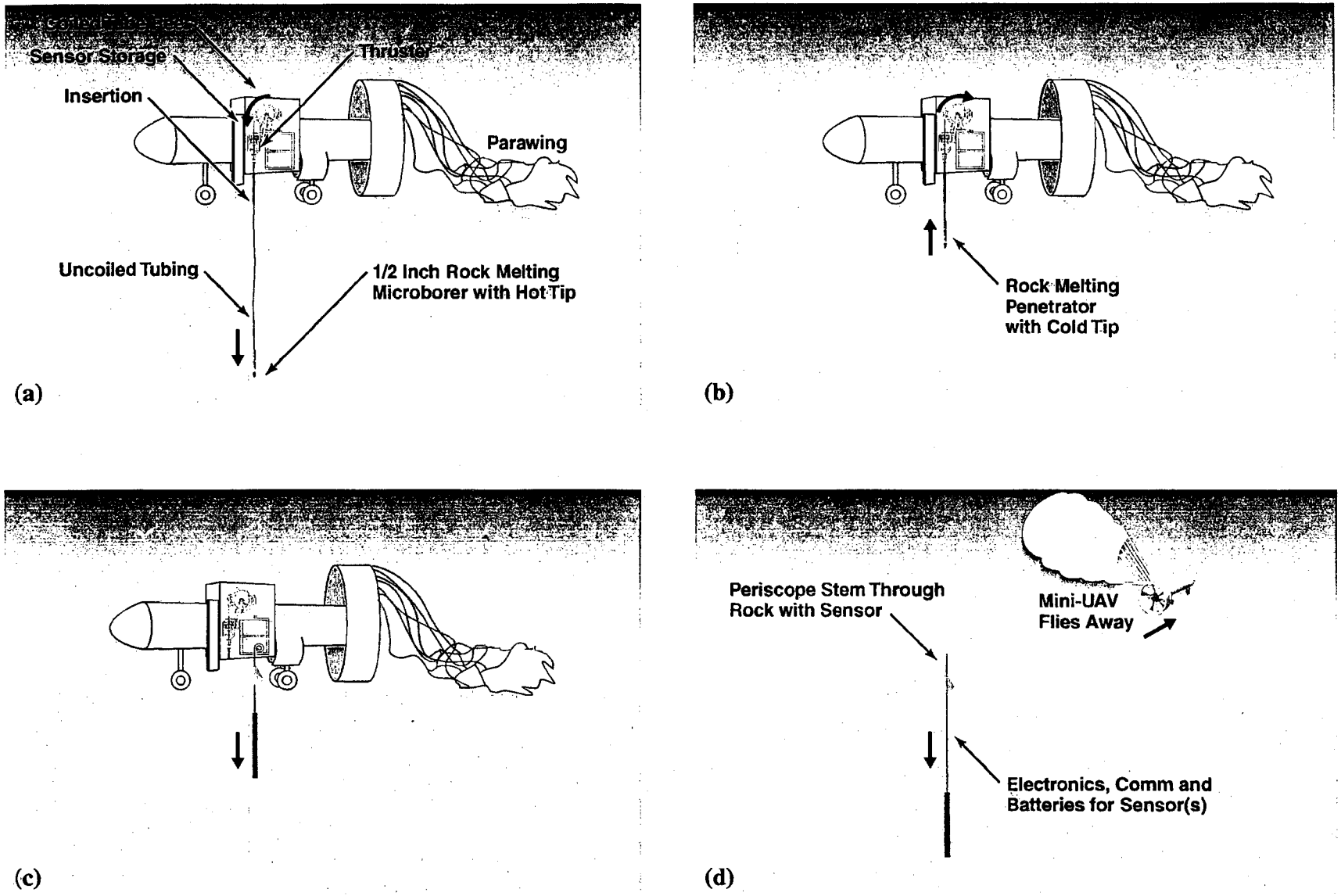

Figure 10. Details of Sensor Emplacement for Continuous Entry Monitoring using Least Complex Microboring Scenario. (a) Microbore a few feet. (b)Withdraw microborer. (c) Insert sensor stem. (d) Cover with exfiltration "rock."

location, another scenario is to have the mini-UAV serve as a surface-base for the microboring, which permits some borehole equipment to stay with the UAV (e.g., a reel of coiled tubing, an insertion device, and a fuel bladder) and a simplified downhole penetrator of smaller diameter to be designed. Once the microboring is finished (one or two days), then the mini-UAV would take the surface-based microboring equipment, leaving only the camouflaged antenna or just a small borehole (as though made by snake or rodent) if the UAV had already relayed the surveilled sensor data, and self-destruct. Figure 11 shows the overall conops approach. The field of view (FOV) for the conops presented in Figure 10 corresponds to the one marked as A in Figure 11.

Insertion. In the original Phase I proposal, upon landing, the penetrator was envisioned to be deployed from an insertion tube on the side of the mini-UAV that tilts to bring it into contact with the ground surface. The penetrator is activated and propulsion mechanisms within the tube, perhaps as simple as a spring, force the penetrator into the ground until the penetrator self-propulsion mechanism can engage the borehole sides that it has created, as illustrated in Figure 6(b). The camouflaged antenna is dropped to the surface from the opposite side of the UAV adjacent to the borehole. Once the entire penetrator has entered the borehole, a tether on the rear end of the penetrator assembly pulls the camouflaged antenna object over the borehole, and then breaks at a certain tension level to disengage from the penetrator. This covers the borehole. The penetrator assembly in our original concept consisted of an articulated linkage of nonmetallic cylinders (nonmetallic composite material to minimize detection by electromagnetic or acoustic means), each about 10 to 15 inches in length, as illustrated in Figure 12. The lead cylinder would have the rock-melting penetrator tip and the propulsion mechanism, as illustrated in Figure 13. This cylinder also has the periscoping sensors that are deployed at the interior chamber wall or at the exterior monitoring location. A second cylinder has the ground-penetrating radar used for navigating and for detection of chamber walls (by creating a radar "image" of the earth and/or UGF walls ahead of the penetrator tip). A third cylinder/module contains batteries to run communications and navigation electronics for the penetrator and sensors onboard. Following that are an arbitrary number of cylinders that carry the fuel for the thermal melting tip and the coiled fiber optic cable. The number of fuel and cable cylinders is determined by the distance of penetration that is required. The fuel is moved under pressure to the lead cylinder with the melting tip through the couplings that connect each cylinder. As the assembly penetrates, the fiber optic cable in tension-relief jacketing, which is attached to the camouflaged antenna, is deployed behind the trailing cylinder. As a fuel cylinder is depleted, it is unlinked with the remainder of the penetrator assembly and left in the borehole. This reduces the mass that the penetrator assembly has to move and it also blocks the borehole if it is later discovered and an attempt is made to explore the borehole from the surface with a fish line. Steering of the penetrator head was envisioned to be accomplished by segmenting

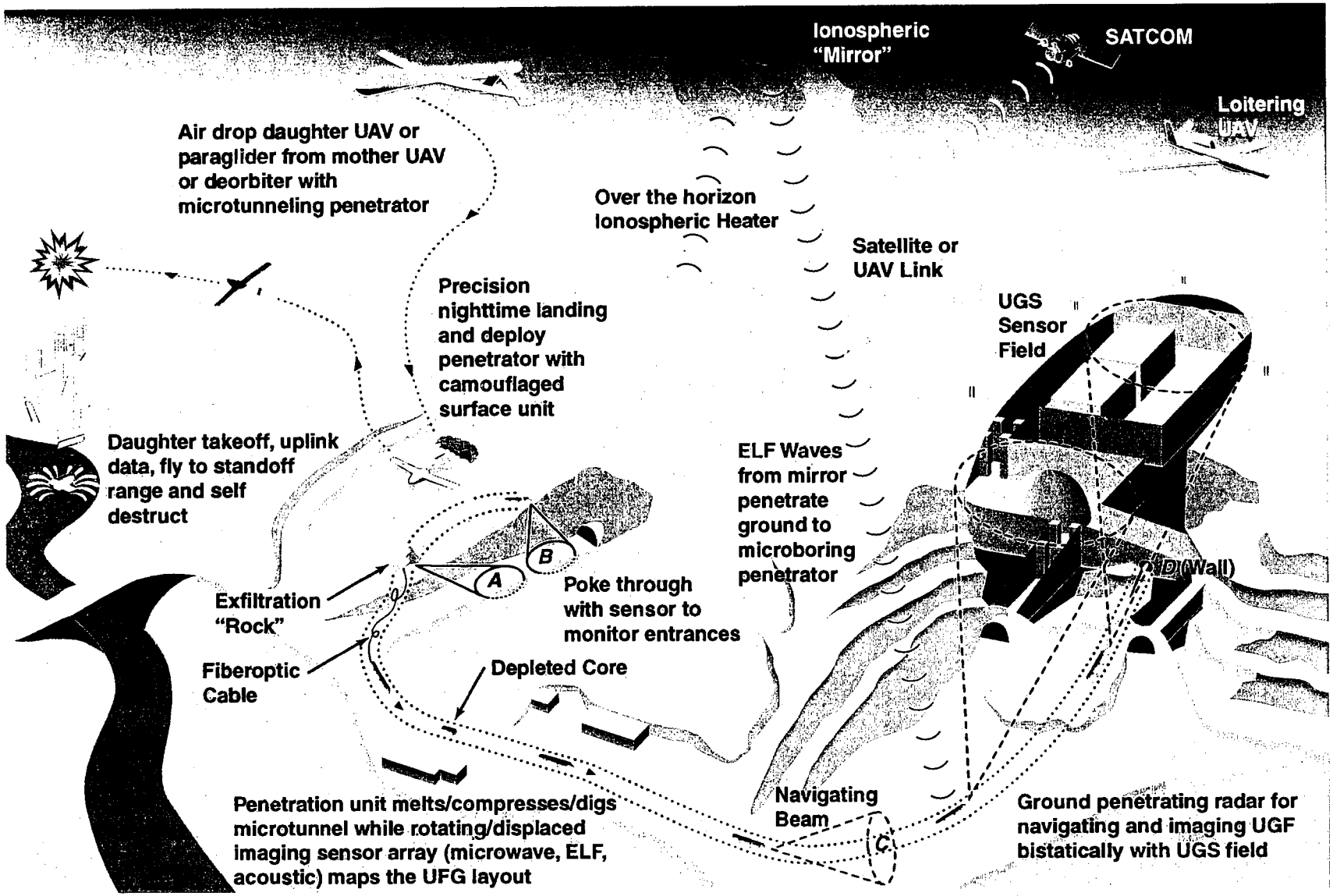

Figure 11. Underground Facility Close Access Characterization Concept of Operations: Sensor Placement/Mapping by Deep Penetration Autonomous Microborer. Delivery by mini-UAV with surveillance data exfiltration via concealed antenna to a SATCOM or loitering UAV serving as comm relay.

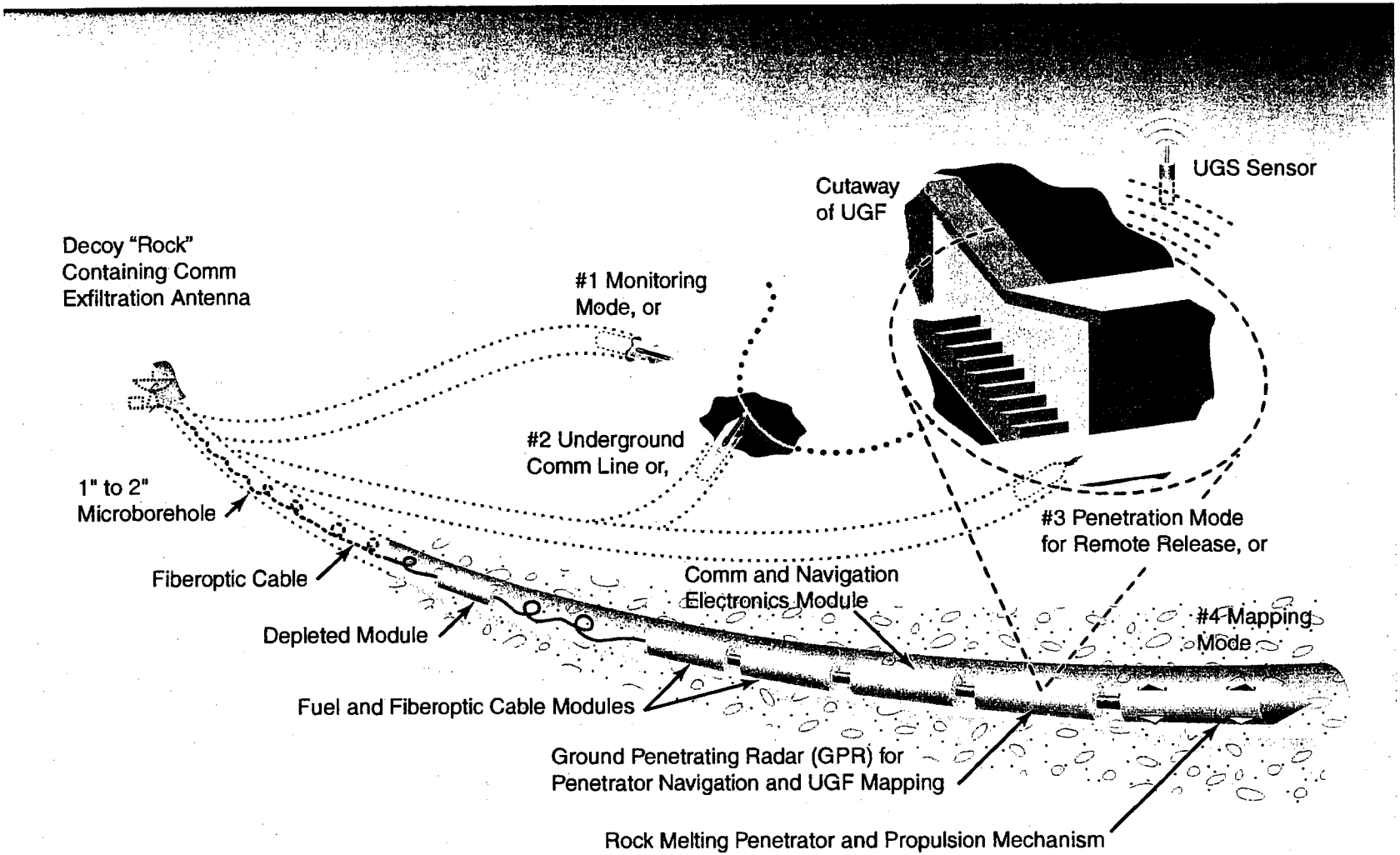

Figure 12. Original Phase I Proposal Configuration of the Proposed Rock-Melting Underground Microborer Showing Penetrator Tip, Navigating and Mapping Ground-Penetrating Radar Plus Sensors Module, a Communications and Underground Navigation Electronics Cylinder, and a Number Of Modules Containing Tip-Melting Fuel and Coiled Fiberoptical Comm Cable

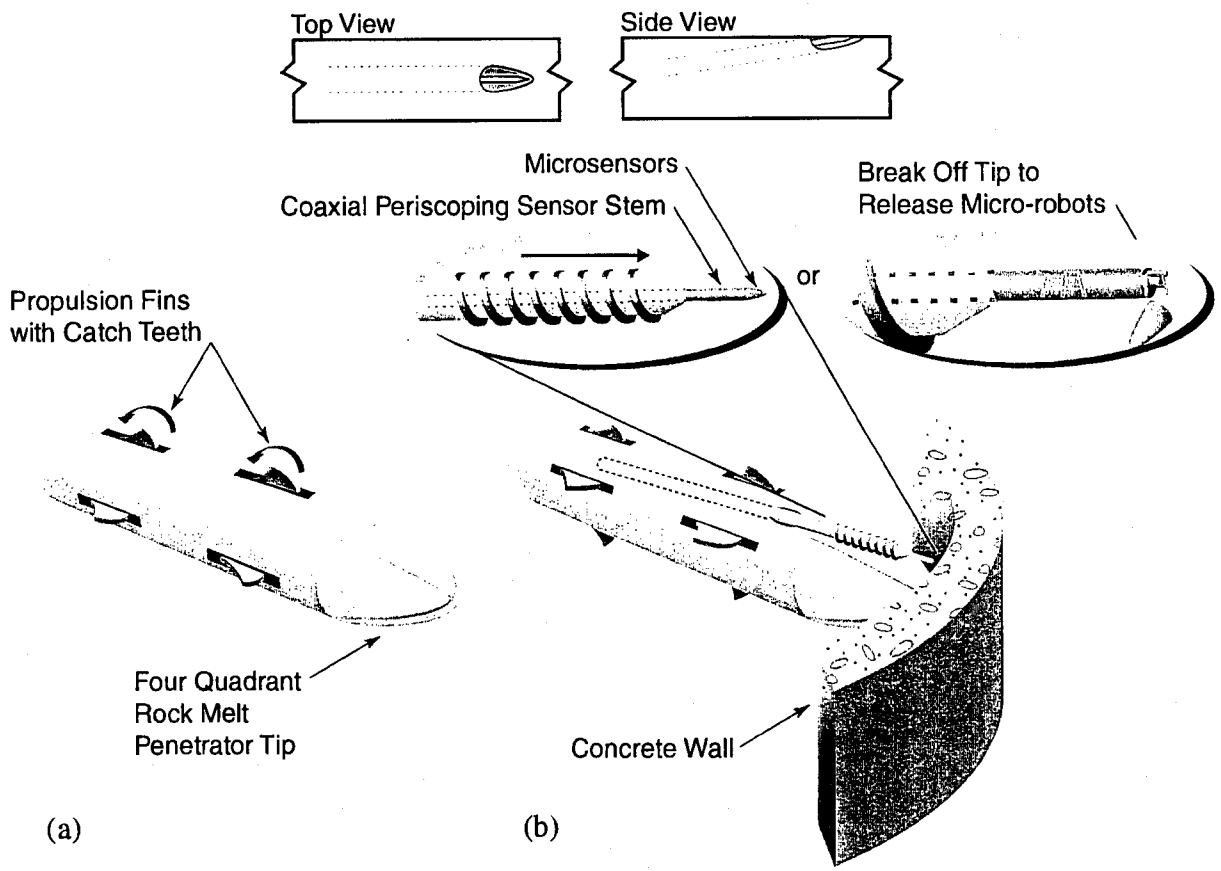

Figure 13. Details of Two Cylinder Modules on the Original Proposed Penetrator Assembly. (a) Penetrator melting tip showing four quadrants of heaters and the propulsion fins along the cylindrical length. (b) Offset microdrilling module showing coaxial periscoping sensor stem

the penetrator tip into four quadrants, each heated separately. Differential heating of the quadrants would lead to different melting rates and therefore would deflect the path of the tip according to the different melting rates.

In the updated conops shown in Figure 14, the diameter of the AUM is reduced from 2 inches to less than 1/2 inch and instead of a self-contained downhole propulsion mechanism, an unreeled coiled-tubing means of thrusting the rock-melting penetrator tip would be operated from the surface as an integrated part of the landed mini-UAV. The significant decrease in AUM diameter allows for over a 25X reduction in energy requirements for microboring by rock melting, which leads to a corresponding increase in standoff distance of perhaps 1 to 2 km. This will provide a greater opportunity to find a covered location for the mini-UAV to operate longer on the surface before departure is needed, and therefore an opportunity to simplify the downhole penetrator by putting some of the microborer insertion equipment on the surface as an integral part of the delivering UAV. In the updated conops, the electric drilling that performs the final drillout and placement of the sensor(s) would follow directly through the centerline of the penetrator, drilling right through the penetrator tip, as illustrated in Figures 14 and 15. The offset drilling of the original conops was not feasible once the diameter was reduced from 2 inches to 1/2 inch. Also, available classified electric drill devices developed by the CIA may be applicable for use in this new scenario.

Penetration. The AUM would penetrate 0.5 to 2 km through the ground and deliver imaging and/or audio sensors to a target position just below ground level in a berm overlooking a tunnel or adit (entrance). This would correspond, for example, to the FOV designated as B in Figure 11. The microsensors would protrude from the electric drill bit by coaxially sliding out of the bit tip to an above ground level on a small stem "periscope" that can monitor visually and acoustically the traffic into and out of the UGF entrance. The periscoping microsensor stem can be pulled below ground level back into the delivering AUM body to prevent detection or when not in operation. The life time of the sensors would likely be weeks, depending on the battery capability.

3.2 Close Access Long-Duration Interior Monitoring

A more complex mission is the placement of sensors into the wall of an UGF. In this scenario, the AUM would rock melt through the ground and a targeted wall of the UGF structure, which is likely to be concrete, stopping short of penetrating all the way through the UGF wall. A small hollow concrete drill stem would be extended from the AUM to penetrate the remaining distance and the microsensors would be deployed on a smaller periscoping stem that would coaxially extend from the drill stem, as depicted in Figure 15 and shown as final destination D in Figure 11. The complexity and power drain for autonomous navigation to the interior and the

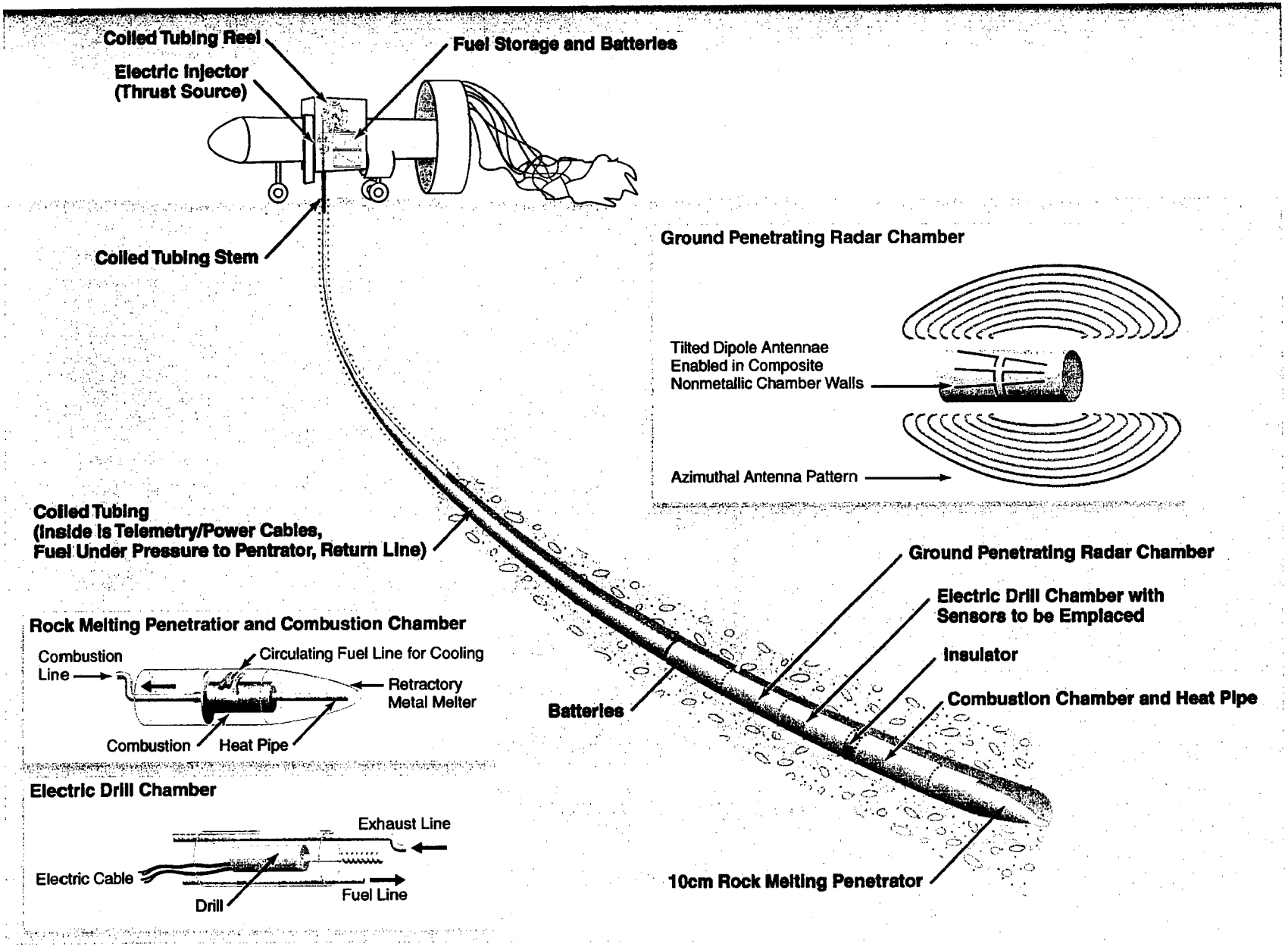

Figure 14. Design Configuration for Rock Melting Autonomous Microborer as a Result of Phase I Study

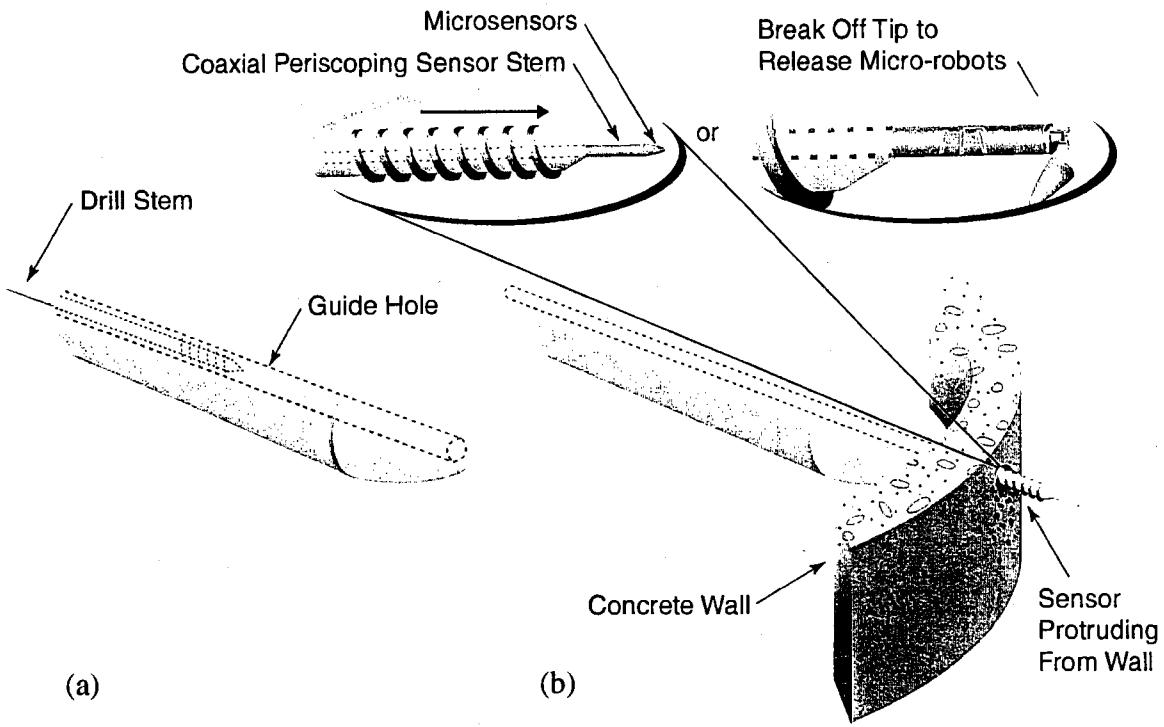

Figure 15. Details of Coaxial Centerline Final Electric Drilling to Emplace Sensor Stem

final drilling will likely drain more battery power, and the monitoring time for surveillance may be somewhat shorter than the exterior monitoring mission, assuming the same weight of batteries are carried in both missions. The intent of this AUM mission is therefore a confirmation of what is inside the UGF for physical characterization/verification of the UGF activities, so the device would likely carry radiation measuring sensors and chemical/biological sniffers rather than imaging sensors.

3.3 Underground Facility Mapping/Imaging

In collaboration with stealthily placed unattended ground sensors (UGS) positioned in the ground above a suspected UGF, the AUM would penetrate underneath the lower floor of the UGF along a path that is likely to traverse the entire extent of the UGF, such as that depicted as C in Figure 11. A ground-penetrating radar (GPR) transmitter carried along with the AUM, which normally serves as the navigating sensor for the AUM, would intentionally have its output impulse power increased in order to serve as a source for the UGS array to bistatically form a microwave image of the underground facility. This approach to imaging will likely be limited to distances between UGS and AUM of at most 100 meters due to the attenuation characteristics of radar frequencies through the ground. Because this is a one-direction (from AUM transmitter to UGS receivers) transmissive ground-penetration radar method of imaging, it has over twice the imaging range of a traditional GPR, requiring a round-trip reflective method of imaging, which has typically in practice achieved ground-penetration imaging through 50 meters or less.

3.4 Other Uses

There will certainly be many other uses for the AUM technology proposed for development in this report. Two other cases that come to mind are as follows:

Neutralization Ordnance Preplacement. The AUM can serve as a vehicle for prepositioning a small ordnance package to a designated target point near to or into a UGF. The AUM has too small a diameter in the revised conops to carry a highly destructive level of ordnance, but its capability to precisely place a small amount could be useful for a neutralization mission to disable a function or a door within the UGF, such as an air defense command center prior to a strike force sortie that would bring the function of the UGF down, allowing allied forces planes to penetrate the airspace. The munition would be commanded via a satellite or loitering UAV link to be set off at a designated time. This ordnance need not destroy the facility, only disable its function. Thus, destruction of a power grid or communication node in or near the UGF may also be sufficient to disable its function, such as a command and control center, during allied operations in previously denied territory.

Special Forces Manual Version. Although this report considers primarily an autonomously deployed underground sensor collection system for UGFs in nonurbanized terrain using a mother/daughter form of UAV delivery, any penetrator technologies and underground navigating and imaging technologies developed to implement the AUM concept will also be applicable for development of a manually operated rock/concrete-melting penetrator. Such a device would be useful for urban settings in which special operations forces would be used to access or place sensors in walls, HVAC, or conduits to denied facilities from adjacent or nearby buildings. A special forces team of four people, each carrying 100 pounds, can carry in more rock-melting penetrator equipment and fuel (400 pounds) than the UAV means of delivery (200 pounds). Thus, safe operating distances of perhaps 2 km should be possible for such manually deployed AUMs.

4.0 ENABLING TECHNOLOGY EVALUATIONS

While Sections 1 and 3 satisfy the requirements of the primary task for the Phase I SBIR project of developing a feasible concept of operations together with the technology roadmap to accomplish the conops and an estimate of the program cost if the roadmap were implemented, this section addresses the requirements of the other tasks cited in the Phase I proposal. These tasks focused attention on the four most critical technologies of the roadmap. Specifically, these tasks were (1) investigate rock melt penetrator and determine its feasibility relative to other microboring approaches, (2) investigate underground navigation technologies that permit the boring system to determine its underground position and the target location, (3) provide a bistatic UGF imaging feasibility assessment, and (4) investigate data exfiltration techniques to transmit the sensor data that are extremely covert. This section provides the results of these evaluation tasks.

4.1 Penetrator Design

The key technology that drives the autonomous underground microborer design is the method of penetration. We surmised as part of our Phase I proposal that a rock-melting technique pioneered during the late 1960s through mid 1970s by a group of scientists at Los Alamos National Laboratory, in what is now called the Geoengineering Group of the Earth and Environmental Science (EES) directorate, would be the appropriate approach. Their work, which has not been widely publicized, was developed for an effort called the Subterrene Program to investigate excavation systems based on melting extruding penetrators for geothermal energy exploration and oil exploration that could employ electricity provided by thermonuclear energy sources to power the penetration. A closer evaluation still leads to the same conclusion that rock-melting is the way to go for stealthy penetration of underground facilities.

A number of penetration methods were considered, including traditional rotary drilling, high-pressure water-jet-assisted rotary drilling, abrasive-jet drilling, percussion types (jackhammer-like), flame-jet spallation drilling, plasma torches, lasers, electron-beam guns, as well as rock-melting penetrators. Although not the most energy efficient of all the methods, the rock-melting approach was the quietest method able to go through concrete; it can be constructed for very small diameters, whereas other methods require larger boreholes; and it involves the least amount of equipment of all the methods that need to be on the surface.

An ultra-high-pressure abrasive waterjet, such as that manufactured by Flow International Corp. of Kent, WA, was one of the several competing technologies that were considered strong contenders as means of penetration. Specialized versions have actually been constructed for manual operation by special operations forces. Although fairly quiet at the abrasive tip and able to be constructed for reasonably small diameters, it still requires very noisy water pump support and water recovery

systems that would have to be left on the surface. Laser drilling was considered too exotic and difficult to navigate in an autonomous system. The electrical usage was also too high. Pneumatic hammering tips (percussive), such as the commercial trenchless technology of the DitchWitch (TM) for near-surface boring used in cable placement, was considered too seismically and acoustically noisy, even though it was more energy efficient than the rock-melting technique. Actual auguring, or rotary drilling, was also considered but was found to have problems disposing of the tailings; also, it was not able to penetrate rocks or concrete.

As an indicator of energy efficiency in drilling/boring, one measure of the performance of a boring technique is an evaluation in terms of its specific energy (energy consumption per unit volume removed) of boring and specific power (amount of power that can be delivered to a unit area of the working face). The rate of penetration is given by the ratio of specific power to specific energy, R=3600P/S where R is the rate of penetration in m/h, P is the power delivered to the working face per unit area in MW/m^2, and S is the specific energy of the technique in use in MJ/m^2. Values of the specific energy vary with the strength, type, and condition of the rock and the technique used. Examples of several techniques for hard rock are [Cook and Harvey, 1974]: percussive (jackhammer) P=3.3 and S=390, rotary P=0.7 and S=840, jet-piercing P=3.8 and S=1500. Novel techniques such as flame jet-piercing, water jet erosion, and laser and electron beams tend to have high values of specific energy. Figure 16 shows that small-hole drilling is the most efficient. Laser and electron beam equipment is too bulky and large to provide large amounts of power. Note in Figure 16 that rock melting is less energy efficient than other approaches. As part of ORINCON's support of class projects at the nearby University of California, San Diego (UCSD) campus, we sponsored a class study to build a percussion tool that could measure energy usage to penetrate various soils as part of this SBIR project. The key measurement for clay soils is shown as point 6 of Figure 16. Figure 17 is a diagram of the device designed by the UCSD mechanical engineering class.

The feasibility of "drilling" holes with rock-melting penetrators was demonstrated by the Los Alamos Scientific Laboratory (now Los Alamos National Laboratories (LANL)) beginning in the mid 1960s and it still appears to be the only facility worldwide that is experimenting with this approach to boring (no other literature references were found, and scientists at LANL were not aware of any others evaluating rock melting techniques). Using an electrically heated laboratory device, holes were drilled in basalt and concrete up to 6 inches (15 cm) deep and 2 inches (5 cm) wide at rates of about 3.3 ft/hr (1 m/hr). Energy requirements for these initial tests were about 2 to 3 times that required to melt basalt, or roughly 10K to 20K J/cm^3. In 1971, a report was published which reviewed, analyzed, and discussed a proposed program of development for large penetrators called Electric Subterrenes or Nuclear Subterrenes [Smith 1971] using compact nuclear reactors. Experiments varying the hole shape were demonstrated (the penetrator does not

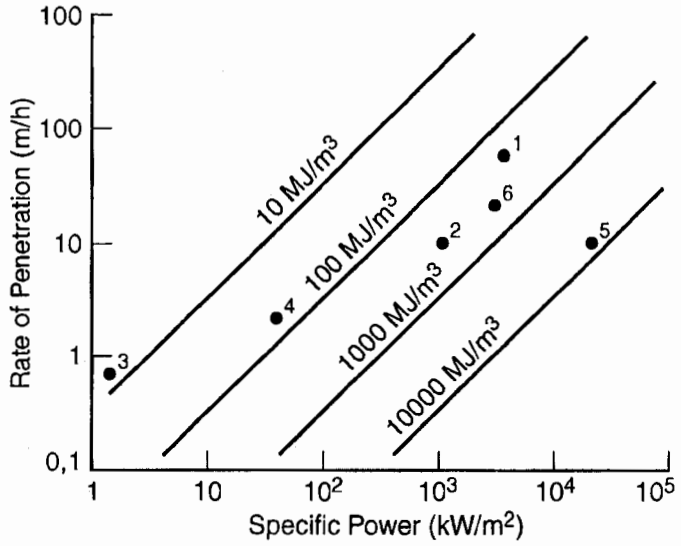

Figure 16. Comparison of Various Drilling/Boring Techniques in Terms of Rate of Penetration, Specific Power, and Specific Energy: (1) Small Percussive Drills, (2) Rotary Drills, (3) Drill-and-Blast Tunneling, (5) Rock Melting and Arc Jet [from Cook and Harvey, 1974], and (6) Measurement by UCSD Mechanical Engineering Percussion Tool

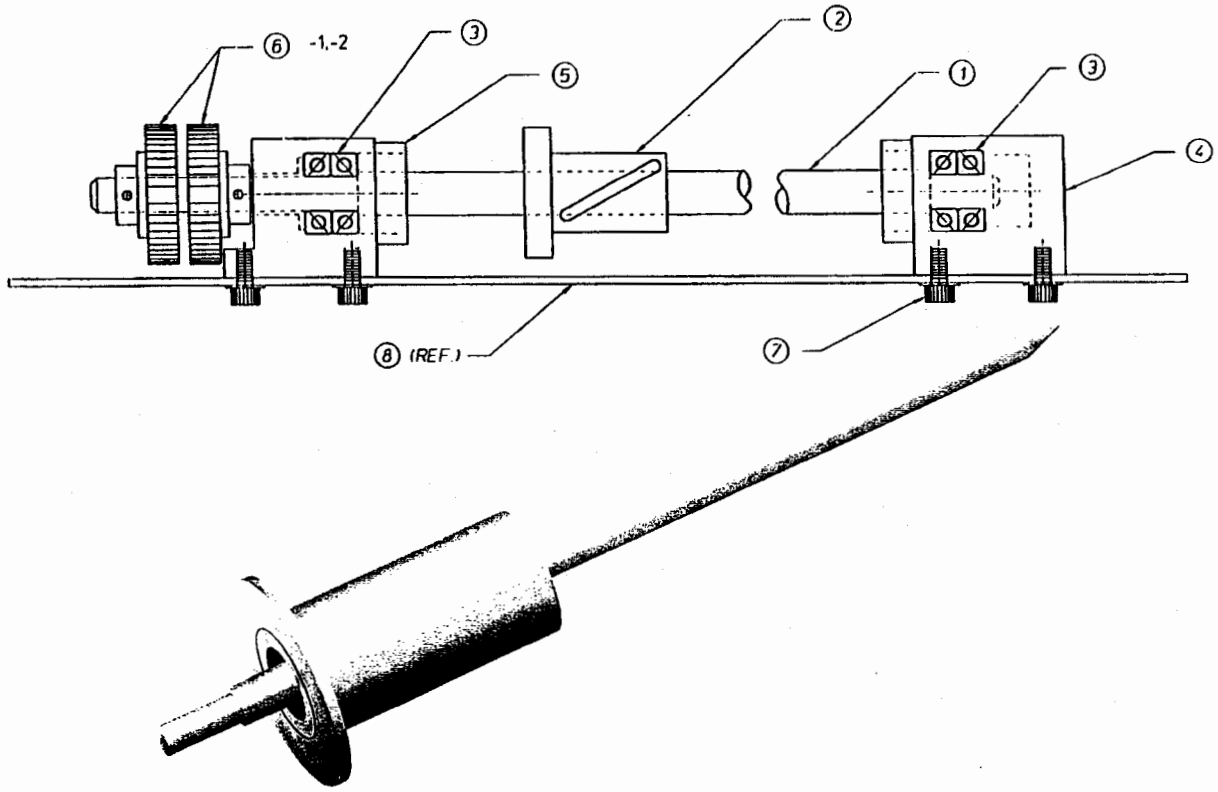

Figure 17. Mechanical Percussive Penetrator Built by UCSD Mechanical Engineering Project Class to Validate Results Shown in Figure 16. (a) Precision driving assembly, and (b) Penetrator.

rotate). Waste rock turned into glass was used for hole lining and/or forced into fissures or removed through the melting bit to the surface.

Rock melting works because soil, rocks, and concrete melt at about 2000 degrees less than the material of the penetrator body, as indicated by Figure 18 and Table 2. Temperatures of approximately 1800 degrees Kelvin are sufficient to melt most rocks and soils encountered in drilling and tunneling. Table 2 provides the melting temperature of refractories and the melting ranges of rock, showing that available structural materials have sufficiently high melting temperatures to allow the construction of rock penetrating devices. The research at LANL investigated materials for melting, the rate of melt, the operating life of the penetrator, analyzed the heat transfer and fluid mechanics of the rock-melting for predicting performance, and experimented with debris handling and removal (mostly in the form of rock glass). Depths up to 100 meters have actually been made with a melting penetrator of approximately 2-inch diameter. Penetrators to date have been heated with electrically powered resistive, pyrolytic-graphite heater elements to achieve melting temperatures between 1700 and 2100 degrees Kelvin. Electrical energy sources were used for convenience and simplicity of the rock-melting penetrator design, although heating by burning an oxidized fuel will be the preferred approach in the design of the AUM. The electrical energy usage was approximately 2 KW with the rate of penetration typically about one foot per hour (i.e., 2 KWH/ft is energy usage as a function of penetration range). A stabilized borehole with glass lining was formed as a result of the rock-melting process. To be investigated is the possibility of using so-called consolidation penetrators in which, by melting out to a diameter larger than that of the penetrator, the molten debris from the melting can be entirely consolidated in the denser glass lining. This would completely eliminate the necessity to remove melt debris and would greatly simplify the microboring penetrator design. Although a 2-inch diameter is likely to be the best diameter to accommodate the electronic components and the mechanical design of the propulsion and sensor periscoping mechanisms, a goal would be a 1/2-inch diameter or smaller. As the energy to penetrate varies with the square of the diameter, considerable fuel and penetrator size can be saved by use of a smaller diameter. In fact, the melting power E and penetration velocity V are related by

$$V\rho A\{C(T-T_0)+H\}=E$$

where ρ is the density of the rock or soil, A is melted cross-sectional area, C is the specific heat, T is the melting temperature, T_0 is the ambient temperature, and H is the effective heat of fusion.

Electrical-powered resistive heating is not going to be an energy efficient method to heat the melting tip of the penetrator. The current LANL design uses a resistively heated pyrolytic-graphite heater element which radiates energy to the refractory metal penetrator body with a heat flux of 2 MW/m^2, which is typically molybdenum. LANL has considered the possibility of arranging the

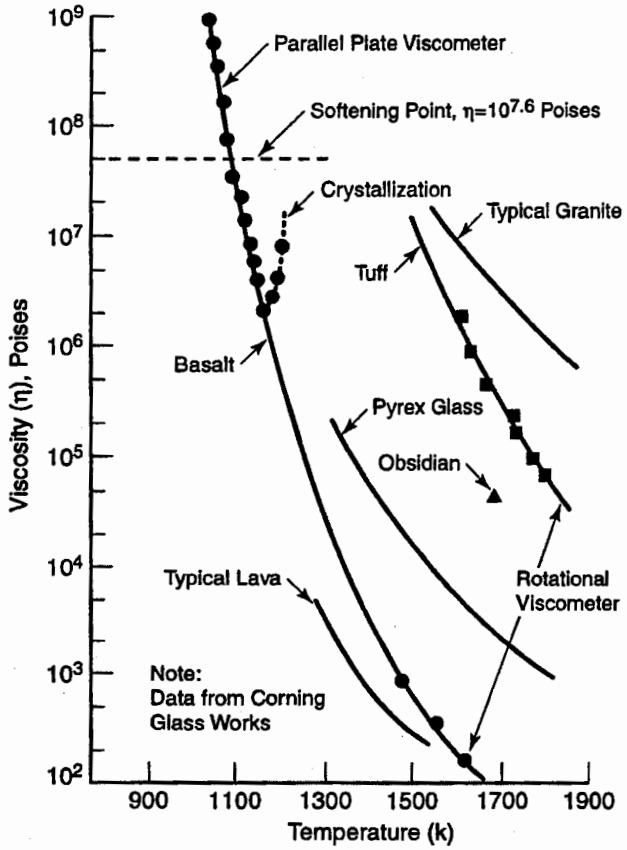

Figure 18. Typical Temperature Dependence of Rock-Melt Viscosity During Melting Based on Theory (line) Versus Measurements (Dots) for Rock in Los Alamos Area [from Rowley, 1974]

electric current of a rock-melting penetrator to pass through the molten region in order to place most of melting power directly in the melt layer just adjacent to the melting interface (direct heat melt) so as to increase the energy efficiency.

Current LANL rock-melt penetrator designs circulate a gas down the pipe stem to which the penetrator is attached, which serves to chill the molten rock to a glass-like lining for hole support (see Figure 22), thus stabilizing the borehole in loose, unconsolidated, wet and dry soils and in low-density rocks. For larger penetrator heads (not to be considered for the AUM), the molten rock can be extruded through ports or flow passages in the penetrator and chilled by a gas coolant; the melt can be formed selectively into glass pellets, glass rods, or rock wool. Both types of penetrators are illustrated in Figure 19 (c) and Figure 20. Both theory and practice show that the penetrator advances at a rate directly proportional to the power applied to melt the rock or soil, where theory models the heat-transfer processes, melt-flow fluid mechanics, and penetrator geometry, as shown in Figure 21. The selected penetrator is relatively insensitive to wide variations in rock or soil type and strength.

Table 2. Comparative Melting Temperatures of Various Refractory Ceramics, Metals, Minerals, and Rocks [from Rowley, 1974]

		Temperature	
Refractory Materials	Formula	°C	K
Silica (quartz)	SiO_2	1723	1996
Corundum	Al_2O_3	2030	2303
Lime	CaO	2570	2843
Boron nitride	BN	~ 3000 (sublimes)	~3273
Graphite	C	~ 3700 (sublimes)	~3973
Metals			
Iron	Fe	~ 1535	1808
Chromium	Cr	1850	2123
Niobium	Nb	2468	2741
Molybdenum	Mo	2620	2893
Tungsten	W	3380	3653
Minerals			
Albite	$NaAlSi_3O_8$	1120	1393
Orthoclase (K-feldspar)	$KAlSi_3O_8$	1150	1423
Anorthite	$CaAl_2Si_2O_8$	1553	1826
Diopside	$CaMgSi_2O_6$	1391	1664
Magnetite	Fe_3O_4	~ 1538 (decomp.)	1811
Rocks[a,b]			
Olivine basalt	—	1080-1220	1353-1493
Biotite granite	—	1100-1250	1373-1523
Bandelier tuff	—	1180-1250	1453-1523
Santa Fe formation (alluvial soil)	—	1100-1200	1373-1473

(a) Rocks do not exhibit sharp melting temperatures as do pure minerals, metals, or compounds. In the geochemical sense, the melting range can be defined as existing between the first appearance of liquid and the disappearance of the last remaining component crystals.

(b) Because rock melting occurs over a temperature range, the rock undergoes a gradual transition from the solid to the liquid phase. The transition may be interpreted and defined in terms of relative viscosity of these phases. Viscosity is a strongly temperature-dependent property. Different rock melts can be compared at either constant viscosity or constant temperature.

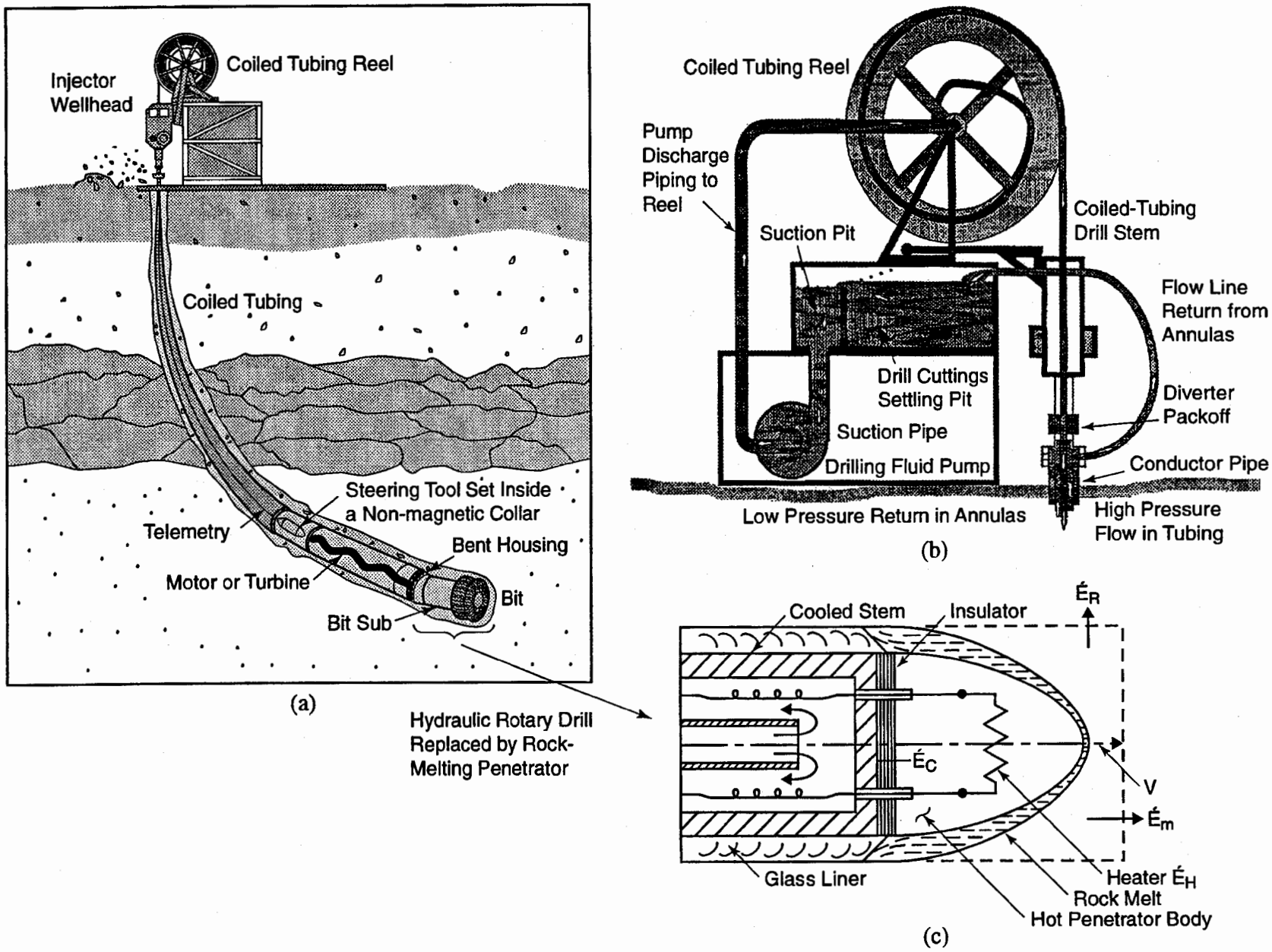

Figure 19. Microboring Components Developed at LANL. (a) Coiled tubing drill stem with hydraulic rotary drill. (b) Details of closed circulation pump for coiled tubing stem approach. (c) Cross-Section of an Electrically Heated, Nonsteerable, Consolidation Penetrator [from Rowley, 1974]

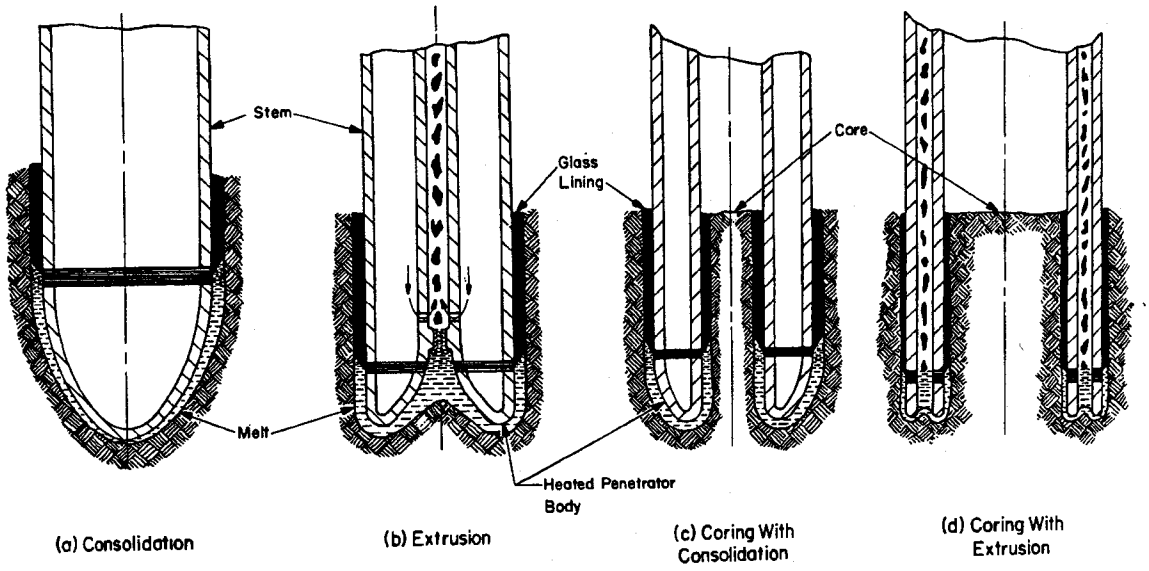

Figure 20. Rock Melting Penetrator Forms Evaluated During the LASL Subterrene Program [from Rowley, 1974]

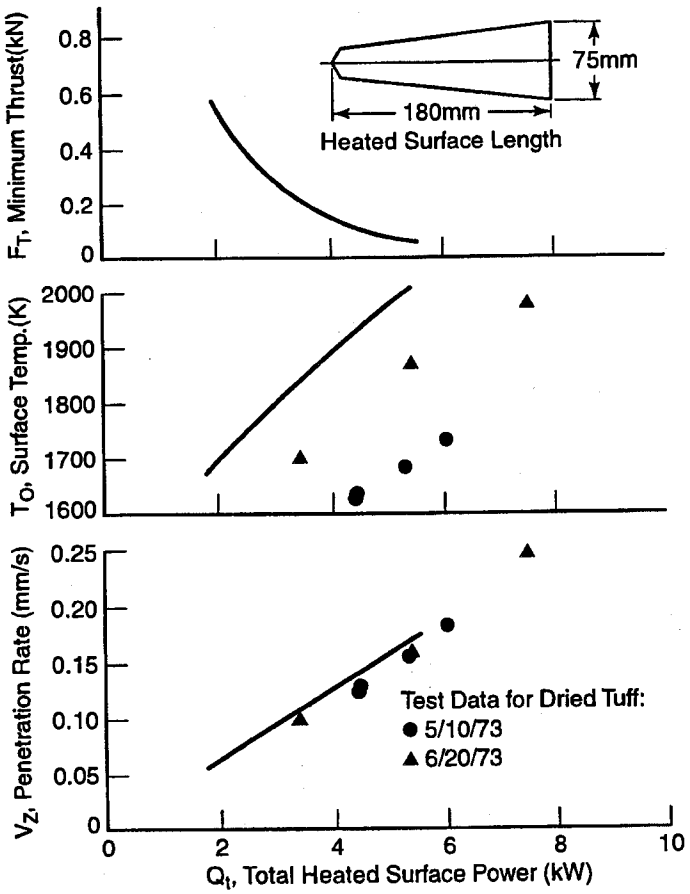

Figure 21. Measurements of Penetration Rate Versus Melting Power Using 50 mm Diameter Consolidating Penetrator Operating in Tuff [from Rowley, 1974]

Figure 22. Photograph of a Section of Glass-Lined, 50-mm Diameter Hole Produced in Tuff in Which the Thickness of the Glass Lining was Approximately 12 mm

Melting penetrator devices are illustrated in Figure 20. One unit is called a density consolidation penetrator because it melts the entire cross section of the hole in loose soil or low-density rock sufficiently to form the glass lining and consolidates the molten debris into the dense glass lining.

The coolant flow through the steel thrusting stem chills the melt into a solid glass-like hole lining. Most consolidators studied have diameters from 10 to 115 mm. Melt is handled by extrusion through flow parts of passages with larger penetrators (66 mm and larger).

4.2 Energy Sources

The energy source for the navigation electronics, exfiltration electronics, and sensor electronics will use electrical energy from batteries, so that mission duration will ultimately be determined by the amount of power energy that can be carried downhole or left on the surface. The energy source for rock melting, however, is one of the critical technologies that ultimately will require experimentation to determine which source will be the most viable from the standpoint of ease of operation and delivered energy density for this microborer application. In this section, we shall cover some of the first order properties that have led to the conclusion that an oxidized hydrocarbon fuel should be used as the energy source. Critical decisions about specific fuels to

use will need to be determined as part of the early phase experiments of a full microborer project. The rock melting experiments performed to date by LANL have used electrical power due to (1) convenience, (2) simplified apparatus to create heating (cable to a resistive heating element), and (3) the desire (at least originally) to use nuclear power converted to electrical power, although there is no limitation in rock melting that requires only electrical-based heating. In fact, Table 3 indicates that self-contained electrical power (batteries, fuel cell, or nuclear reactor with electrical converter) is orders of magnitude less efficient than the most energy dense sources, which tend to be hydrocarbon-based fuels. Thus, to deliver a minimum weight microboring apparatus, we will need to explore hydrocarbon fuels as the source of penetrator heating. LANL had also pumped cooled gas down the boring stem to the penetrator head to cool the molten rock to solidify it into glass and to push debris and glass fragments back through an internal smaller-diameter coaxial tube to the surface. Discussions with LANL indicate that, due to much smaller diameters being considered for the microborer application, a penetrator design that controls the heating and penetrating rates and rock material displacement can obviate the need for cooling and debris removal, thus avoiding yet another energy source to run cooling apparatus pumps on the surface. If the coiled tubing approach to microboring is used, a coaxial return-to-surface inner tubing may be required to exhaust gas byproducts of the combustion. However, as no air will be pumped from the surface to the combustion chamber where the fuel is burned, the fuel will need to be self-oxidized.

Table 3. Energy Densities for Selected Fuels and Electrical Sources

Source	Energy Density (watt-hours/kilogram)
Nickel-Cadium Battery	40
Li/SO_2 Battery	175
Rechargeable Auto Battery	200
Fuel Cells	800
High Explosive	1,000
Torpedo Fuel (estimated)	2,000
HEDM Rocket Propellant	4,000
Methanol	5,000
Diesel Fuel	10,000

The investigation during this Phase I study found the most likely candidate for oxidized hydrocarbon fuel for use in the microborer device to be torpedo fuel. The Indian Head Division

of the Naval Surface Warfare Center (NSWC) at Indian Head, Maryland, is the only energetics manufacturer of torpedo fuel (and several other specialty chemicals used for rocket motors and warheads). However, there appear to be some classified aspects of this special fuel, and only an estimated energy density is reported in Table 3. Both the Air Force and NASA conduct research programs in high energy density materials (HEDM), primarily for use as rocket propellants. The Air Force HEDM program is run by the Phillips Laboratory, and the NASA program is run by the Space Propulsion Technology Division of the Lewis Research Center. Both programs prefer cryogenically cooled high energy density fuels, which are not practical for use in the microborer application. Nevertheless, detailed discussions should be held with both the Air Force and NASA organizations to determine if any ambient temperature fuels have been developed that could be used on the proposed microborer program.

We can project fuel requirements based on some of the experimental measurements already made by LANL on their rock-melt microdrilling programs. Using a 2 Kw electrical source and a 2-inch diameter rock-melting penetrator, LANL achieved a penetration rate of approximately one foot per hour, with very little dependence on the type of rock, soil or concrete material penetrated for either the penetration rate or the amount of energy used. This corresponds to an energy volumetric density rate of roughly 0.05 watt-hours per cubic centimeter (.05 w-h/cm^3) of material rock-melted and penetrated. Using the fact that diesel fuel has a mass density of 0.82 grams per cubic centimeter (somewhat less dense than water at one gram per cubic cm) and the energy density from Table 3, one can conclude by taking the ratio of the mass and energy densities that the hydrocarbon diesel fuel has an energy volumetric density rate of approximately 8.2 watt-hours per cubic centimeter for an equal volume of diesel to rock material removed or melted. However, in practice one must account for the loss of volume due to the coiled tubing shell thickness and the displacement of volume due to the internal return-to-surface coaxial tubing and the telemetry cabling (assume a 50 percent displacement of volume), the use of a fuel other than diesel (e.g., torpedo fuel, which appears to have 20 percent of the energy density of diesel), and the efficiency of combustion and radiating the heat via a heat pipe to the penetrator head (assume a 60 percent efficiency). This yields a net energy volumetric density rate of (.5)(.2)(.6)(8.2 w-h/cm^3)=0.49 w-h/cm^3, which is still denser than the energy for melting an equivalent amount of rock or concrete material. This suggests that the fuel will only need to be stored in the coiled tubing and no external tank or bladder would be required to hold fuel.

We note that the penetration rate of one foot per hour (faster penetrations may be possible due to the smaller diameter proposed for the microborer relative to the much larger penetrators used to obtain the measurements) implies that a 1 km boring would require approximately eight weeks.

This needs to be considered carefully in the conops of any operation where a microborer may be used.

4.3 Propulsion and Steering

In the original AUM concept presented in the Phase I SBIR proposal, we suggested a self-propulsion scheme as depicted in Figures 12 and 13. Because the borehole is cooled to hard glass as a byproduct of the rock-melt action of the penetrator tip, this provided an exploitable option to engage the walls like a pick to pull the penetrator assembly along. Gas under pressure from burning fuel as a byproduct of the heating process can be exploited to create a pneumatic-driven mechanism for propulsion. A specific scheme was visualized in Figure 14 in which engaging fins that move outward from the sides of the lead cylinder, contacting the glass borehole, shifting position to the rear while engaged against the wall of the borehole, then disengaging and recessing back into the cylinder was proposed. This process is periodically repeated by a number of fins around the cylinder circumference to provide the forward thrust needed to propel the penetrator assembly. Steering was proposed to be accomplished by dividing the penetrator tip into four heating zone quadrants. By varying the amount of fuel fed to each quadrant, heating variances could be created that change the amount of rock material melted in each quadrant. The thrust action would tend to move the penetrator assembly in the direction with the most melted material (line of least resistance).

Discussions with LANL have caused a significant change in the conops approach to self-propulsion to an alternative approach that appears to be simpler and that supplies the thrust for forward motion from the surface. The current LANL Microboreholes Project [Dressen, 1997] is examining a portable, reeled, non-rotating, coiled-tubing-deployed, hydraulically-powered microdrilling platform (rotary driller; not a rock-melting penetrator) for 2.25-in and 1.125-in diameter microboreholes. A surface platform is used that has a tubing injector unit to develop high load insertion (thrust) of the tubing into the sealed borehole; the tubing, in effect, forms a continuous drill/penetrator stem (in contrast to the traditional coupled short-section rotating drill stems). LANL has proposed that the coiled-tubing approach be conjoined with the rock-melting penetrator as the best solution for the AUM application. Issues of tubing buckling and friction loading need to be evaluated, although these are less likely to be issues with rock-melters than with hydraulic drillers as less thrust is required and no rotary mechanical devices are at the end of the coiled tubing. The coiled-tubing technology is provided to LANL by Coiled Tubing Engineering Services (CTES), who also provides coiled-tubing performance modeling, analysis, and designs. Coiled-tubing manufacturing has been recently augmented by insertion of telemetry cables and small hydraulic tubing inside the coiled tubing. The tubing is plastically deformed as it is coiled onto the reel and

uncoiled from the reel and inserted into the borehole. The power to deform the tubing during unreeling is proportional to the product of the tubing velocity, the yield stress of the steel tubing, and the tubing diameter cubed and inversely proportional to the reel diameter.

Even though surface-based insertion force may solve the propulsion problem, it may be useful to consider designing a pick-and-slide side-cylinder propulsion downhole to assist the propulsion if it can reduce surface-based equipment size and weight. Such a pick device downhole would also be useful for security purposes. If the borehole is discovered and removal of the coiled tubing is attempted, the picks could hold the penetrator assembly in place and cause the coiled tubing to break off, leaving the penetrator assembly (with sensors) downhole undiscovered; only the coiled tubing would be brought to the surface.

Rather than the four-quadrant heating scheme as originally proposed, it is better to have one integral melting head and bring three or four heat pipes with energy to the penetrator head. By cycling the heat on/off at specific pipes, a differential heating of the penetrator tip is accomplished, thus causing the penetrator to steer due to the differential in melting rates. Alternatively, if a downhole pick-and-slide propulsion is designed, then using or not using some of these picks can impose a mechanical differential force that causes the penetrator head to steer.

4.4 Navigational Sensors

Another key technology area to create in an autonomous device for microboring underground is navigation: knowing where the penetrator is located with respect to its penetration point on the surface and knowing what is in the path ahead of the penetrator. We address these two navigational requirements with two separate proposed technologies. Simple tiltmeters or magnetometers are proposed for the location capability. A miniaturized impulse ground-penetrating radar (GPR) is proposed to provide the look-ahead capability, as well as possibly serving as a signal source for the UGF bistatic imaging capability described in the next subsection.

Inclinometers are the simplest devices that can indicate attitude (angular orientation in 3D-space) of the AUM at its current path location; they are sometimes called tiltmeters as they generally are a planar piece of metal that rotate under gravity depending on their rotation; a mechanical or electrical readout of the rotation angle is then made. Very small ones already exist and have been used in low-cost applications such as video arcade games. If the inclinometer angles are periodically sampled and combined with an optical reading of length of coiled tubing into the borehole (markings on side of tubing are read by optical sensor on the reel to determine number of meters uncoiled), a simple integration path through the angular readings will permit the position to be determined easily. Magnetometers are an alternative to tiltmeters and use no moving parts that

might bind, in order to measure relative changes in orientation. Off-the-shelf devices also exist that approach the one-half form factor proposed for the AUM. For example, Applied Physics System model 544 miniature angular orientation sensor measures roll, pitch, and yaw and measures 0.75 inches x 0.75 inches x 4.6 inches. It contains both a 3-axis fluxgate magnetometer and a 3-axis accelerometer, both of which are sampled by an internal A-to-D converter and output as digital data on an internal microprocessor. There are other devices under sponsorship of DARPA that might have use as navigational aids to fix the position of the underground microborer, in particular, the micro-inertial navigation systems under development by the DARPA Electronics Technology Office (ETO) or NASA. For example, Jet Propulsion Laboratory (JPL) is developing a micro-inertial reference system chip consisting of micromachined silicon gyroscopes and accelerometers for future space missions. It measures 1 cm x 1 cm x 0.2 cm and consumes less than 0.2W. Figure 23 shows a photo of this device. Sandia National Laboratories is developing an integrated circuit MicroNavigator which not only has micro gyros and accelerometers, but also has an integrated GPS receiver and navigation computer.

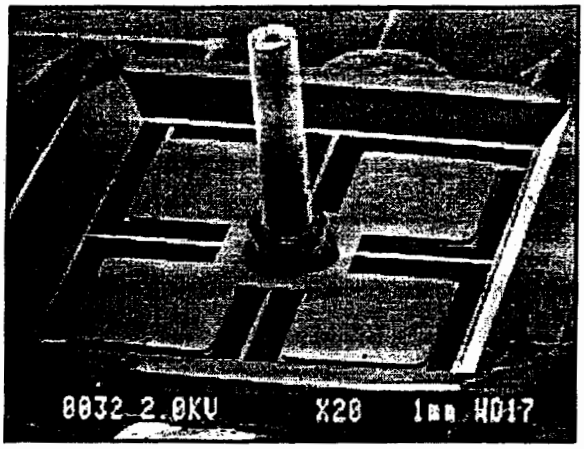

Figure 23. Illustration of Silicon Gyro in JPL Micro Inertial Reference System Chip

For the look-ahead capability, we have settled on a ground penetrating radar with a possible dual use. The look-ahead mode of the GPR can be used to look out a meter or so ahead of the penetrator to crudely image, by pulse echo return timing, the area about to be penetrated. This can determine if major obstacles lie ahead, or if an underground facility wall is about to be penetrated, or if the ground surface is about to be breeched. A second serendipity would be a phased array mode to transmit microwave energy upward through suspected UGF tunnels and chambers in order to image the UGF in bistatic tomographic collaboration with an UGS array previously buried stealthily above the UGF, as indicated in Figure 12. We are specifically proposing to use the ultrawideband (UWB) micropower impulse radar (MIR) developed by

Lawrence Livermore National Laboratory and now being commercially licensed. The MIR technology currently fits on a 1.5-inch square circuit board and uses a 1.5-inch dipole antenna at its current operational frequency. A development effort is underway at LLNL to place the radar electronics, currently costing about two dollars, onto an even smaller chip that would be compatible with the half inch AUM form factor. LLNL is willing to develop a customized prototype for the AUM concept.

The MIR was developed by Tom McEwan of LLNL as part of the Laser Fusion program at LLNL. The MIR generates and detects subnanosecond (0.2ns) pulses, roughly at a rate of two million per second, and averages many returns in order to increase sensitivity and detectability to a desired level. The MIR requires only microamperes and can last two years on an AA battery. Range gating is used to determine range from the radar; such gating is also useful in the proposed AUM system by being able to gate the reflection of the radar energy off the side of the AUM assembly. The current circuit board for the MIR is 4 cm^2. The MIR randomizes the exact pulse emission and detection times for purposes of interference rejection, which also permits multiple co-located MIR operation (needed for the AUM design that may use five or six of these radars to cover the azimuthal region about the penetrator) and makes it hard to detect due to the randomization. The current MIR design has been proven in field test to be able to penetrate at least 33 cm of soil looking for mines (15 cm wavelength currently), in which the MIR specs are 2 or 6.5 Ghz center frequency with 500 Mhz emission bandwidth, 1 microwatt or less transmitted at 2 Mhz PRF.

The performance of the GPR would need to be adjusted depending on conditions encountered underground, primarily by the number of pulses that are integrated. Soil condition and type at site determine the conductivity through which radar EM signal propagation will occur, and therefore the depth of penetration. Figure 24 illustrates the relationship of penetration depth versus conductivity for various rock and soil media. The amount of moisture in the soil/rock has the largest effect on conductivity, with low moisture content leading to low soil conductivity and consequently low EM absorption and therefore generation penetration depth; vice versa with high moisture content. That is, the radar wave is attenuated less and has better penetration in dry sandy soils, and has reduced penetration in moist clay or similar conductive soils. GPR systems constructed by Earp et al. [1996] and Giglio and Ralston [1993] at 900 and 500 MHz operational frequencies, were able to penetrate 5 to 15 feet with resolution 0.5 to 2 inches, respectively. This provides the confidence that the MIR device from LLNL will be adequate as a look-ahead imaging sensor for the proposed AUM.

4.5 Surveillance Sensors and Bistatic Imaging

The primary mission of the AUM is to deploy imaging, acoustical, chemical/biological sniffing, or nuclear material monitoring sensors at the targeted UGF sensing location. Figures 13 and 15 depicted concepts for that deployment using a coaxial periscope mechanism pushing through the final electric drilling bit. For an entrance monitoring mission, the AUM would typically carry low-light-level EO/IR imaging and/or audio sensors to be periscoped to ground level near an entrance by protruding from the AUM, as shown in Figure 9. For an internal access mission, the AUM would carry EO/IR, audio, and/or radiological/chemical sniffers to be placed in or through walls of a UGF chamber, as illustrated in Figures 11 and 12. An IR source may also be required if chambers of interest are in the dark. For this application, a microdrill would actually be deployed at a slight offset with respect to the cylinder body to drill the remaining couple of inches into a UGF concrete wall. Once penetration through the wall is sensed by a change in torque, the sensors would deploy coaxially through the hollow core of the drill stem. The walls of the UGF may not be the only target of opportunity. It may be advantageous to locate communication or power conduits in order to tap into them, as illustrated in Figure 12. It is expected that current battery technology will permit a few days or weeks of monitoring in order to keep the penetrator assembly as small as possible. The TRW ASG operations in Sunnyvale is a possible source for some of the sensor technology; JHU APL for the low-light-level imaging sensor; and DARPA's STO office for other sensors under development. Specifics of sensors are not catalogued here as this report was directed primarily at the means of delivery for such sensors.

A more exotic concept for the AUM penetrator assembly is the capability to use the coiled-tubing deployed in the placement of the AUM as an antenna to detect deep ground-penetrating ELF waves (30 to 300 Hz), which have been in use for years for submerged submarine communications and geophysical exploration. The ELF wavelength is too long (many kilometers at the lowest ELF frequencies) to be used for traditional phase comparison geolocation. However, with novel modulation of the ELF waves [Ferraro and Werner, 1995, and Kuo et al., 1997] and long integration times (order of an hour), algorithms should be possible to geolocate with even weak ELF that can penetrate through the UGF and down to the depth of the AUM below the UGF. ELF penetrates deep but diffusion dominates over wave propagation so that sharp boundaries cannot be resolved, and therefore correlating type receivers need to be used. ELF waves can be generated remotely and "beamed" down to a designated over-the-horizon location currently from a facility called the High-frequency Active Auroral Research Program (HAARP) located at a DOD-owned site near Gakona, Alaska, scheduled for completion in 2002. The HAARP is primarily an ionospheric research instrument that uses a ground-based 15x12-antenna-element phased array radio transmitter in the HF frequency range to excite the

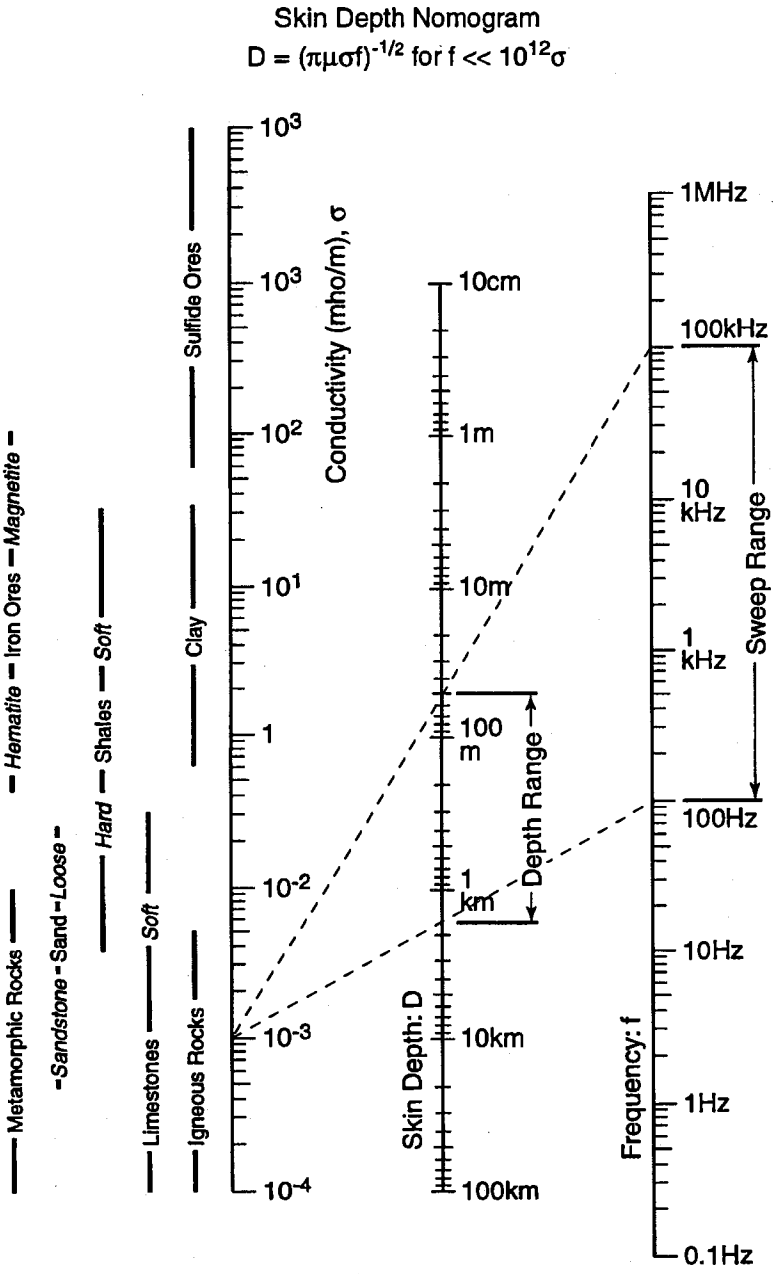

Figure 24. Nomogram Showing the Relationship Between Transmitter Frequency, Ground Conductivity, and Depth of Penetration for Typical Earth Materials. Magnetic permeability is assumed to be that of free space. As an example, a source with frequency content from 100 Hz to 100KHz in an igneous rock area would have penetration depth ranging from about 40 to 1500 meters [from Won, 1980]

ionosphere to induce a small, localized volume change in ionospheric temperature that becomes an ionospheric "mirror" to some RF frequencies. Even though the HAARP does not transmit in the ELF frequency range, it can induce modulated (mostly on-off) underground probing ELF waves by modulation in the ionosphere at an altitude of about 80 km. This could be an experimental source of ELF waves into denied areas by modulating the strong electrojet current system that occurs naturally at high latitudes in the ionosphere and forming arrays of low frequency ionospheric dipole elements in the upper atmosphere. When this energy is injected into the earth-ionospheric waveguide it can be steered over the earth's crust in directions preferred by the experimenter to create underground propagation confined to a region of several kilometers. The HAARP is operated jointly by NRL and the Space Effects Division, Geophysics Directorate, Air Force Phillips Laboratory, Hanscom AFB, MA, and was built by Advanced Power Technologies Inc. (APTI), a subsidiary of E-Systems.

Figure 25 illustrates the basic geometry behind the approach for generating ELF/VLF radiation by HF heating of a local region of the existing ionospheric current system. The ionospheric plasma is irradiated by a high power HF electromagnetic wave (a heater) which is modulated at an ELF/VLF rate. The electrons within the volume of plasma irradiated by the HF beam experience periodic heating at the HF modulation frequency. Since the conductivity of the ionosphere is electron-temperature dependent, the conductivity also varies periodically. The natural ionospheric currents which pass through the heated region are modulated by these conductivity changes. The plasma effectively demodulates the envelope of the heating wave which results in injection of radio wave, at the ELF/VLF modulation rate, into the earth-ionosphere waveguide. Thus, the HF heating process creates a wireless antenna in the ionosphere, such as that illustrated in Figure 25(b). By moving the modulated "clouds" in a 2- or 3-D pattern in the ionosphere and having the AUM receive the transmissive ELF waves at its underground position, a synthetic spatial aperture is created which can be used for imaging the UGF. Note that in order to make a half-wavelength antenna of the coiled tubing deployed to emplace the AUM, an insulating ring needs to be fabricated at the middle of the tubing antenna and at the ends, in order to create a dipole antenna.

If two or more AUMs are deployed simultaneously about a UGF, then it may also be possible to perform cross borehole EM imaging among the AUMs (sometimes called electric resistive (conductivity) tomography) by joint use of the GPR on board each AUM; the transmit power may need to be increased to make the signal level detectable.

Another possible application of the AUM for placement of surveillance sensors in UGFs is to deploy micro-robotic rovers once the AUM has penetrated the UGF wall, as illustrated in

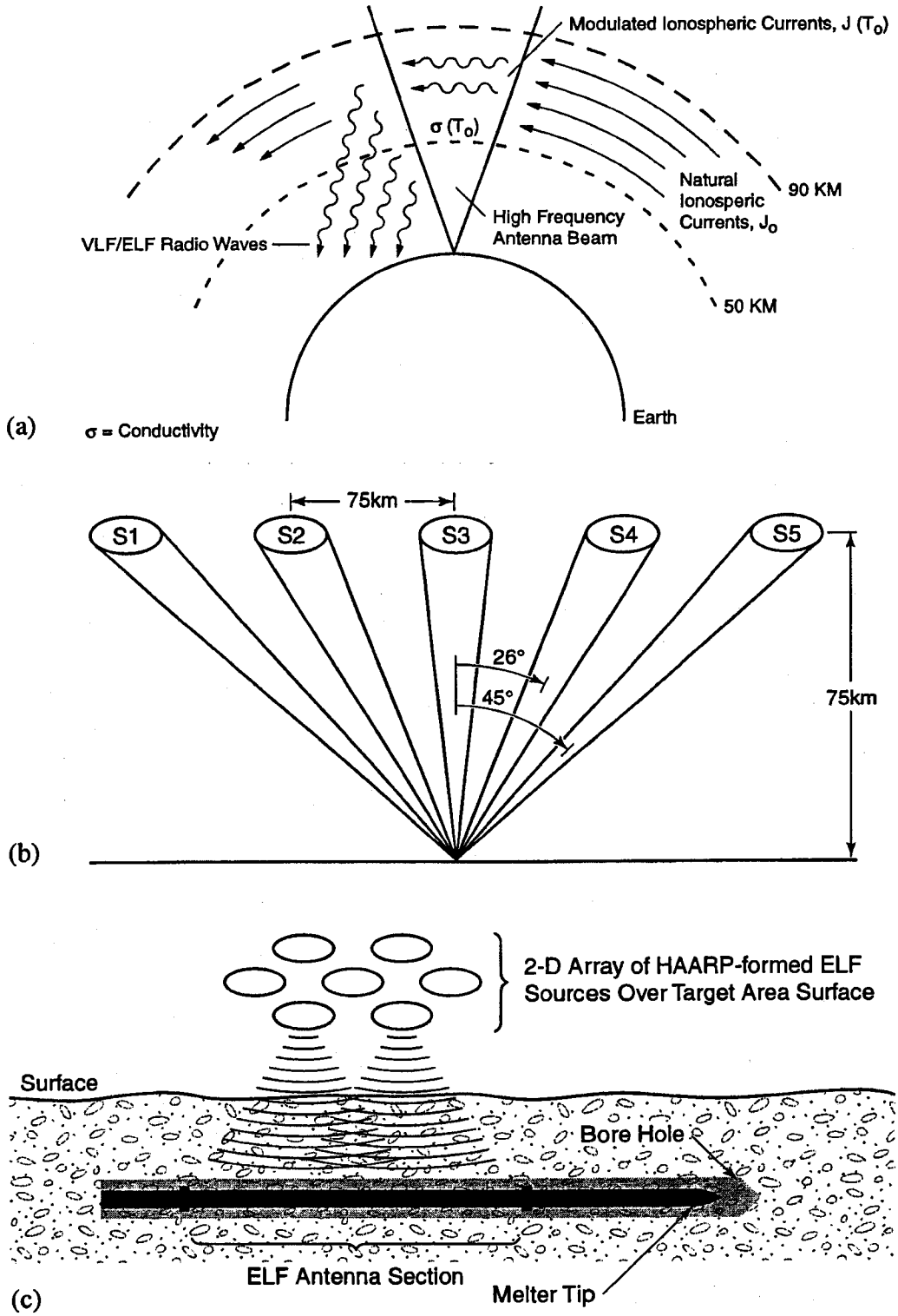

Figure 25. Using HAARP to Beam ELF Waves at Underground Facilities. (a) Ionospheric heating geometry for creating a single ionospheric dipole, (b) Illustration of a five-element linear array with half-wave spacing formed by five beams from a high-frequency ionospheric modulation facility like HAARP, (c) 2-D array possibility over UGF target

Figure 13. The rovers would transmit LPI sensor data to the AUM, which would relay the data to the surface antenna for exfiltration. This would be useful for UGFs that have enclosed buildings or huts within an underground chamber that need further exploration that would not be accomplished with a simple concrete wall penetration.

4.6 Data Exfiltration

The surface-based antenna will need to be camouflaged as a culturally blending object and will need to service the two-way communications needs of the AUM (control to the AUM and data from navigation or sensors from the AUM). Commands from a SATCOM or loitering UAV can instruct the AUM to modify its penetration operation. The AUM can send both compressed imagery from the GPR and other navigational data to status the boring progress and compressed data from its sensors once they are in position near or inside the UGF. There will be opportunities to develop specialized sensor data compression algorithms to minimize the number of bits that need to be transmitted, such as sending data only when imagery content changes.

We are proposing a data exfiltration communications approach based on merging two key technologies. These two technologies are (1) retrodirective phased array antennae implemented on microstrip and (2) active integrated antennae, in which the microwave circuitry is integrated with the antenna array elements on the microstrip. Dr. Tatsuo Itoh, the director of the Millimeter Wave Electronics group at the University of California, Los Angeles (UCLA), is a pioneer of the active integrated antenna technology, and we have had several technical discussions with him. These technologies enable a relatively simple integrated antenna assembly with much lower cost and power requirements than a comparable discrete element antenna and microwave electronics module implementation, and which due to its conformal capability can be fabricated into a camouflaged structure. The use of a retrodirective phased array antenna approach also offers some additional advantages over previously developed prototype data exfiltrators.

Retrodirective antennae are special self-adaptive phased arrays that reflect and focus incident RF waves coherently back toward the source without prior knowledge of either the source's location or the effects of phase distortion during propagation. Retrodirectivity is achieved by transmitting an outgoing wave from the transmit aperture that is the antiphase (phase-conjugate) of the incoming wave on the receive aperture. We are proposing for the AUMs that a data exfiltrator be developed based on a two-dimensional retrodirective phased array antenna consisting of phase-reflecting antenna microstrip patch elements integrated with heterodyning mixers and amplifiers. The antenna patch elements will utilize a cross-polarized mode scheme to permit *simultaneous* reception and transmission. Each antenna element in the array receives an incoming RF wave at one polarization and, after heterodyning with a self-generated local oscillator (LO) of twice the

frequency of the incoming signal using a mixer integral to the antenna patch, transmits it after amplification with an orthogonal polarization and a conjugate phase shift imparted to it. This process avoids complex and power-consuming data exfiltrator schemes that require sophisticated phase-locking to the received RF pulse in order to regenerate a time-delayed coherent modulated pulse after the incident pulse has passed or the use of high-speed RF switching (chopping) and coax line delays to alternate between receive and transmit functions in order to utilize the same antenna. The use of orthogonal receive and transmit polarizations provides an additional benefit for a polarization-sensitive radar (many modern synthetic aperture radar (SAR) systems have implemented this capability), which can exploit the polarization change to distinguish the retrodirective beam from incidental backscatter off the array and its surroundings.

The proposed implementation of a data exfiltrator based on a retrodirective phased array of integrated active antenna elements has two additional benefits. First, the retrodirective phased array antenna data exfiltrator, when activated by an interrogating radar and with no transponded sensor data modulation, will simply reflect an amplified signal back to the interrogating source exactly as received with zero temporal latency due to simultaneous receive and transmit capability. In essence, the retrodirective array acts as an electronic corner reflector with gain. No special signal processing operations or adjustments for delays are necessary in order for the interrogating radar's signal processor to locate and highlight the position of the tag in the processed radar scene or image, because the return signal looks like any other strong target echo signal. Second, the use of the heterodyning technique with the proposed retrodirective array data exfiltrator will properly create a phase-conjugated reflection of any irregular wavefront. Thus, the antenna array is not restricted to be planar or symmetric in its arrangement of antenna elements. In fact, the antenna can be conformal to any convenient shape that can be fabricated with microstrip. For example, a flat planar retrodirective array data exfiltrator form factor as shown in Figure 26(a) would be easy to camouflage and hide as a flat surface. Also possible is a conformal antenna that could be shaped as a natural feature such as a rock in Figure 26(b) or as a man-made object such as a helmet in Figure 26(c)). There is no change in the interrogating radar's processing to accommodate arbitrary tag shapes as the retrodirective array will produce a coherent echo back to the radar independent of tag shape.

Prior implementations of retrodirective arrays have been small 1-D or 2-D arrays involving totally passive or nonamplified active microwave circuit components. These designs satisfied applications for retrodirective arrays, such as packaging RF identification, where the interrogating RF source was close to the array. The retrodirective array data exfiltrator that we are proposing adds two new microwave design dimensions: larger arrays and distributed amplification over individual antenna elements. Both are required to provide gain in order for the

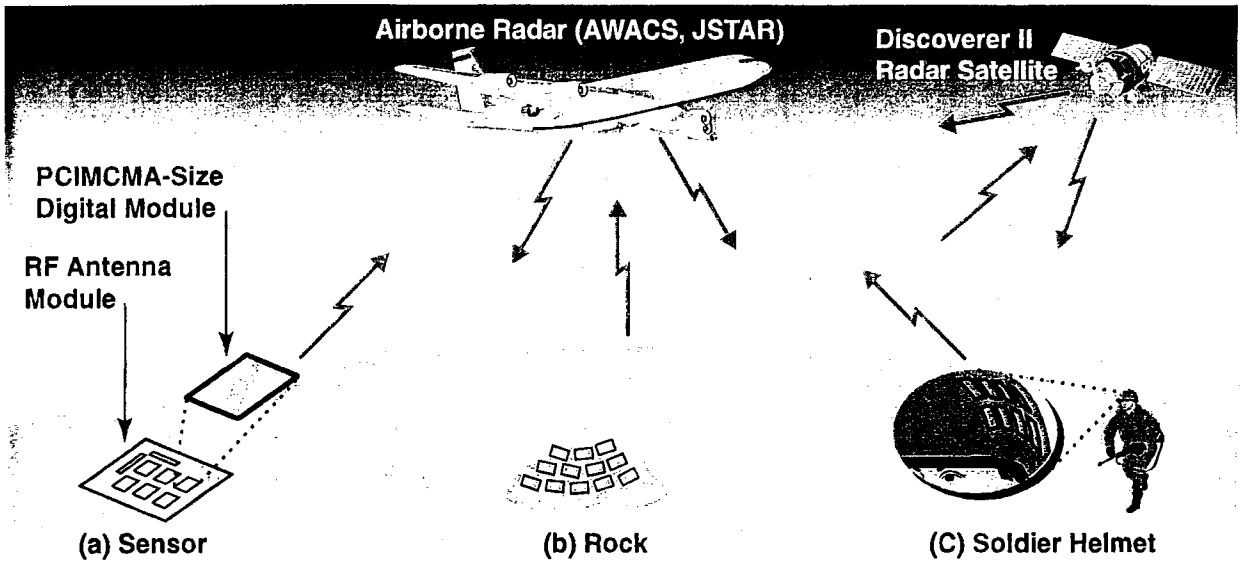

Figure 26. Representative Data Exfiltrator Form Factors Possible for Retrodirective Phased Array Antenna With Integrated Active Microwave Components

retrodirective array data exfiltrator to have link margins that work with airborne or space-borne radar systems that are far from the tag. Critical design issues to develop integrated mixer and amplifier designs that can operate successfully with the microwave RF behavior of patch antennae will need to be resolved in the phased program described in Section 5, as these have not been studied previously. Similarly, high drive capable local oscillators (LOs) that can provide a common LO frequency to a large array of antenna elements will need to be studied, fabricated, and tested to develop appropriate designs for retrodirective arrays. The technique can be scaled for radar bands from UHF to Ka.

For modulation of the data to be exfiltrated, we are proposing binary phase shift keying (BPSK), with the modulated ID of the AUM and data being applied to the common heterodyning LO before it is distributed to all antenna elements of the phased array. Classical direct sequence spread-spectrum (DS-SS) with code-division multiple-access (CDMA) compatible orthogonal spread sequences (to permit separation of simultaneously received responses in case multiple AUMs have been deployed) is proposed to provide LPI security of the AUM's data. Because the data exfiltrator approach simply reflects coherently the impinging radar pulse back to the source, the modulation can only be applied during the pulse duration of the impinging radar pulse. One design to accomplish this would use a crystal-controlled relatively low-frequency modulation clock at the chip rate of the spreading sequence, suggested to be in the 10- to 50-MHz range depending on link margin requirements. This clock will be synchronized with the detected start of the impinging pulse, but will not be phase coherent or synchronized with the phase of the

received pulse. This greatly simplifies the modulation scheme over more traditional comm link approaches that use phase lock loops. This modulation is radar platform independent. Rather than tie into the radar's processor to retrieve the exfiltrated data, we believe it will be more cost effective to have an independent processor operate on the baseband output of the radar receiver with pulse timing cues provided by the radar processor to the independent processor in order to recover the AUM navigation or sensor data.

We envision a data exfiltrator that has two components. First, the RF component would be the planar or conformal surface retrodirective array antenna with integrated microwave components tuned for the radar band of the radar system expected to interrogate the data exfiltration antenna (most likely will be X band). Second, a special universal digital component would be connected to the antenna component of any band to complete the data exfiltrator. This digital component has the ID, encryption, modulation formatting, exfiltrator triggering hardware, and crystal oscillator that would fit into a PCMCIA-size sealed module. It would be a one-time use module with a volatile encryption memory that would erase when the battery dies or the device is tampered with. It is anticipated this one-time use digital module would cost about $10 in production quantities. The throw-away cost effectiveness is a low probability of exploitation (LPE) security feature. The length of the pulse transmitted from the radar interrogator source to the data exfiltrator determines the duration that modulation can be applied, so it is conceivable that one long pulse could read out the entire data stream. A radar system that is not pulse-duration agile could recover portions of the data to be exfiltrated with each transmitted pulse, and it would take longer to recover the data to be exfiltrated.

The use of a phase array antenna for the data exfiltrator provides an additional low probability of detection (LPD) security feature because the antenna is not omnidirectional, unlike the available exfiltration devices, which are omnidirectional. Due to reduced sidelobes and source directionality of the retrodirective phased array, it is difficult to intercept unless one is directly in line between the interrogating radar system and the data exfiltration antenna. The standby power of this proposed comm scheme will likely be sub-milliwatt as the amplifiers in the antenna array will not draw power unless stimulated with an applied signal. This helps conserve battery power for long mission life.

The microstrip integrated antenna approach used in this proposed data exfiltrator design could be expanded to create a patch antenna for feeding signals to a GPS receiver. This makes it possible to integrate compactly a GPS-receiver so that location as well as sensor can be exfiltrated. This could be important for the bistatic mapping missions where the AUM location must be known accurately in order to create undistorted volumetric images.

Technical Details. In this subsection, we review some of prior work and benefits of integrated antenna retrodirective arrays. We also introduce some of the design issues in the use of active integrated antenna technology to implement such arrays. Active integrated antennae, a technology area pioneered by Dr. Tatsuo Itoh of UCLA [Lin and Itoh], integrate passive antenna elements and active microwave circuitry on the same substrate, using modern MIC and MMIC fabrication technology, to realize compact, lightweight, low-cost active integrated antennae. A retrodirective array represents a special type of phased array antenna that reflects any incident signal primarily back toward the source, without prior knowledge of the source's location. From the antenna's point of view, a retrodirective array has an omnidirectional receive coverage capability while simultaneously maintaining a high antenna transmission gain directionality, which is difficult to achieve with conventional types of antennae or nonretrodirective antenna arrays [Hewitt, Margerum, Skolnk, and King]. To realize retrodirection, each element in the array must radiate an outgoing wave whose phase is conjugate to that of the incoming signal, relative to a common reference. One of the most well-known retrodirective arrays is the Van Atta array, where conjugated elements of a symmetric array are connected by transmission lines of equal length to form a totally passive retrodirective array [Sharp and Diab].

To overcome the limitations on the requirement of symmetry of the array and a linear uniformity of the phasefront (i.e., a plane wave) in the Van Atta array, a more general approach of phase conjugation based on heterodyne mixing has been explored [Culter et al., Pon]. This method exploits the conjugate phase shift induced in the lower-sideband product of a frequency mixing operation; by mixing the incoming signal with a reference signal at twice the frequency, the original frequency is obtained as the difference and the resulting phase is inverted. Specifically, if the incoming signal is $\cos(2\pi ft + \theta)$ and an LO of form $A\cos(2\pi[2f]t + \phi)$ with amplitude A and phase component ϕ is used as the mixing source, then the resultant output is

$$(A/2)\cos(2\pi - \theta + \phi) + (A/2)\cos(4\pi f - \theta + \phi).$$

The sum frequency component is filtered out, leaving the difference frequency component with a sign-inverted (conjugated) phase term -θ. Note that an automatic gain control (AGC) of the output of all array elements can be accomplished by adjusting the LO amplitude A. Also, a BPSK phase modulation can be applied to all antenna elements through the mixer by phase modulating the ϕ phase term. Since inversion of the wavefront phase occurs directly at each element of the array, retrodirectivity does not depend on the symmetry of the array or the linear uniformity of the wavefront. This means that irregularly spaced, nonplanar arrays can be made retrodirective, which is an attractive feature when antennae conformal to the surface of an object must be

designed. Early heterodyne-retrodirective arrays were built from packaged mixer modules and separate antennae, using rectangular or coaxial waveguide [Pon, 1964].

There is a misconception in the literature that the phase conjugation of retrodirectivity compensates for the time delays of the impinging wavefront on the antenna array, as shown in Figure 27(a). Retrodirectivity only causes phase alignment of the retrodirected beam to create a coherent response back to the interrogating source. There is still temporal misalignment that causes edge effects in the retrodirected pulse back to the radar, as illustrated in Figure 27(b). For an X-band retrodirective array data exfiltrator, for example, this transition edge effect on the echoed pulse is less than 1 ns in duration. The effect is usually negligible and the retrodirective array will perform quite well in its intended function as a data exfiltrator when interrogated by airborne or space-borne radar systems.

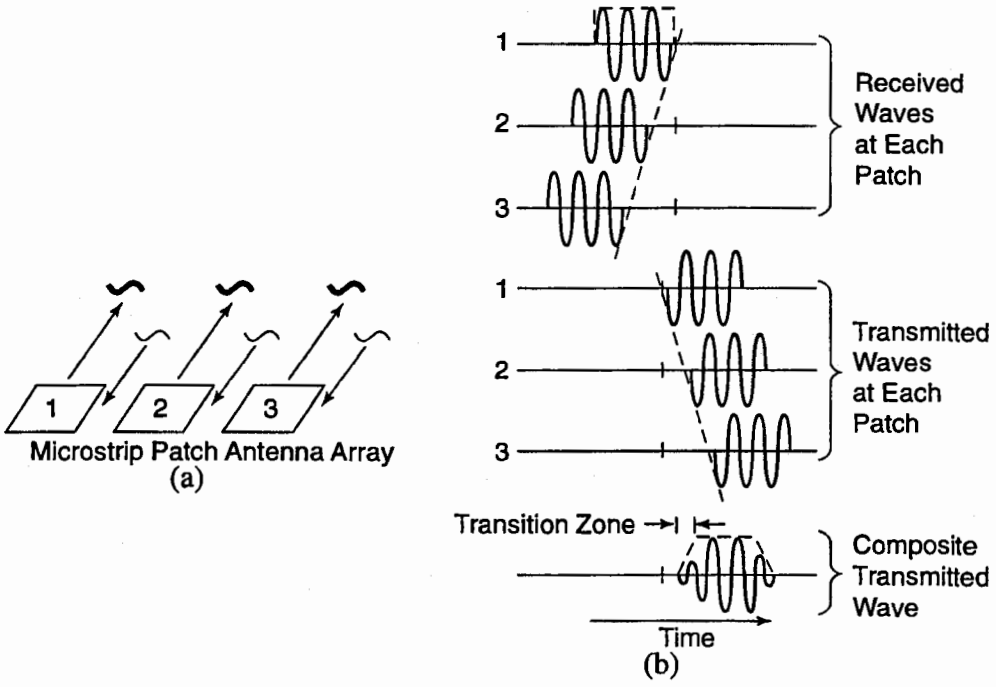

Figure 27. Illustration of the Transition Effect of Echoed Pulses From Retrodirective Phase Array Antennae. (a) Impinging wavefront on a linear array. (b) Time diagram of the phasing of the echoed pulse from the retrodirective array.

Microstrip circuits are an attractive alternative to discrete packaged microwave implementations due to their thin profile, their capability of forming conformal antennae, and their ability to design low-power antenna systems for long operation off battery power. The development of active integrated antennae based on microwave circuits built from microstrip has been used by

Dr. Itoh to produce the first RF identification (ID) transponder by such a technology, [Pobanz and Itoh, 1995] as illustrated in Figure 28, for use in noncontact tagging of inventory. As this device was only intended for use as a transponder within a few feet of the RF interrogating source, it did not require a transponding antenna array. The RF ID device of Figure 28 has a single slot antenna for receive detection and a single bowtie transponding antenna. This RF ID device demonstrated the capability of integrated active antenna technology to create a compact, low-cost, low-power RF transponding device.

To make the data exfiltrator transponder response more directional in order to enhance detectability, several researchers have started investigating integrated active antennae that implement retrodirective arrays [Pobanz and Itoh Karode and Fusco, Chen and Chung]. The most challenging part in designing mixers for retrodirective arrays fabricated from microstrip is the separation (radio frequency isolation) of input and output signals, which correspond respectively to the RF and IF ports of the mixer, even though they may share the same frequency if an LO of double the input frequency is employed. Isolation between these signals is required in order to preserve the desired conjugate-phase relationship, or else the beam radiated by the array will waste power in the specular direction or be otherwise distorted. Since filtering is impossible due to the shared frequency, alternative approaches to RF/IF isolation are required. Figure 29 is a photo of a one-dimensional (1-D) linear retrodirective array designed by Dr. Itoh's team at UCLA [Pobanz and Itoh, 1995]. The implementation used a novel heterodyne-phased scattering element, employing a square patch antenna, and a modified "rat race" mixer where the LO and IF are interchanged so that effective RF/IF isolation is realized. Figure 29 illustrates that the prototype was an eight-element linear array using a spacing of 0.8 wavelengths between antenna elements and a 6-GHz operational frequency (a 12-GHz LO was therefore used to create a conjugate phase response along the array). The array was proven during laboratory tests to redirect the interrogating microwave signal back to its source, for any angle of incidence and any type of polarization, linear and circular of either rotational sense. The omnidirectional receive capability of the linear retrodirective array was proven by measurements to have a retrodirective response over a 100-degree azimuthal range. Similar microstrip designs employing two-element retrodirective arrays involving power dividers or dual polarized patch antennae have also been reported by Karode and Fusco recently [Karode and Fusco, September 1997 and December 1997].

Dr. Itoh's UCLA group has also designed and fabricated a 6-MHz two-dimensional 4x4 retrodirective array based on slot ring antennae and the heterodyne-phasing technique [Pobanz and Itoh, 1996], which is illustrated by the Figure 30 photo. The array spacing was 7/8 of the wavelength of the 6-GHz operation frequency. Each array element comprises a balanced FET resistive mixer, integrated in a ring slot that serves as both the radiating antenna and the hybrid for RF/IF isolation.

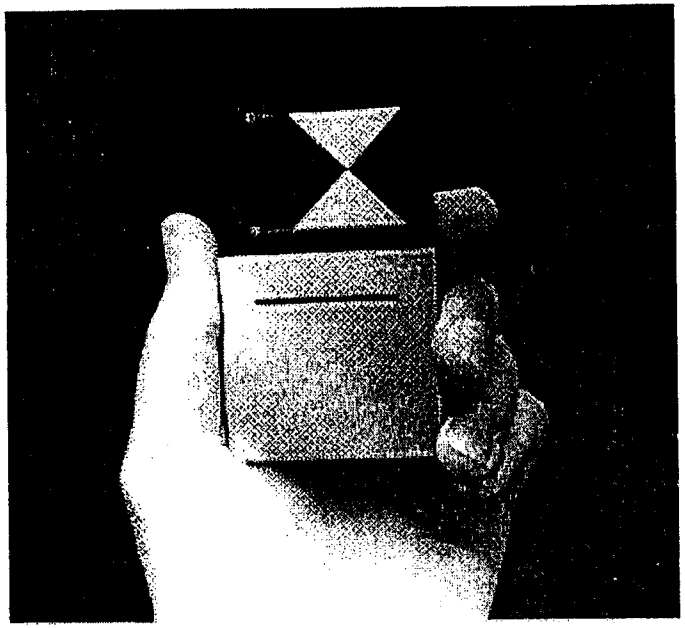

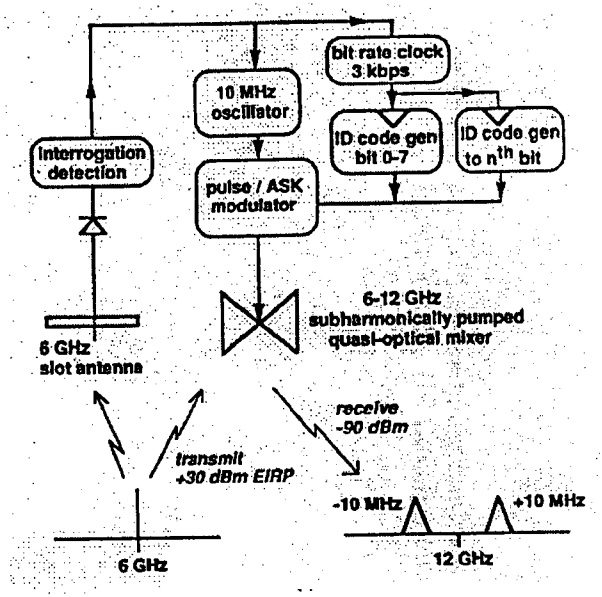

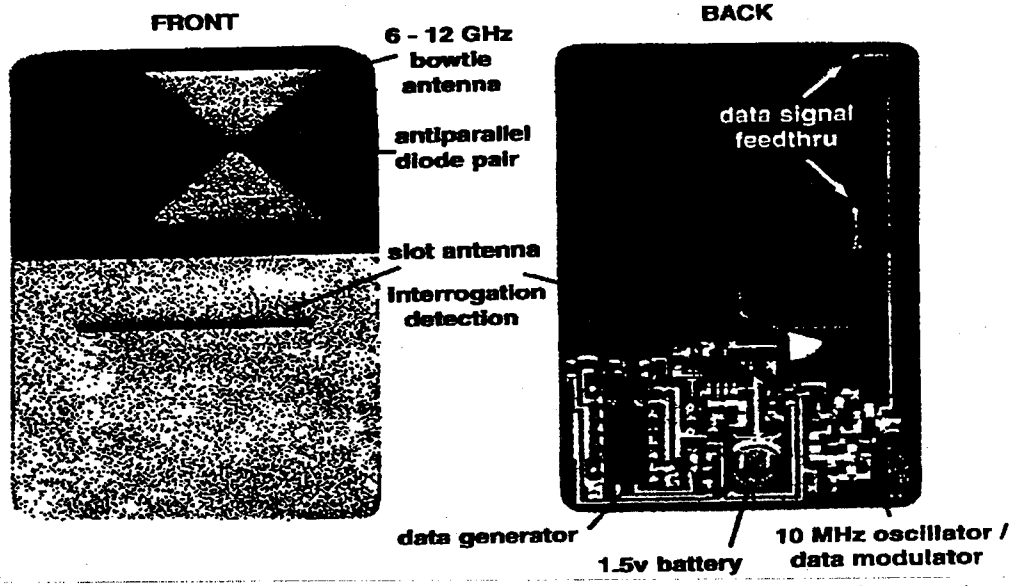

Figure 28. Single Transponding Integrated Active Antenna Transponder. (a) Credit-card size form factor transponder in RF tag application. (b) Circuit design. (c) Close-up of front and back views of the microstrip.

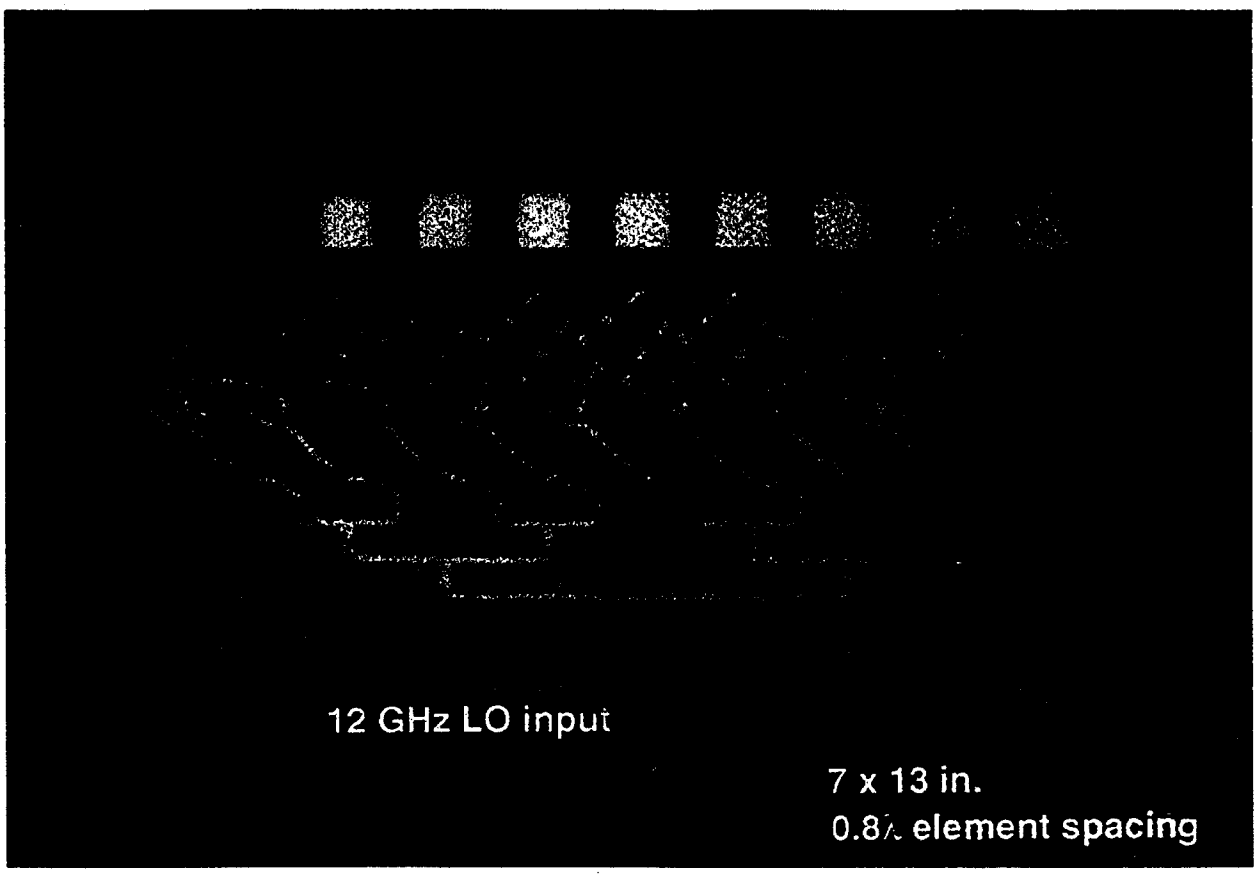

Figure 29. One-Dimensional Retrodirective Phased Array Implemented as an Active Integrated Antenna on Microstrip

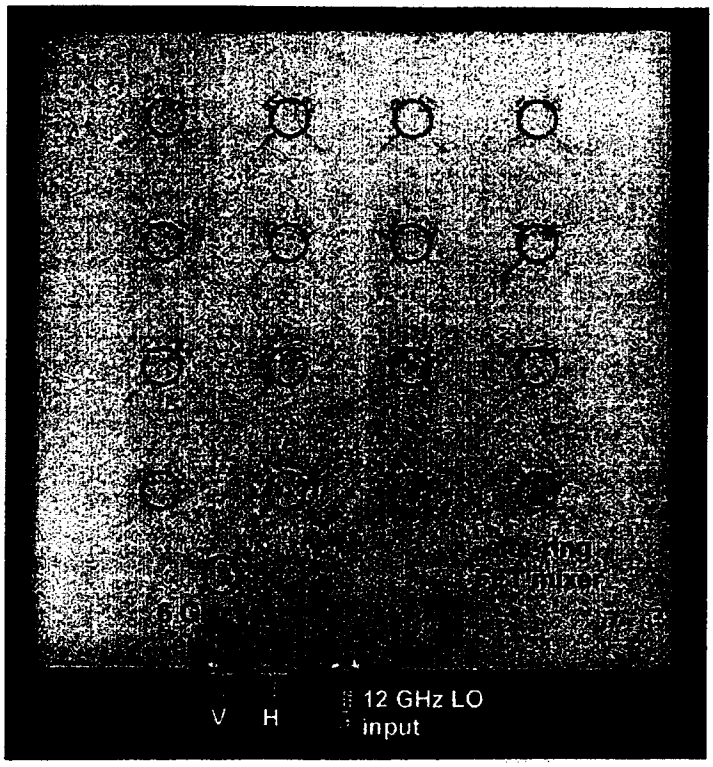

Figure 30. Two-Dimensional Retrodirective Phase Array Implemented as an Active Integrated Antenna on Microstrip

The backscatter pattern of this array exhibits over 100 degrees of scan range in both azimuth and elevation planes. A free-running 12-GHz LO was used as the reference slightly offset in frequency in order to separate the array backscatter from room reflections to make measurements more easily. However, in practice, a frequency-doubling of the signal received by a reference element with orthogonal feeds could be performed and applied to the array, enabling a self-contained retrodirective transponder to be formed. One interesting capability of 2-D retrodirective arrays was demonstrated with this unit. Retrodirective arrays, being self-adaptive, have a graceful degradation in response as a percentage of obstruction. Figure 31 illustrates the roll-off in performance obtained with the 4x4 array to such obstruction or failure of antenna elements.

Technical Approach. Figure 32 depicts the proposed retrodirective phased array data exfiltrator architecture. It consists of two sections: an RF section and a digital section containing the ID, data formatting and modulation, and encryption (security) components of the data exfiltration system. The RF section is further subdivided into the active phased array component and a reference monitoring receiver with a separate pair of orthogonally polarized antennae to detect the interrogating radar signal.

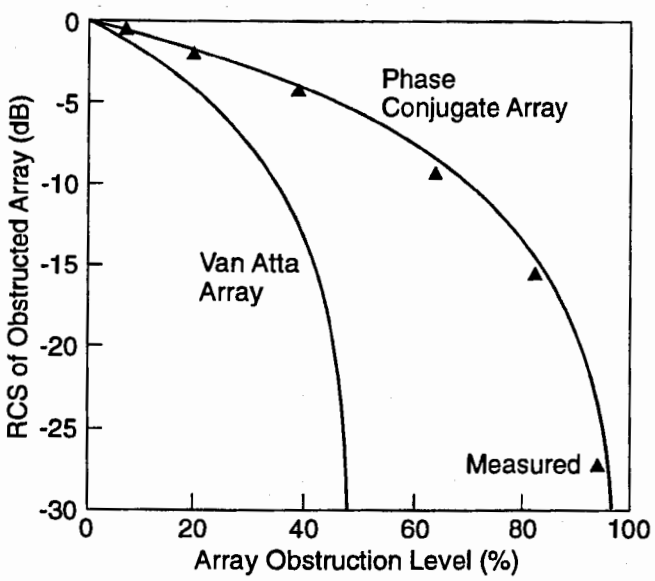

Figure 31. Effect of Obstruction (Array Elements Blocked or Out of View) or Element Failure on the Radar Cross-Section (Transponder Response Magnitude) of a 4x4 Retrodirective Array

The monitoring receiver is constantly powered and detects energy within its RF band. The detected energy is thresholded to one bit and passed to pattern analysis logic in the digital section. A temporal analysis of the pulse interval durations and pulse width durations, such as that depicted in Figure 33, will determine if the interrogating signal is from a recognized interrogating radar source. This analysis can be coded into the memory of the digital section and changed for security purposes. If a recognized pulse sequence is detected, then a powering up from the very low-power monitoring state will activate the retrodirective array circuitry for transmission and will activate the sensor data modulation and encryption circuitry. We envision a one-time encryption pad in volatile memory that would be erased if the battery dies or the device is tampered with. The data message would be ANDed with the one-time pad and concatenated with the ID number, then formatted for presentation to the BPSK modulator in the RF section of the tag (basically a +1 or -1 gain switcher). The BPSK modulator would act on an LO signal created by frequency-doubling circuitry off a tap from the monitoring receiver that has its own reference slot antenna elements fabricated on the microstrip. The LO driver to the phased array would optionally have an AGC control. The purpose of the AGC is to provide, based on received signal strength, a constant signal level retrodirected back to the interrogating source regardless of range. This is needed so that the CDMA spread-spectrum decoding will work properly (the near/far problem of multiple access spread-spectrum signaling) to separate simultaneously received signals from multiple AUMs that may have been deployed. However, we are proposing a processing scheme based on range gating, so the overlap of tag signals will tend to only occur for tags at about the same range. If this works out in practice, then the AGC will not be needed. The common LO is fed to all antenna patch elements of the phased array.

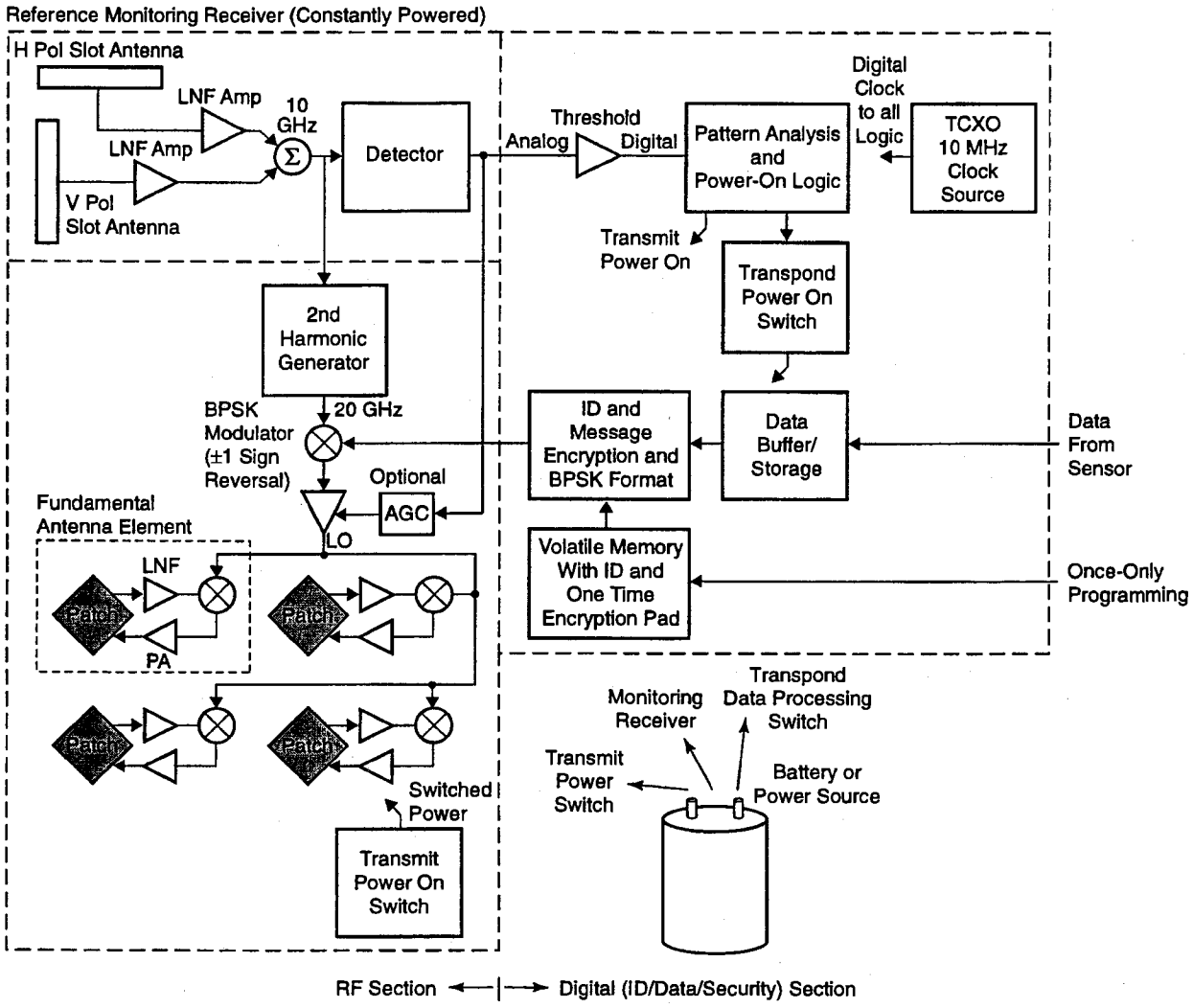

Figure 32. Architecture of Proposed Retrodirective Phased Array Data Exfiltration System

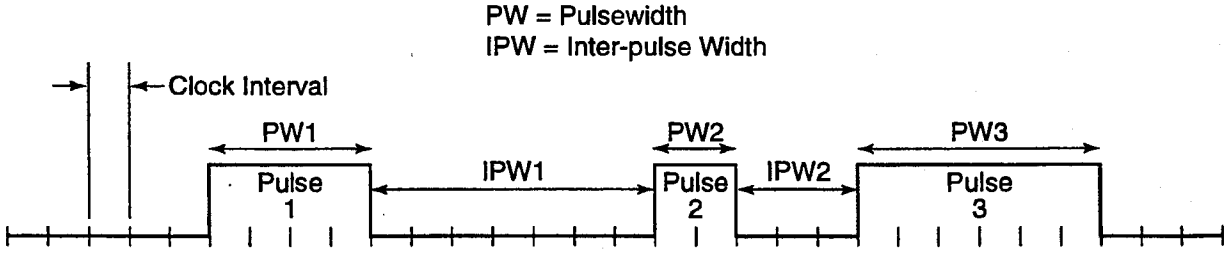

Figure 33. Depiction of Pulse Interval and Pulsewidth Parameters That Could be Used to Activate the Proposed Data Exfiltrator

Mixing and amplification occurs locally to each antenna element. The mixer performs the phase conjugation needed to make the array behave as a retrodirective antenna.

A net signal to noise ratio (S/N) of about 8 dB is needed to achieve a fairly high probability of correct bit detection in BPSK. Adding a link margin of about 2 to 3 dB is typically done to ensure good detection performance over changing EM conditions. The S/N is determined fundamentally by the formula

$$S/N = \frac{PG_tG_r\lambda^2G_p}{(4\pi)^2R^2KTB}$$

where P is the transmit power from the retrodirective array, G_t is the retrodirective array gain, G_r is the slot receive antenna gain, λ is the signal wavelength, G_p is the spread-spectrum processing gain, R is the range between the exfiltration antenna and the interrogating radar, K is Boltzman's constant, T is time interval of transmission/retrodirectivity, and B is the signal bandwidth (the dB form of the formula would be used). Assuming an X-band radar, typical design parameters for the retrodirective method of exfiltration would need 4W transmit power, 52 dB of receiver gain (received power assumed to be in the range of -90 to -20 dBm), and 20 dB of retrodirective array gain (yielding a transmit power of +24 dBm), which provides 70 dB isolation between the receive and transmit operations.

While the prior work of Dr. Itoh's group has demonstrated both linear and two-dimensional retrodirective arrays that are very compact, conformal, and low-cost, the previous designs emphasized the highest degree of integration, and did not allow the insertion of either low noise amplifiers (LNA) in the receiving path or power amplifiers (PA) in the transmitting path. If fact, the incoming RF and outgoing IF, which are at the same frequency, share the same antenna as well as the same feed lines, in order to take full advantage of the intrinsic diplexing capabilities of the antenna.

To realize a retrodirective array for application as a data exfiltrator, we need to modify the design topology so that both LNAs and PAs can be inserted at each element of the array. Figure 34 shows the schematic of a 4x4 element array configuration of the proposed phased array component of the data exfiltrator and Figure 35 details one element of the proposed structure for this amplified retrodirective transponder serving as a data exfiltrator. The incoming RF and IF will share the same patch antenna, using the two orthogonal modes (TM10 and TM01) of the patch. An LO signal at twice the RF frequency will mix with the RF signal, generating an IF with the same frequency as the RF, but a reversed phase. Since this heterodyne mixing and phase conjugation occur at each element of the 2-D array, a compact, high-gain retrodirective array is realized.

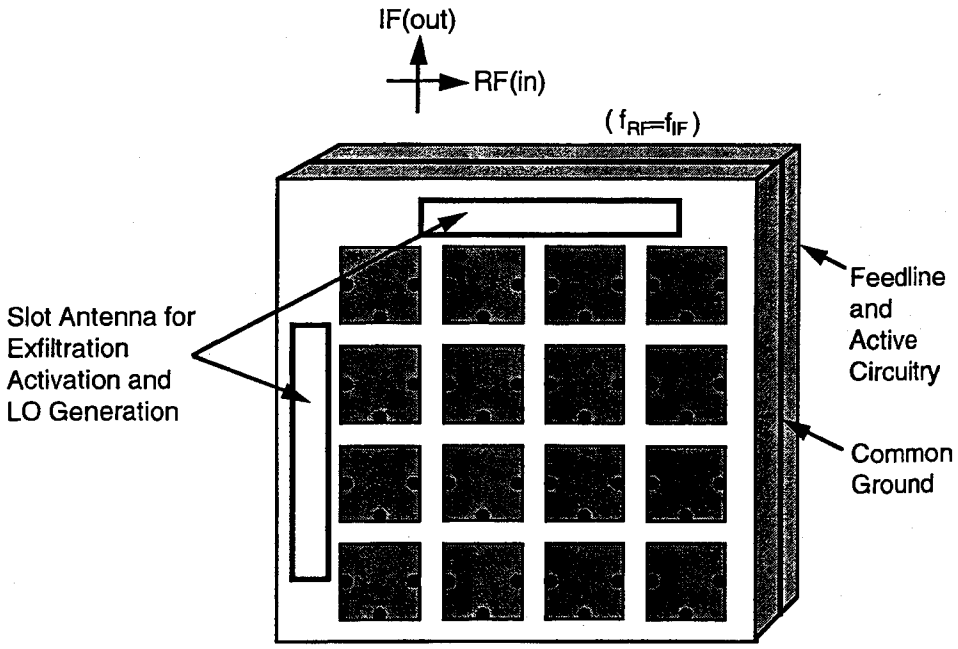

Figure 34. Depiction of the Microstrip Layout of the Proposed Data Exfiltrator. A 4x4 array is shown, although a larger array may be required to satisfy link margins.

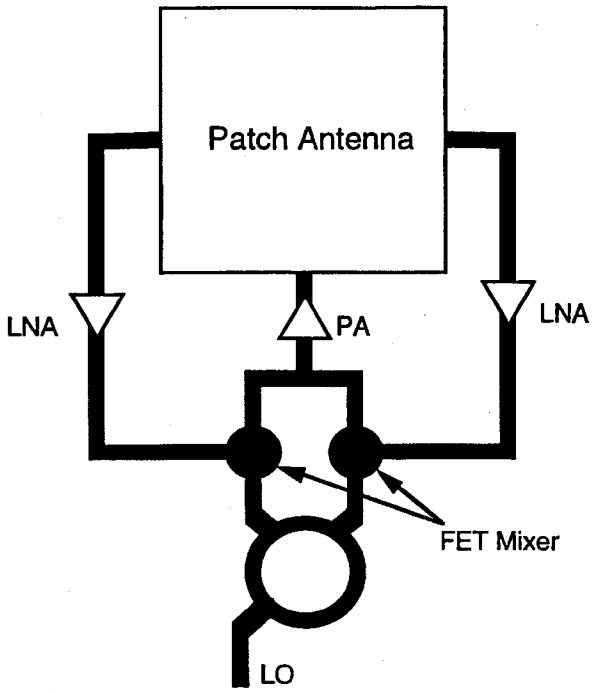

Figure 35. Details of Microwave Topology at One Antenna Patch Element of the Retrodirective Phased Array

Several very challenging technical issues exist, however, that need to be investigated as part of the proposed AUM technology development program before a full-scale design of a data exfiltrator is initiated:

(1) Since the element spacing in a 2-D retrodirective array cannot exceed one wavelength in both directions, we have a very stringent limit on substrate real estate to accommodate the heterodyne mixer. As shown in Figure 35 it is desirable to use the two opposite radiating edges of the patch to realize a 180-degree hybrid for the RF, and a pair of FET mixers with a rat race ring to cancel LO and RF and combine the IF signal. It must be verified with the proposed design topology that a reasonable level of conversion loss and signal cancellation can be achieved.

(2) The maximum isolation between the two orthogonal modes of the patch antenna will also put an upper limit to the maximum gain achievable at each element. This can be compensated for by the increased gain of the 2-D antenna array to some extent (a 5x5 array, for example, provides a 28-dB gain). A design trade-off between amplifier gain and array gain will need to be studied in detail.

(3) Because of the unconventional port arrangement of the balanced mixers that is essential to the proposed design architecture, a higher level of LO power is required in order to make the two FETs work in a switching mode. Additional difficulties might arise when this LO signal has to be distributed over the whole 2-D array. Another issue is to cope with the possible sweeping in RF frequency when a SAR-based interrogating radar is used. One approach is to use a separate receiving antenna with frequency doubler and amplifiers to generate the required LO signal for the mixers as proposed for the monitoring receiver. The advantage is that the LO will be able to track the RF sweep and keep an exact phase conjugation even if the RF frequency deviates to a substantial extent. The technical challenge is to design an efficient circuitry to meet this requirement, which at the same time can be integrated comfortably into the retrodirective array without causing major system degradation.

We note here that the integrated antenna approach we have proposed makes it possible to incorporate multiple arrays on the same substrate. For example, two orthogonally polarized retrodirective arrays can match to all the incident energy on the exfiltration antenna, regardless of its polarization. Other radar frequency bands can be accommodating by scaling the antenna patch size to "tune" to the band frequency, as shown in Figure 36. The substrate can accommodate the slot antennae of the monitoring receiver, and antenna patches can also be added for a GPS receiver for those data exfiltrators that message back their geoposition as well as the sensor data.

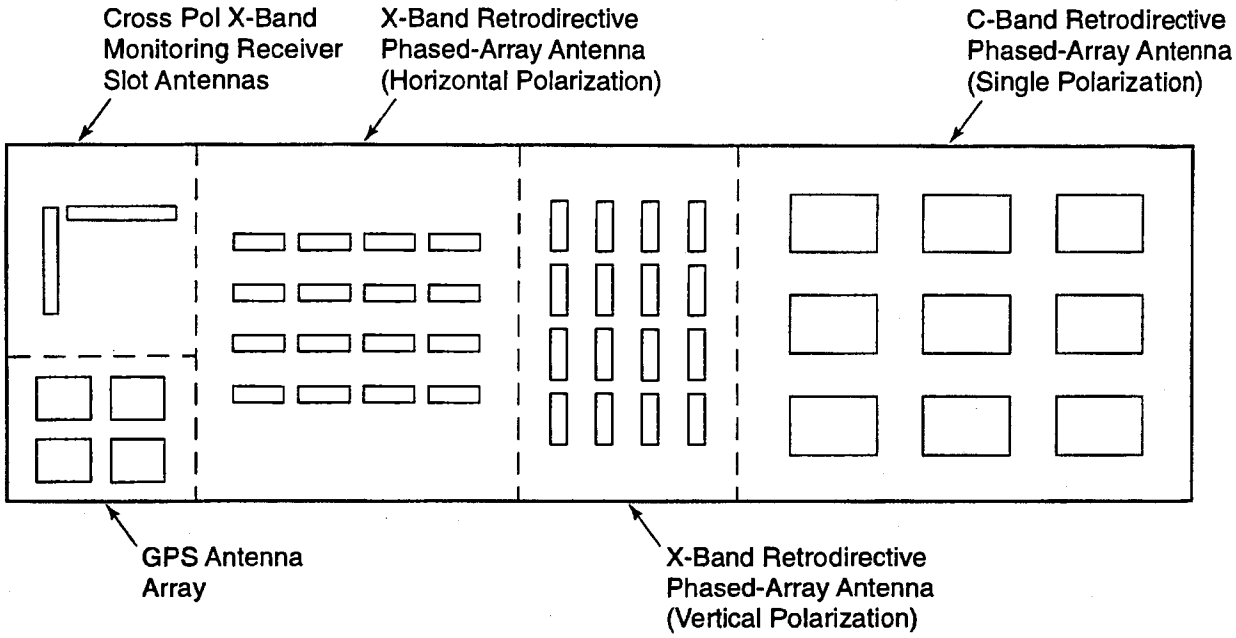

Figure 36. Multiple Antenna Configuration on a Microstrip to Handle Multiple Radar Bands and GPS Reception

5.0 PROPOSED PROGRAM PLAN

5.1 Objectives

This section proposes a multiphased program for developing the autonomous underground microborer to spread the development risk, attacking the highest risk technology items first before advancing to more sophisticated mission scenarios. Three mission scenarios (entrance monitoring, chamber/tunnel bistatic mapping using either GPR or ELF waves from HAARP, interior sensor placement) were proposed in the conops section in an increasing order of complexity. The entrance monitoring mission involves the least complexity and the least accuracy in sensor placement, and it does not involve penetrating concrete walls. Thus, technology development should be directed first to this mission as it involves the least risks. If an AUM collection system based on a monitoring mission succeeds, then the mission of slightly higher complexity is the mapping mission. This involves development of an associated UGS sensor array, which is currently in development by DSWA (TUGS contractors LLNL and Sandia) and DARPA (IUGS contractor Hughes). The mission of most complexity involves placement of sensors through UGF chamber walls, which necessitates more sophisticated navigation, quiet drilling, and accurate placement of sensors. This would represent upgraded onboard electronics from that needed to support the monitoring mission AUM and the addition of the final drilling mechanism. The mission that places sensors in walls of chambers would likely occur after an earlier AUM mapping mission had scouted the details of the underground facility.

The following subsections propose a multiphased effort to provide near-, mid-, and far-term AUM systems of increasing complexity.

Phase 0. Detailed Project Planning and Requirements. This phase is the preparatory phase to establish the specific requirements, program schedule, and program cost to which DARPA will sign up. Funding for preliminary design concepts from the major technology sources identified in this report may be required to obtain better first-order design concepts to firm up the requirements and schedule may be required. The Phase II SBIR process can be utilized for some of the funding in the Phase 0 effort.

5.2 Phase 1

Phase 1. System Requirement and Basic Autonomous Underground Microborer Design. The basic specifications and performance and payload weight goals for all phases would be developed in this phase. The modules that make up the penetrator assembly and the assembly insertion mechanism are the primary components to be developed and tested in this phase. The penetrator tip design, the fuel source, the propulsion mechanism, and the first system-level

underground navigational subsystem would be the technical focal points. Goals of Phase 1 are to demonstrate that a fuel-heated melting tip can maneuver the assembly underground while microboring, that the thrusting mechanism will force penetration, and that the navigational system can detect underground obstacles and can accurately determine the penetrator's location underground. A fixed surface insertion unit (not flown in by UAV) for limited penetrations (less than 500 m) to test the insertion mechanism and the capability to deliver an EO sensor to a designated target location is proposed for Phase 1. The estimated cost for Phase 1 is $3.5M, plus additional costs for the microsensors specified to be used, over a 24 month period. The cost breakdown is $1.5M to LANL for the rock-melt penetrator, $0.75M to LLNL for adaptations of the micropower impulse radar for the underground navigation role, $0.75M for system engineering, and the balance for miscellaneous engineering, including early work on the exfiltration retrodirective array. Phase 1 will validate the most risky critical technologies and provide data on energy usage per kilogram of fuel per meter of penetrated earth and the refine the diameter to use for microboring with the proposed coiled-tubing inserted/thrusted penetrator.

5.3 Phase 2

Phase 2. Integration of AUM Assembly with Mini-UAV. The next stage of AUM development would integrate the AUM assembly and insertion mechanism developed and tested in Phase 1 with the delivering mini-UAV. The insertion mechanism would be mated with the mini-UAV and a prototype exfiltration communication system would be integrated with the AUM electronics and a delivery mechanism on the mini-UAV. Tests would be conducted in which the mini-UAV would fly a prototype AUM to a designated penetration target location on the DSWA NTS test range in Nevada and would deploy it. This phase would test the integration of the mini-UAV and a prototype transportable AUM, now coupled to its exfiltrating communication subsystem, for delivery and insertion. The estimated cost for Phase 2 is $3M over a 24 month period, some of which could be concurrent with Phase 1. The cost includes $1M for purchase and re-engineering of an Omega Technologies TUSA to serve in the mini-UAV role, $0.5M for the prototype exfiltration communication subsystem, $1M for design and integration of the AUM with the mini-UAV, and $0.5M for range testing and recovery of the buried AUM. Phase 2 will validate the next most risky technology of precision soft-landing delivery of the AUM assembly at night. A monitoring mission will be simulated at the NTS.

5.4 Phase 3

Phase 3. Integration of Infiltrating UAV with Mini-UAV/AUM Payload. Phase 3 is envisioned as a full system demonstration of the monitoring mission. We propose that the designed and tested mini-UAV and AUM unit be integrated as a payload into the most mature UAV program that can

support the payload weight. The only near-term mature UAV is the Predator, and we have verified that wing-mounted payloads are possible. Although a stealth UAV would seem to be required for the AUM conops, the Predator has proven in Bosnia that it is quite difficult to aurally and visibly detect it unless it is at a very low altitude (below 1000 feet), so it should still be a satisfactory stealthy delivery vehicle to bring the mini-UAV and AUM payload within deployment range of a targeted UGF, especially if a 10-km or better standoff range can be supported. Phase 3 would provide a full monitoring mission demonstration, including launch from several hundred miles away from the target with a Predator, deployment of the mini-UAV carried as payload by the Predator, soft-landing and insertion and surveillance operation of the AUM, and simulated self-destruction of the mini-UAV(actually, have it dunk into a pond and be recovered). The estimated cost of Phase 3 is $6M over a 24-month duration. This includes $2M for purchasing a Predator with payload modification and the associated support facilities, $1M for the purchase of a second modified mini-UAV, $1M for additional AUM assemblies and upgrades, $1M for additional navigational, sensor, and drill mechanism design and integration and data compression algorithm development, and $1M for range testing and recovery of the AUM. If additional testing in more complicated terrain sites (e.g., UGFs in the United States that are in forested areas) than those in Nevada or Ft. Huachuca is deemed needed, additional test expenses will be required.

5.5 Phase 4

Phase 4. Demonstration of the Bistatic Mapping Mission. The additional electronics and augmentation of the ground-penetration radar not only to handle the underground navigational requirements, but also to act as the transmitted pulse source for bistatic radar imaging of underground facilities is a major focus of Phase 4. The demonstration must also include the deployment of available UGS sensor array over the test site so that the penetrating AUM with its modified GPR can be used to bistatically image the UGF tunnels and chambers. Tomographic imaging algorithms and UGS deployment scenarios will be developed in this phase. The proved system from Phase 3 with a modified GPR will be used to support the Phase 4 demo. Experiments with the HAARP transmitter in Alaska may optionally be performed to see if ELF waves can be detected by the antenna on the coiled tubing stem and used for purposes of imaging the UGF. The estimated cost of Phase 4, not including any experiments with HAARP, is $4M over a 24-month duration. This includes $1M to modify the ground-penetrating radar used for underground navigation to transmit focused impulses to support the bistatic imaging operation, $.5M to develop imaging algorithms and software, $1M for a UGS sensor array, and $1.5M for range testing and recovery of the AUM.

5.6 Phase 5

Phase 5. Demonstration of the Interior Wall Penetration Mission. An AUM with a coaxial drill component integrated with a coaxial sensor stem will be developed, integrated, and tested during this phase. Improved navigational and chamber wall detection GPR electronics and signal processing will be added to provide accurate location and wall boundary detection for placing in wall or through wall sensors in an UGF chamber or tunnel. A full mission demonstration by UAV infiltration, mini-UAV delivery to and insertion at the surface of a test range target, and penetration into and insertion of a sensor in a test range UGF wall at Nevada Test Site (NTS) will be performed. Another option would be to substitute delivery with the Boeing mini-spaceplane in lieu of the UAV employed in Phases 3 and 4 if this device is sufficiently operational at this point in the AUM program. The estimated cost of Phase 5 is $6M if the UAV of Phases 3 and 4 is used, plus optional expenses for the Boeing spaceplane demonstration of orbital re-entry means of delivering the AUM if it is considered. Base expenses without option include $2M for the drilling stem development and fabrication, $2M in AUM and UAV hardware mods, and $2M in range tests.

5.7 Technology Sources

Table 4 is a summary of the various key technologies identified in the concepts of operation section to produce the proposed autonomous underground microborer system. Candidate contractors and national labs that can provide the technologies are also indicated. The highest risk item is the rock-melting penetrator. Developing the most energy density efficient heating mechanism and maneuvering the heating tip underground are the two biggest challenges. The next highest risk item is the underground navigation techniques, both to determine position relative to the penetration point on the surface and to image/detect obstacles and chamber walls as the system approaches the targeted location. Deploying a mini-UAV of the proper payload weight and shape factor from a larger UAV is the next level down in risk. There are also operational risks in determining airspace infiltration scenarios for penetrating denied access territories, but those are not considered as they are not technology-driven risks.

5.8 ORINCON Capabilities

As the originator of the autonomous underground microborer, ORINCON is uniquely positioned to serve as the system engineers and system integrator for the proposed AUM program, and possibly the developer of the exfiltration comm system as well. A number of system engineers are on staff who have run programs as large or larger than this proposed program, including at least three who previously were Government employees who ran large technology programs for the CIA or the Navy. As a company, ORINCON is centrally located near to the companies,

Table 4. Technology Development to Support Autonomous Underground Microboring (AUM) System

Technology Development Areas	Technology Sources	Comments
Rock-Melting Maneuvering Penetrator Tip Design	LANL	Phase 1 - 5
Penetrator Fuel Source	LANL	Phase 1 - 5
AUM Cylinder Design and Propulsion Mechanism	System Integrator (TBD) and LANL	Phase 1 - 5
AUM Assembly Insertion	System Integrator (TBD)	Phase 1 - 5
Hi-Energy Density Batteries for Comm, Nav, Sensors	DARPA-ETO program	Phase 1 - 5
AUM-Insertion Mini-UAV	Omega Aerospace	Re-engineer for AUM (Phase 2)
Covert Communications Technologies	UCLA Microwave Dept TRW ASG Harris Comm.	Phase 2 - 5
Coaxial Drilling Mechanism	CIA	Phase 2 - 5
Micro Sensors, Imagers, Mics, Sniffers for Periscope Stem	DARPA-ETO JHU APL TRW ASG	MEMS Program Sensors (Phase 3) Mini-CAM Phase 2 - 5
Underground Navigation	DARPO-TTO USAF HAARP Program LLNL	Micro Inertial Nav Systems (Phase 3 - 5) ELF Communication (Phase 5) Micropower Impulse Radar (Phase 2 - 5)
Airspace Infiltrating UAV with Mini-UAV Payload Capability	General Atomics Teledyne-Ryan Lockheed-Boeing	Predator UAV (Phase 3 - 5) Global Hawk UAV (Phase 3 - 5) Dark Star UAV (Phase 3 - 5)
UGF Bistatic Radar Imaging	HAARP Program LLNL	USAF Phillips Lab, Hanscom AFB Micropower Impulse Radar (Phase 4 - 5)
UGS Sensors for Bistatic Imaging	DARPA-TTO (through Hughes) DSWA (through LLNL)	IUGS Program (Phase 4 - 5) TUGS Program (Phase 4 - 5)
Data Compression	DARPA-DSO Various Contractors	Image Data Compression Programs and IRAD Studies (Phase 3 - 5)
Mini Unmanned Space Plane	Boeing North American	Deployment from orbit (Phase 5)
ELF Comm and Geoposition	USAF FSR Phillips Lab, Hanscom AFB	HAARP Program (Phase 5)

national labs, and test ranges that would provide the proposed technologies and test sites to produce and demonstrate the envisioned autonomous underground microborer, which is essential to the level of collaboration needed to produce a successful near-term demonstration of the proposed AUM technology. Both General Atomics-Aeronautical Division and Teledyne-Ryan, respective manufacturers of the Predator and Global Hawk UAVs that are possible infiltration UAVs proposed here, are within miles of the ORINCON facility. Boeing North American Division in Seal Beach, CA has a prototype mini spaceplane that is being tested starting this fall. TRW Avionics and Surveillance Group in both Sunnyvale, CA and Space Park is proposed as a source for sensors and components of the exfiltration communications hardware. Lawrence Livermore National Laboratory (LLNL) in northern California is proposed as a source for micropower impulse ground penetration radar technology. Boeing, TRW, and LLNL are all within state. Los Alamos National Laboratory is proposed as a source for the rock-melt microboring technology and is a short commute flight to New Mexico. The DOE Nevada Test Site (NTS) is proposed as a demonstration location, and this site is within driving distance of San Diego. Omega Technologies, the proposed source for a mini-UAV, is located in Washington state, completing the western US consortium of technology companies and national labs.

6.0 RECOMMENDATIONS

Due to the highly critical need for the new technology concept to characterize UGFs that are currently impossible to characterize with available remote sensors, it is strongly recommended that DARPA initiate the proposed AUM development program.

7.0 REFERENCES AND BIBLIOGRAPHY

Anro Engineering, "Ultra-wideband (impulse) radar array systems for the detection of buried mines and bunkers, volume 2," technical report under contract DAAK70-93-C-0058, 12 March 1996.

Azevedo, S.G., and McEwan, T.E., "Micropower impulse radar," IEEE Potentials, pp. 15-20, April/May 1997.

Bailey, P.G., "History and applications of HAARP technologies: the high frequency active auroral research program," Proceedings of the Thirty-Second Intersociety Energy Conversion Engineering Conference, 27 July-1 August 1997, pp. 1317-1322.

Chen, H.-T., and Chung, S.-J., "Design of a planar array transponder with broad responding beam," *IEEE Microwave and Guided Wave Letters*, vol. 7, pp. 297-299, September 1997.

Cook, N.G., and Harvey, V.R., "An appraisal of rock excavation by mechanical, hydraulic, thermal, and electromagnetic means," Proceedings of the Third Congress of the International Society for Rock Mechanics, vol. 1, part B, pp. 1599-1615, September 1974.

Culter, C.C., Kompfner, R., and Tillotson, L.C., "A self-steering array repeater," *Bell System Technical Journal*, vol. 52, pp. 2013-2027, Sept. 1963.

De Gaudenzi, R., Garde, T., Giannetti, F., and Luise, M., "A performance comparison of orthogonal code division multiple-access techniques for mobile satellite communications," *IEEE Journal on Selected Areas in Communications*, vol. 13, pp. 325-331, February 1995.

Dressen, D.S., "DOE NN-20 Microboreholes Project," Los Alamos National Laboratory project report LA-UR-97-1052, 12 March 1997.

Earp, S.L., Hughes. E.S., and Elkins, T.J., "Ultra-wideband ground-penetrating radar for the detection of buried metallic mines," IEEE Aerospace and Electronic Systems Magazine, pp. 30-34, September 1996.

Ferraro, A.J. and Werner, D.H., "A technique using an ionospheric modification instrument to produce controllable and steerable low frequency ionospheric arrays for remote sensing applications", Proceedings Ninth International Conference on Antennae and Propagation, 4-7 April 1995, pp. 199-202.

Field, E.C., and Bloom, R.M., "Excitation of earth-ionosphere waveguide in the ELF and lower VLF bands by modulated ionospheric current," technical report to Phillips Laboratory, Hanscom AFB, under contract F19628-90-C-0100, 21 May 1993.

Flikkema, P.G., "Spread-spectrum techniques for wireless communication," *IEEE Signal Processing Magazine*, vol. 14, pp. 26-36, May 1997.

Giglio, D., and Ralston, J., "Perspective on underground and obscured target detection and imaging," SPIE Proceedings on Underground and Obscured Object Imaging and Detection, 15-16 April 1993, volume 1942, pp. 2-7.

Hanold, R.J., "Rapid excavation by rock melting (LASL subterrene program)," Los Alamos National Laboratories, technical report LA-5979-SR, 1 February 1977.

Hewitt, B.S., "The evolution of radar technology into commercial systems," *IEEE MTT-S Int. Microwave Symp. Dig.*, pp. 1271-1274, June 1994.

Karode, S.L., and Fusco, V.F., "Novel retrodirective beam forming techniques," *Proc. of 27th European Microwave Conference*, pp. 81-86, Sept. 1997.

Karode, S.L., and Fusco, V.F., "Use of an active retrodirective antenna array as a multipath sensor," *IEEE Microwave and Guided Wave Letters*, vol. 7, pp. 399-401, December 1997.

Kuo, S.P., Lee, M.C., and Kossey, P., "Study of ELF/VLF wave generation by HF heater-modulated electroject," Proceedings Conference on Plasma Science, 19-22 May 1997, pp. 265-266.

Leismer, D., Williams, B., and Pussel, J., "Coiled tubing drilling: real time MWD with dedicated powers to the BHA," paper SPE 37199 presented at the Offshore Technology Conference, Houston, TX, 1996.

Lin, J., and Itoh, T., "Active Integrated Antennae," IEEE Transactions on Microwave Theory and Techniques, vol. 42, pp. 2186-2195, December 1994.

Margerum, D.L., "Self-phased arrays," in *Microwave Scanning Antennae*, vol. III, Ch. 5, R. C. Hansen, Ed., Los Altos, CA: Pennisula, 1985.

Milstein, L.B., "Interference rejection techniques in spread spectrum communications," *Proceedings of the IEEE*, vol. 76, pp. 657-671, June 1988.

Pobanz, C.W., and Itoh, T., "A conformal retrodirective array for radar applications using a heterodyne phased scattering element," *IEEE MTT-S Int. Microwave Symp. Dig.*, pp. 905-908, May 1995.

Pobanz, C.W., and Itoh, T., "A microwave noncontact identification transponder using subharmonic interrogation," *IEEE Transactions on Microwave Theory and Techniques*, vol. 43, pp. 1673-1679, July 1995.

Pobanz, C.W., and Itoh, T., "A two-dimensional retrodirective array using slot ring FET mixers," *Proc. of 26th European Microwave Conference*, pp. 217-220, Sept. 1996.

Pon, C.Y., "Retrodirective array using the heterodyne technique," *IEEE Trans. Antennae Propagat.*, vol. AP-12, pp. 176-180, Mar. 1964.

Rowley, J.C., "Rock melting applied to excavation and tunneling", Proceedings of the Third Congress of the International Society for Rock Mechanics, vol. 1, part B, pp. 1447-1453, September 1974.

Sarwate, D.V., and Pursley, M.B., "Crosscorrelation properties of pseudorandom and related sequences," *Proceedings of the IEEE*, vol. 68, pp. 593-619, May 1980.

Sharp, E.D., and Diab, M.A., "Van Atta reflector array," *IRE Trans. Antennae Propagat.*, vol. AP-8, pp. 436-438, 1960.

Skolnik, M.I., and King, D.D., "Self-phasing array antennae," *IEEE Trans. Antennae Propagat.*, vol. AP-12, pp. 142-149, Mar. 1964.

Smith, M.C., editor, "A preliminary study of the nuclear subterrene", Los Alamos Scientific Laboratory report 4547, April 1971.

Won, I.J., "A wide-band electromagnetic exploration method—some theoretical and experimental results," Geophysics, vol. 45, pp. 928-940, 1980.